# General Disclaimer

One or more of the Following Statements may affect this Document

- This document has been reproduced from the best copy furnished by the organizational source. It is being released in the interest of making available as much information as possible.

- This document may contain data, which exceeds the sheet parameters. It was furnished in this condition by the organizational source and is the best copy available.

- This document may contain tone-on-tone or color graphs, charts and/or pictures, which have been reproduced in black and white.

- This document is paginated as submitted by the original source.

- Portions of this document are not fully legible due to the historical nature of some of the material. However, it is the best reproduction available from the original submission.
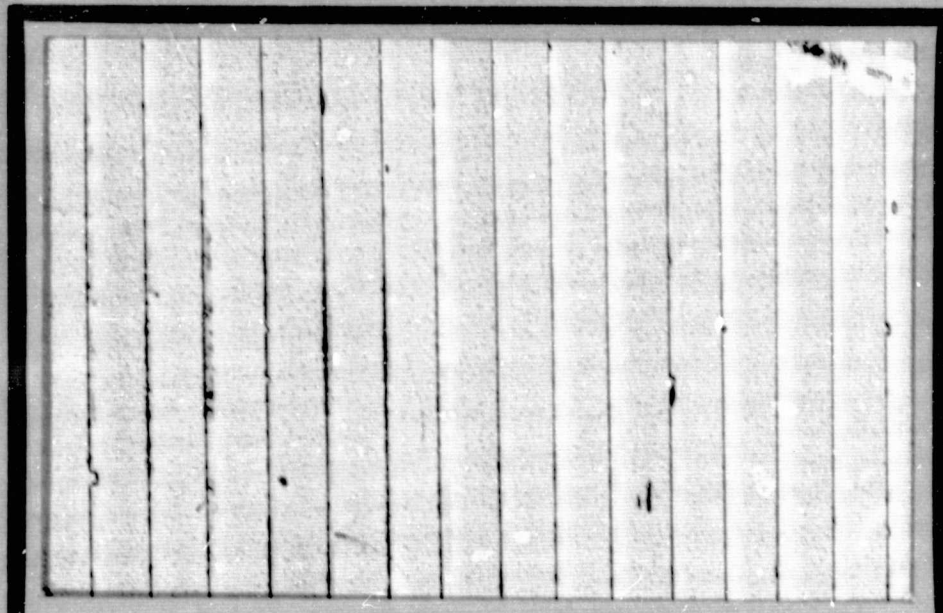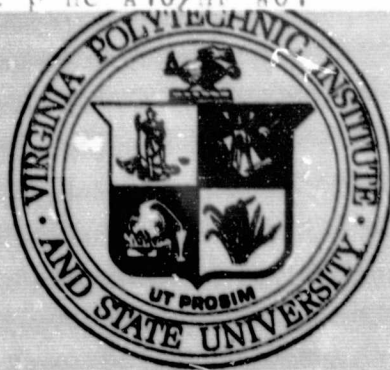
Produced by the NASA Center for Aerospace Information (CASI)

NASA CR-156841

Virginia Polytechnic Institute
and State University

Electrical Engineering
BLACKSBURG, VIRGINIA   24061

Interim Report 1978-2

on

A DEPOLARIZATION AND ATTENUATION EXPERIMENT USING THE CTS AND COMSTAR SATELLITES

The Phase of the Crosspolarized Signal Generated
By Millimeter Wave Propagation Through Rain

Text by

W. P. Overstreet and C. W. Bostian

Electrical Engineering Department
Virginia Polytechnic Institute and State University
Blacksburg, Virginia 24061

Prepared for

NASA Goddard Space Flight Center
Greenbelt, Maryland 20771

June, 1978

1. Report No.	2. Government Accession No.	3. Recipient's Catalog No.
4. Title and Subtitle The Phase of the Crosspolarized Signal Generated by Millimeter Wave Propagation Through Rain		5. Report Date June, 1978
		6. Performing Organization Code 1978-2
7. Author(s) W. P. Overstreet and C. W. Bostian		8. Performing Organization Report No.
9. Performing Organization Name and Address Department of Electrical Engineering 340 Whittemore Hall VPI&SU, Blacksburg, Virginia 24061		10. Work Unit No.
		11. Contract or Grant No. NAS5-22577
		13. Type of Report and Period Covered
12. Sponsoring Agency Name and Address NASA Goddard Space Flight Center Greenbelt, Md. 20771 E. Hirschmann, Code 953, Technical Officer		Interim Report 1978-2
		14. Sponsoring Agency Code

15. Supplementary Notes

16. Abstract

Proposed schemes for cancelling rain-induced crosstalk in dual-polarized communications systems depend upon the phase relationships between the wanted and unwanted signals. This report investigates the phase relationship of the rain-generated crosspolarized signal relative to the copolarized signal. Theoretical results obtained from a commonly accepted propagation model are presented. Experimental data from the Communications Technology Satellite beacon and from the Comstar beacon are presented and the correlation between theory and data is discussed.

An inexpensive semi-adaptive cancellation system is proposed and its performance expectations are presented. The implications of phase variations on a cancellation system are also discussed.

17. Key Words (Selected by Author(s)) depolarization,isolation,phase, millimeter wave propagation, rain, CTS, COMSTAR, satellite communica- tions, crosstalk, cancellation, antenna-wave interraction	18. Distribution Statement Unlimited		
19. Security Classif. (of this report) U	20. Security Classif. (of this page) U	21. No. of Pages 190	22. Price

* For sale by the National Technical Information Service, Springfield, Virginia 22151

TABLE OF CONTENTS

LIST OF FIGURES

v

LIST OF TABLES

CHAPTER 1

INTRODUCTION

1.1 Purpose of Thesis

Overcrowding of the radio frequency spectrum is forcing users to
consider operating at higher and higher frequencies and to investi-
gate the practicality of orthogonal polarization frequency reuse [1].
However, this combination of higher frequencies and dual polariza-
tions poses certain problems. Atmospheric effects, principally
rain, depolarize the transmitted wave. This depolarization results in
a crosspolarized signal component which creates undesired crosstalk
between otherwise independent channels.

The phase of this crosspolarized signal is probably the most
difficult rain propagation effect to measure. In general, theoretical
predictions of phase are either absent from the literature, or they
are presented as a byproduct of an attenuation-isolation model.
Theoretical phase predictions are often suspect for these reasons.

This thesis investigates the crosspolarized signal phase in
detail. This investigation was motivated by several factors. First,
the phase has implications in the theoretical modelling of rain
propagation. It is a particularly sensitive function of certain
properties of a rain-filled medium and its measurement aids in the
determination of these properties. In addition, phase can have a
direct bearing on communications system performance. To illustrate
the system implications consider a cancellation system (or a cross-

coupling system as it is often called) which injects a signal from channel A of a dual-polarized receiver into channel B of the receiver. If the injected signal has the correct amplitude and phase the result is a cancellation of the crosstalk in channel B. A signal from channel B is similarly injected into channel A. The phase of the cancellation signal must be 180° different from that of the interfering signal. It is therefore necessary to know something about the characteristics of the crosspolarized signal phase in order to implement a cancellation network.

The questions to be answered by this these are: (1) what can be learned of the rain propagation medium from phase measurements; (2) how will phase variations affect a cancellation system; and (3) is there a particular set of conditions that will enhance the operation of a cancellation system? In the work to follow a brief section of definitions is followed by the development of a mathematical model to predict the phase. This chapter, 2, will also present several phase predictions for different frequencies and polarizations. Chapter 3 describes the VPI&SU Satellite Communications experiment with emphasis on the hardware and software related to the measurement of phase. Presented in Chapter 4 are experimental data for a wide range of propagation events at 11.7 GHz and 28.56 GHz along with a discussion of the correlation between data and theory. Explanations for observed differences are proposed and substantiated. Chapter 5 addresses the cancellation system and its performance in a real communications link. An inexpensive cancellation device suitable for

the small earth terminal will be proposed as a conclusion to this thesis.

1.2 Definition of Phase

Phase is defined as "the fraction of a complete cycle elapsed as measured from a specific reference point" [2]. In this thesis the phase of concern is that of the crosspolarized wave and the reference point is defined as the beginning of a cycle of the copolarized wave. The copolarized wave is the wave of the desired polarization and the crosspolarized wave is the undesired rain-induced wave. These definitions are equivalent to stating that the relative phase of the crosspolarized wave with respect to the copolarized wave is to be measured. As in most electrical engineering work the phase will be expressed as an angle in degrees.

Electromagnetic waves and their corresponding waveguide fields and circuit voltages may be expressed as sinusoids in the general form

$$v_1(t) = Vm \sin(\omega t + \phi) \tag{1}$$

where ϕ is the phase angle relative to the sinusoid

$$v_2(t) = Vm \sin(\omega t) \tag{2}$$

and Vm is a positive number.

The angle ϕ represents the amount by which $v_1(t)$ leads $v_2(t)$. This is illustrated in Figure 1-1 where $v_1(t)$ and $v_2(t)$ are plotted.
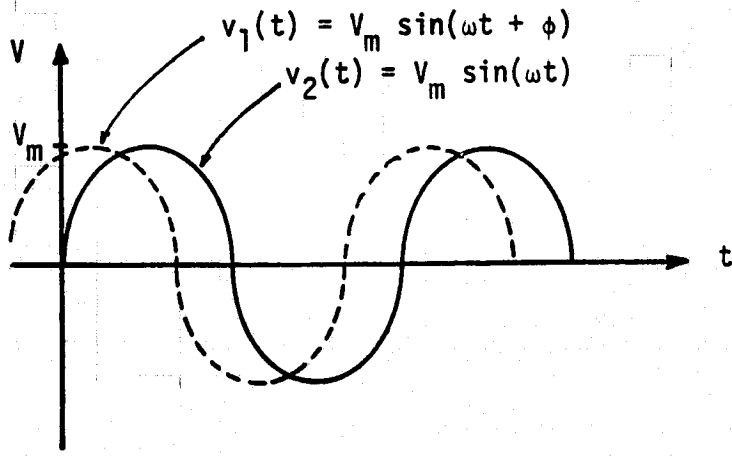
Figure 1-1. The relative phase of two sinusoids.

Here ϕ is the angle by which v_1 (broken line) is shifted to the left of v_2. Corresponding points of $v_1(t) = Vm \sin(\omega t + \phi)$ occur ϕ/ω seconds earlier than $v_2(t) = Vm \sin(\omega t)$.

Similarly if

$$v_3(t) = Vm \sin(\omega t + \phi_3) \qquad (3)$$

and

$$v_4(t) = Vm \sin(\omega t + \phi_4) \qquad (4)$$

v_3 leads v_4 by $\phi_3 - \phi_4$ where v_4 is assumed to be the reference sinusoid. If v_3 lags v_4 then the sign of $\phi_3 - \phi_4$ is negative which indicates this condition.

The copolarized wave is the reference sinusoid and is analogous to $v_4(t) = Vm \sin(\omega t + \phi_4)$. The crosspolarized wave is analogous to $v_3(t) = Vm \sin(\omega t + \phi_3)$. The phase of the crosspolarized wave referenced to the copolarized wave is then $\phi_3 - \phi_4$.

Expressed mathematically,

$$\phi_{co} = \text{Phase}\{V_4(t)\} = \text{Phase}\{Vm \sin(\omega t + \phi_4)\} = \phi_4 \qquad (5)$$

and

$$\phi_{cross} = \text{Phase}\{V_3(t)\} = \text{Phase}\{Vm \sin(\omega t + \phi_3)\} = \phi_3 \qquad (6)$$

and the relative phase is

$$\phi_3 - \phi_4$$

$$= \text{Phase}\{Vm \sin(\omega t + \phi_3)\} - \text{Phase}\{Vm \sin(\omega t + \phi_4)\}$$

$$= \phi_{cross} - \phi_{co} \ . \tag{7}$$

Therefore the relative phase is defined as

$$\Delta = \phi_{cross} - \phi_{co} \ . \tag{8}$$

With this definition of relative phase a retardation of the cross-polarized signal phase results in a negative change in Δ and an advance in the crosspolarized signal phase causes a positive change in Δ.

The phase of the crosspolarized wave with respect to the copolarized wave, Δ, will henceforth be termed the crosspolarized phase or simply the phase.

1.3 The Phase of a Circularly Polarized Wave

In dealing with linearly polarized waves, linearly polarized fields in a waveguide, or circuit voltages, the phase is completely specified as in the discussion above. The electric (and magnetic) field vectors of a linearly polarized wave oscillate in amplitude at the radian frequency of the wave. However, the field vectors of a circularly polarized wave are constant in amplitude and this leads to an ambiguity in the meaning of phase. Several definitions have been proposed for the phase of a circularly polarized wave [3]. The definition to be used here requires a reference direction in space

to be established. Figure 1-2 illustrates a right-hand circularly polarized (RHCP) wave in space with the E-vector rotating in the x-y plane. Also shown is a left-hand circularly polarized (LHCP) wave. A reference direction in the x-y plane is established along the positive x-axis and the phase of the wave is measured by the angle through which the E-vector has rotated beyond this reference direction. The sense of the positive angle or the RHCP wave and the LHCP wave is opposite. The phase difference between the two waves remains constant as the vectors rotate in their respective directions.

If a new reference direction were chosen or if two different reference directions were chosen for the two waves a constant value is added to the relative phase. In the studies to follow only changes in the relative phase and the correlation between these changes and weather phenomena are important. Many constant terms appear; for example, differences in the waveguide structure of a practical receiver introduce a constant term. Therefore the choice of reference directions is completely arbitrary.

1.4 Differential Phase Shift

The term differential phase shift, or the more concise term differential phase, will be used throughout this thesis. Differential phase (and differential attenuation) refer to the difference in propagation constants for a wave polarized in a direction parallel to the major axes of an ensemble of raindrops and a wave polarized parallel to the minor axes of the raindrops. The propagation
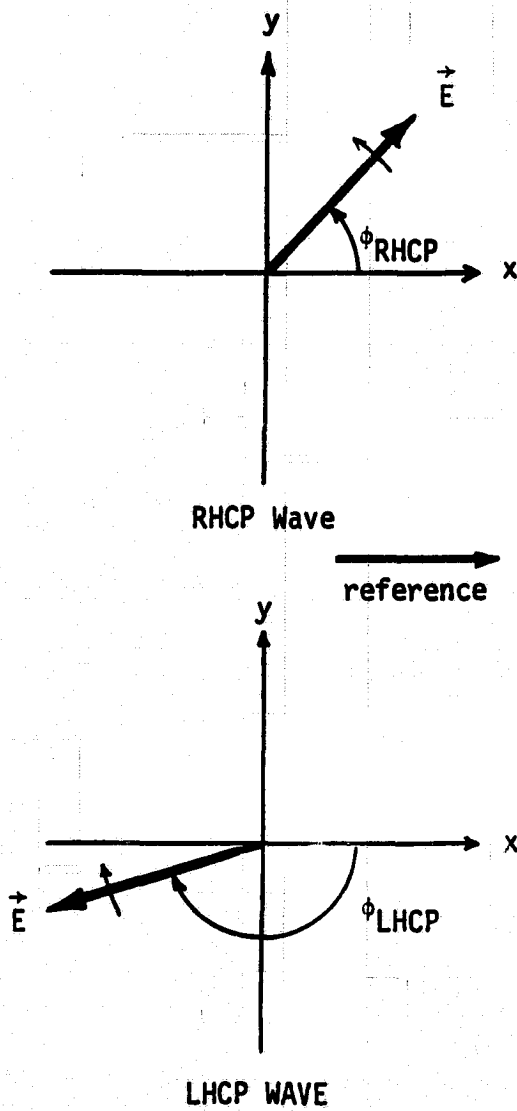
Figure 1-2. The phase of a circularly polarized wave.

difference exists because most raindrops are elongated in an approximately horizontal direction.

Differential phase and crosspolarized phase are different quantities. A relationship between the two is developed in the next chapter. The differential phase will henceforth be referred to by its complete name.

CHAPTER 2

A MATHEMATICAL MODEL FOR PHASE

2.1 Review of the Rain Medium Propagation Properties

In this section expressions are developed which relate cross-polarized phase directly to the properties of a rain-filled propagation medium. These new expressions were developed in order to provide simple equations from which the effects of the medium are readily apparent. These equations lead in turn to relatively straightforward computer routines for predicting phase behavior.

The properties of a rain-filled medium which are of concern are path length, canting angle of the raindrops, differential attenuation, and differential phase. For convenience all raindrops in the medium are assumed to have the same canting angle θ. This assumption, while not ideal, is realistic and is necessary to the development of simple equations for phase. The assumption of equal canting angles for all drops is equivalent to defining an effective canting angle for the medium. It has been stated that by defining an effective canting angle the cancelling effects of drops canted positive from the effective angle and those canted negative from the effective angle are approximated [1].

A rain-filled propagation medium is shown in Figure 2-1 with an x-y coordinate system along the horizontal and vertical directions. One raindrop is shown in order to define a 1-2 coordinate system which is rotated from the x-y coordinate system by the
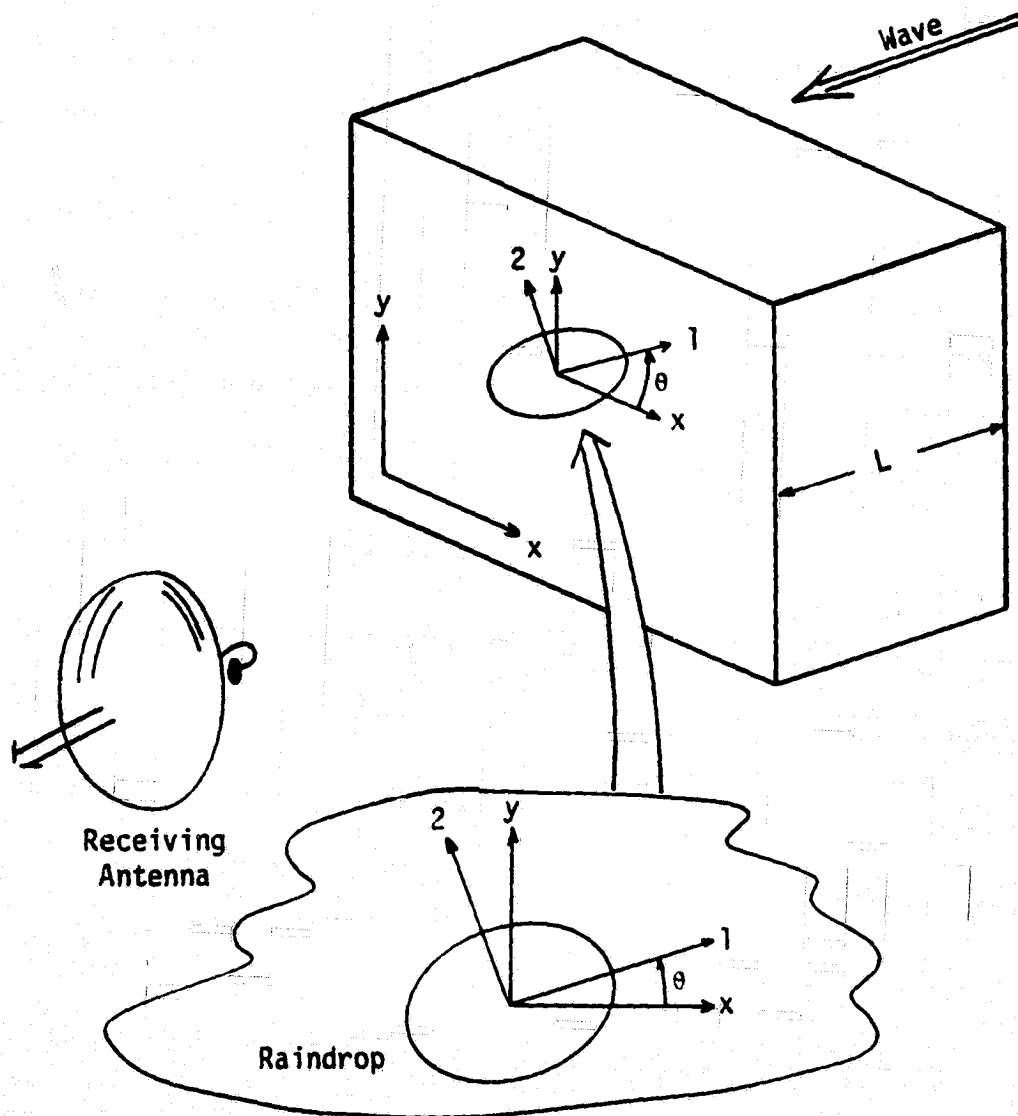
Figure 2-1. A rain-filled propagation medium.

canting angle θ. Differential attenuation and differential phase are
defined as properties of the medium and are related to the propagation
of two waves, one polarized in the 1-direction and the other in the
2-direction.

A wave which is polarized in the direction of the 1-axis
experiences an attenuation of α_1 and a phase delay of β_1 upon
propagation through one kilometer of the rain medium. A wave polar-
ized in the direction of the 2-axis experiences an attenuation and
phase delay of α_2 and β_2 respectively. Differential attenuation is
defined as

$$\alpha = \alpha_1 - \alpha_2 \tag{9}$$

and differential phase is defined as

$$\beta = \beta_1 - \beta_2 . \tag{10}$$

The differential quantities α and β are properties of the total
rain-filled medium. They are related to the scattering properties of
the individual raindrops by [4]

$$\alpha_{1,2} = 0.434 \frac{\lambda^2}{2} \ \Sigma \ Re\{S_{1,2}\} \ n(\overline{a}) \qquad dB/km \tag{11}$$

and

$$\beta_{1,2} = - \frac{36 \ \lambda^2}{4\pi^2} \ \Sigma \ Im\{S_{1,2}\} \ n(\overline{a}) \qquad degr/km \tag{12}$$

where

λ = wavelength in cm

$n(\overline{a})$ = density of drops with equivolumic radius $\overline{a}$

$S_{1,2}$ = complex scattering functions

and where the summation is performed over all drops in the medium.

The scattering functions S_1 and S_2 represent the effects on a wave propagating perpendicularly to the axis of symmetry of the raindrop. In the case of a satellite communications link the wave propagates along a slanted path through the atmosphere. This path intersects the plane containing the raindrop axes of symmetry at an angle of less than 90°. Therefore an additional factor must be included in the above relations since they use the scattering functions S_1 and S_2.

The geometry of this situation is shown in Figure 2-2. The angle γ is the elevation angle from the earth station to the satellite. The angle between the direction of propagation of the incident wave and the axis of symmetry of the raindrop is $\zeta = 90° - \gamma$. It has been shown that [5]

$$\alpha = \alpha_\perp \sin^2 \zeta \qquad (13)$$

and

$$\beta = \beta_\perp \sin^2 \zeta \qquad (14)$$

where
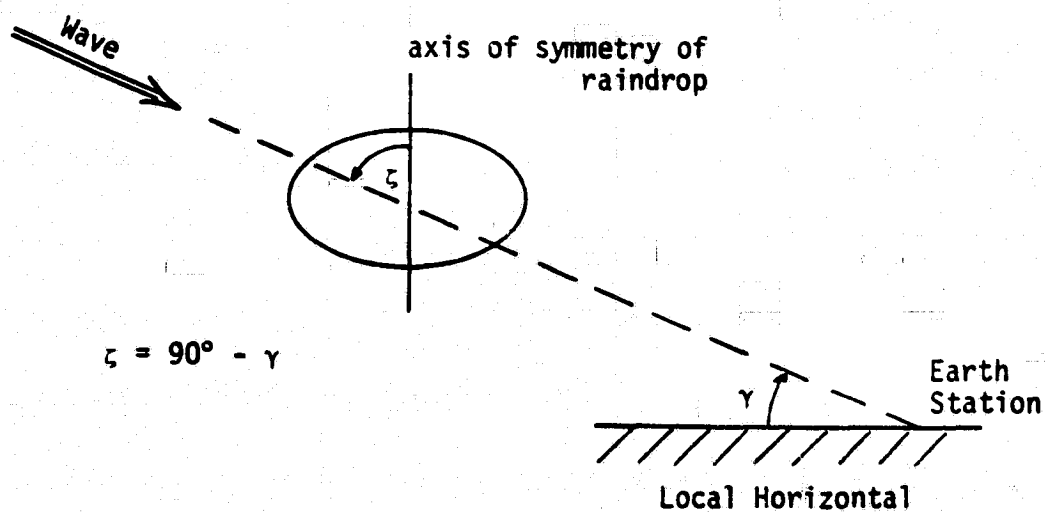
Figure 2-2. The geometry of an earth-satellite link.

α, β = differential attenuation and phase values for incidence angle < 90°

$\alpha_{\perp}$, $\beta_{\perp}$ = differential attenuation and phase values for perpendicular incidence

ζ = angle between raindrop symmetry axis and direction of propagation .

Substituting $\zeta = 90° - \gamma$ into these expressions yields

$$\alpha = \alpha_{\perp} \sin^2(90° - \gamma)$$
$$= \alpha_{\perp} \cos^2 \gamma \tag{15}$$

and

$$\beta = \beta_{\perp} \sin^2(90° - \gamma)$$
$$= \beta_{\perp} \cos^2 \gamma \tag{16}$$

where

γ = elevation angle of the satellite .

These relationships will be used in the sections to follow.

2.2 Development of the Model

2.2.1 The Rain Transmission Matrix

A wave entering the rain medium can be decomposed into two orthogonal wave components. A convenient choice is to decompose the wave such that one of the components is linearly polarized in

the x-direction and the other component is linearly polarized in the y-direction. However, the attenuation and phase properties of the medium are defined for waves polarized along the 1 and 2 axes. Therefore it is necessary to transform the incident wave with x and y polarization components into a wave with 1 and 2 polarization components. After accounting for the propagation of the wave through the medium it is necessary to transform back into the original x and y component representation.

Figure 2-3a illustrates an x-polarized electric field vector (representing the E-field of a propagating wave) and a y-polarized E-vector and their projections onto the 1 and 2 axes. It is seen that

$$E_1^i = E_x^i \cos \theta + E_y^i \sin \theta \tag{17}$$

and

$$E_2^i = -E_x^i \sin \theta + E_y^i \cos \theta \tag{18}$$

where the superscript i is included to represent the wave incident upon the rain medium. In matrix form these equations are

$$\begin{bmatrix} E_1^i \\ E_2^i \end{bmatrix} = \begin{bmatrix} \cos \theta & \sin \theta \\ -\sin \theta & \cos \theta \end{bmatrix} \begin{bmatrix} E_x^i \\ E_y^i \end{bmatrix} \tag{19}$$

The resulting components propagate through the rain-filled medium according to their respective propagation constants,
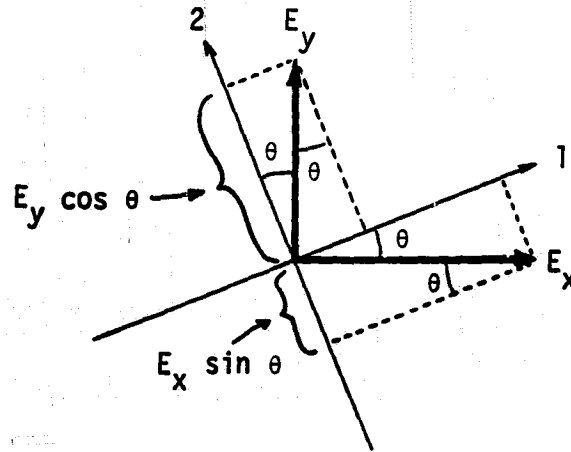
Figure 2-3a. Decomposition of vectors.
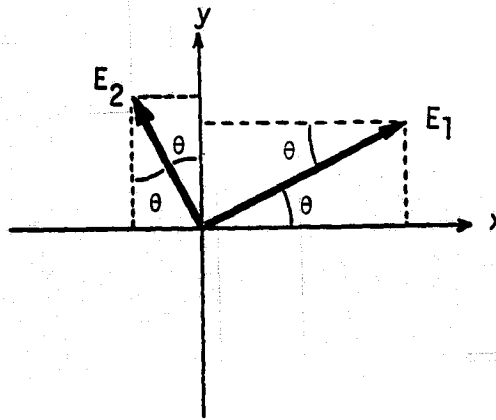
Figure 2-3b. Recomposition of vectors.

Figure 2-3. Decomposition and recomposition of vectors representing a wave propagating through rain.

$$d_1 = e^{-(\alpha_1 + j\beta_1)L}$$
$$d_2 = e^{-(\alpha_2 + j\beta_2)L} \tag{20}$$

where

$$\alpha_{1,2} = \text{attenuation} \qquad \text{nepers/km}$$
$$\beta_{1,2} = \text{phase delay} \qquad \text{radians/km}$$
$$L = \text{path length} \qquad \text{km} \quad .$$

Both α and β are positive numbers and the negative sign on the exponents in these relations assures that the wave is attenuated and phase delayed.

The effects of the rain are expressed in matrix form as [6]

$$\begin{bmatrix} E_1 \\ E_2 \end{bmatrix} = \begin{bmatrix} d_1 & 0 \\ 0 & d_2 \end{bmatrix} \begin{bmatrix} E_1^i \\ E_2^i \end{bmatrix} \tag{21}$$

In a manner which is analogous to the decomposition of the wave into 1 and 2 components, the wave leaving the rain medium is recomposed into x and y components. This is illustrated in Figure 2-3b. The results are

$$\begin{bmatrix} E_x \\ E_y \end{bmatrix} = \begin{bmatrix} \cos\theta & -\sin\theta \\ \sin\theta & \cos\theta \end{bmatrix} \begin{bmatrix} E_1 \\ E_2 \end{bmatrix} . \tag{22}$$

The three steps of decomposition, propagation, and recomposition

are integrated into a single expression by forming the matrix product

$$
\begin{bmatrix} E_x \\ E_y \end{bmatrix} = \begin{bmatrix} \cos\theta & -\sin\theta \\ \sin\theta & \cos\theta \end{bmatrix} \begin{bmatrix} d_1 & 0 \\ 0 & d_2 \end{bmatrix} \begin{bmatrix} \cos\theta & \sin\theta \\ -\sin\theta & \cos\theta \end{bmatrix} \begin{bmatrix} E_x^i \\ E_y^i \end{bmatrix}
$$

$$
= \begin{bmatrix} \cos\theta & -\sin\theta \\ \sin\theta & \cos\theta \end{bmatrix} \begin{bmatrix} d_1\cos\theta & d_1\sin\theta \\ -d_2\sin\theta & d_2\cos\theta \end{bmatrix} \begin{bmatrix} E_x^i \\ E_y^i \end{bmatrix}
$$

$$
= \begin{bmatrix} d_1\cos^2\theta + d_2\sin^2\theta & (d_1 - d_2)\sin\theta\cos\theta \\ (d_1 - d_2)\sin\theta\cos\theta & d_1\sin^2\theta + d_2\cos^2\theta \end{bmatrix} \begin{bmatrix} E_x^i \\ E_y^i \end{bmatrix} . \tag{23}
$$

The transmission matrix

$$
\begin{bmatrix} d_1\cos^2\theta + d_2\sin^2\theta & (d_1 - d_2)\sin\theta\cos\theta \\ (d_1 - d_2)\sin\theta\cos\theta & d_1\sin^2\theta + d_2\cos^2\theta \end{bmatrix} \tag{24}
$$

is a compact expression which includes the total effect of the rain medium. This expression is in agreement with expressions derived by others [6].

2.2.2 Circular Polarization

In this section a pure circularly polarized wave is assumed to

be transmitted and the medium effects are modelled with the
transmission matrix developed in the previous section. The wave
which exits the depolarizing rain medium will have both a RHCP
component and a LHCP component. These components are to be extracted
and the relative phase of the two determined. This yields the
crosspolarized phase assuming the receiving antennas are perfect
circularly polarized antennas. Deviations in the crosspolarized
phase because of imperfect antennas will be discussed in sections
2.6 and 2.7.

Assuming that the incident wave is right-hand circularly
polarized, the x-component of the wave leads the y-component by 90°.
This is expressed in vector notation as

$$
\begin{aligned}
\vec{E}^i &= E_x^i \, \hat{x} + E_y^i \, \hat{y} \\
&\propto \hat{x} + e^{j\delta} \, \hat{y} \\
&= \hat{x} + e^{j(-90°)} \, \hat{y} \\
&= \hat{x} - j \, \hat{y}
\end{aligned}
\tag{25}
$$

and in matrix notation as

$$
\vec{E}^i = \begin{bmatrix} E_x^i \\ E_y^i \end{bmatrix} \propto \begin{bmatrix} 1 \\ -j \end{bmatrix} .
\tag{26}
$$

The magnitude is suppressed and proportionality signs are used here

because the phase is not dependent upon the magnitude of the incident wave. This concept will be used in several places in this derivation in order to reduce the complexity of equations.

This representation of the incident wave is multiplied by the transmission matrix. The results are the x and y components of the wave leaving the rain medium:

$$
\begin{bmatrix} E_x \\ E_y \end{bmatrix} \propto \begin{bmatrix} d_1 \cos^2 \theta + d_2 \sin^2 \theta & (d_1 - d_2)\sin \theta \cos \theta \\ (d_1 - d_2)\sin \theta \cos \theta & d_1 \sin^2 \theta + d_2 \cos^2 \theta \end{bmatrix} \begin{bmatrix} 1 \\ -j \end{bmatrix}
$$

$$
= \begin{bmatrix} d_1 \cos^2 \theta + d_2 \sin^2 \theta - j(d_1 - d_2)\sin \theta \cos \theta \\ (d_1 - d_2)\sin \theta \cos \theta - j(d_1 \sin^2 \theta + d_2 \cos^2 \theta) \end{bmatrix}
$$

$$
= \begin{bmatrix} d_1(\cos^2 \theta - j \sin \theta \cos \theta) + d_2(\sin^2 \theta + j \sin \theta \cos \theta) \\ d_1(\sin \theta \cos \theta - j \sin^2 \theta) - d_2(\sin \theta \cos \theta + j \cos^2 \theta) \end{bmatrix}
$$

$$
= \begin{bmatrix} d_1 \cos \theta(\cos \theta - j \sin \theta) + j d_2 \sin \theta(\cos \theta - j \sin \theta) \\ d_1 \sin \theta(\cos \theta - j \sin \theta) - j d_2 \cos \theta(\cos \theta - j \sin \theta) \end{bmatrix}
$$

$$
= (\cos \theta - j \sin \theta) \begin{bmatrix} d_1 \cos \theta + j d_2 \sin \theta \\ d_1 \sin \theta - j d_2 \cos \theta \end{bmatrix}
$$

$$= e^{-j\theta} \begin{bmatrix} d_1 \cos\theta + j\ d_2 \sin\theta \\ \\ d_1 \sin\theta - j\ d_2 \cos\theta \end{bmatrix}. \tag{27}$$

Although it is not obvious from this expression, the pure RHCP wave has been depolarized into a wave with RHCP and LHCP components. It is necessary to extract these two components.

The copolarized wave is RHCP and will be received by a RHCP antenna, the output voltage of such an antenna will be proportional in magnitude and phase to the RHCP wave. The vector representation of this antenna is determined by the wave that it transmits, and, as in the case of the incident RHCP wave, this is

$$\vec{e}_{a_{(co)}} \propto \hat{x} - j\ \hat{y} \tag{28}$$

The phasor voltage at the antenna output port as a result of the received wave is expressed as the dot product of the wave vector and the complex conjugate of the receiving antenna vector:

$$\overline{V}_{co} = C\ \vec{E} \cdot \vec{e}_{a_{r(co)}}^* \tag{29}$$

where

$\overline{V}_{co}$ = phasor output voltage of the copolarized antenna

C = constant of proportionality .

The subscript r appearing on the antenna vector indicates that the receiving polarization state of the antenna must be used. The

polarization vector of an antenna upon receiving is not necessarily the same as the polarization vector of the wave which it transmits. A transformation is required to obtain $\vec{e}_{a_r}$ from $\vec{e}_a$.

This transformation is discussed in detail in Appendix 1 where it is shown that the required transformation is

$$\delta_r = 180° - \delta \tag{30}$$

where δ is the phase angle of the y-component of the wave transmitted by the antenna in question.

In this case,

$$
\begin{aligned}
\vec{e}_{a(co)} &\propto \hat{x} - j\,\hat{y} \\
&= \hat{x} + e^{j(-90°)}\,\hat{y} \\
&= \hat{x} + e^{j\delta}\,\hat{y} \quad \text{where } \delta = -90° \ .
\end{aligned}
\tag{31}
$$

Therefore

$$\delta_r = 180° - \delta = 180° - (-90°) = 270° \tag{32}$$

and

$$
\begin{aligned}
\vec{e}_{a_{r(co)}} &= \hat{x} + e^{j\delta_r}\,\hat{y} \\
&= \hat{x} + e^{j(270°)}\,\hat{y} \\
&= \hat{x} - j\,\hat{y} \ .
\end{aligned}
\tag{33}
$$

The output of the copolarized antenna is

$$\overline{V}_{co} = \vec{E} \cdot \vec{e}_{a_{r(co)}}^*$$

$$= (E_x \hat{x} + E_y \hat{y}) \cdot (\hat{x} - j\hat{y})^*$$

$$= (E_x \hat{x} + E_y \hat{y}) \cdot (\hat{x} + j\hat{y})$$

$$= E_x + j E_y \tag{34}$$

and the phase of this voltage is simply

$$\phi_{co} = \text{Phase}\{E_x + j E_y\} . \tag{35}$$

Substituting the E_x and E_y components of the wave leaving the rain medium (from (27)) yields

$$\phi_{co} = \text{Phase}\{[e^{-j\theta}(d_1 \cos\theta + j d_2 \sin\theta)]$$
$$+ j[e^{-j\theta}(d_1 \sin\theta - j d_2 \cos\theta)]\} \tag{36}$$

and simplifying

$$\phi_{co} = \text{Phase}\{e^{-j\theta}[d_1(\cos\theta + j\sin\theta) + d_2(\cos\theta + j\sin\theta)]\}$$
$$= \text{Phase}\{e^{-j\theta}[e^{j\theta}(d_1 + d_2)]\}$$
$$= \text{Phase}\{d_1 + d_2\} . \tag{37}$$

Similarly, the crosspolarized LHCP antenna is represented by

$$\vec{e}_{a_{(x)}} \propto \hat{x} + j\hat{y}$$
$$= \hat{x} + e^{j(+90°)} \hat{y} . \tag{38}$$

The angle of the y-component, δ, is +90°, therefore

$$\delta_r = 180° - \delta = 180° - (90°) = 90° \tag{39}$$

and

$$\vec{e}_{a_{r(x)}} = \hat{x} + e^{j\,90°}\,\hat{y}$$
$$= \hat{x} + j\,\hat{y} \ . \tag{40}$$

The voltage at the crosspolarized antenna output is

$$\overline{V}_x = \vec{E} \cdot \vec{e}^{\,*}_{a_{r(x)}}$$

$$= (E_x\,\hat{x} + E_y\,\hat{y}) \cdot (\hat{x} + j\,\hat{y})^*$$

$$= (E_x\,\hat{x} + E_y\,\hat{y}) \cdot (\hat{x} - j\,\hat{y})$$

$$= E_x - j\,E_y \tag{41}$$

and the phase of the voltage is[1]

$$\phi_x = \text{Phase}\{E_x - j\,E_y\}$$
$$= \text{Phase}\{[e^{-j\theta}(d_1 \cos\theta + j\,d_2 \sin\theta)]$$
$$\qquad -j[e^{-j\theta}(d_1 \sin\theta - j\,d_2 \cos\theta)]\}$$
$$= \text{Phase}\{e^{-j\theta}[d_1(\cos\theta - j\sin\theta) - d_2(\cos\theta - j\sin\theta)]\}$$
$$= \text{Phase}\{e^{-j\theta}[e^{-j\theta}(d_1 - d_2)]\}$$
$$= \text{Phase}\{e^{-j2\theta}(d_1 - d_2)\}$$
$$= -2\theta + \text{Phase}\{d_1 - d_2\} \ . \tag{42}$$

Recalling the definition of the phase of the crosspolarized

---

[1] The phase ϕ_x is the same as ϕ_{cross} defined in Chapter 1.

signal with respect to the copolarized signal, the crosspolarized phase is

$$\Delta = \phi_x - \phi_{co}$$
$$= -2\theta + \text{Phase}\{d_1 - d_2\} - \text{Phase}\{d_1 + d_2\} \tag{43}$$

for the case in which the transmitted wave is RHCP.

Consider now a LHCP transmitted wave. The matrix representation of the wave incident upon the medium is

$$\begin{bmatrix} E_x^i \\ \\ E_y^i \end{bmatrix} \propto \begin{bmatrix} 1 \\ \\ j \end{bmatrix} . \tag{44}$$

Multiplying this by the transmission matrix of the medium yields the x and y components of the wave exiting the medium.

$$\begin{bmatrix} E_x \\ \\ E_y \end{bmatrix} \propto \begin{bmatrix} d_1 \cos^2 \theta + d_2 \sin^2 \theta & (d_1 - d_2)\sin \theta \cos \theta \\ \\ (d_1 - d_2)\sin \theta \cos \theta & d_1 \sin^2 \theta + d_2 \cos^2 \theta \end{bmatrix} \begin{bmatrix} 1 \\ \\ j \end{bmatrix}$$

$$= e^{j\theta} \begin{bmatrix} d_1 \cos \theta - j \, d_2 \sin \theta \\ \\ d_1 \sin \theta + j \, d_2 \cos \theta \end{bmatrix} . \tag{45}$$

This result was obtained in a manner idential to that of (27).

Again this represents a depolarized wave with both LHCP and RHCP components. The copolarized antenna in this case is a LHCP

antenna. Its vector representations are

$$\vec{e}_{a_{(co)}} = \hat{x} + j\,\hat{y} \tag{46}$$

and

$$\vec{e}_{a_{r(co)}} = \hat{x} + j\,\hat{y} \ . \tag{47}$$

The crosspolarized antenna (RHCP) vector representations are

$$\vec{e}_{a_{(x)}} = \hat{x} - j\,\hat{y} \tag{48}$$

and

$$\vec{e}_{a_{r(x)}} = \hat{x} - j\,\hat{y} \ . \tag{49}$$

Using these, the expression $\vec{V} \propto \vec{E} \cdot \vec{e}^{\,*}_{a_r}$, and (45) the copolarized signal phase and the crosspolarized signal phase are determined.

$$\phi_{co} = \text{Phase}\{\overline{V}_{co}\} = \text{Phase}\{\vec{E} \cdot \vec{e}^{\,*}_{a_{r(co)}}\}$$

$$= \text{Phase}\{E_x - j\,E_y\}$$

$$= \text{Phase}\{[e^{j\theta}(d_1 \cos\theta - j\,d_2 \sin\theta)]$$

$$-j[e^{j\theta}(d_1 \sin\theta + j\,d_2 \cos\theta)]\}$$

$$= \text{Phase}\{d_1 + d_2\} \tag{50}$$

and

$$\phi_x = \text{Phase}\{V_x\} = \text{Phase}\{\vec{E} \cdot \vec{e}^*_{a_{r(x)}}\}$$

$$= \text{Phase}\{E_x + j\, E_y\}$$

$$= \text{Phase}\{[e^{j\theta}(d_1 \cos \theta - j\, d_2 \sin \theta)]$$

$$+ [e^{j\theta}(d_1 \sin \theta + j\, d_2 \cos \theta)]\}$$

$$= \text{Phase}\{e^{j2\theta}(d_1 - d_2)\}$$

$$= 2\theta + \text{Phase}\{d_1 - d_2\} \quad . \tag{51}$$

The relative phase between the crosspolarized signal and the copolarized signal is

$$\Delta = \phi_x - \phi_{co}$$

$$= 2\theta + \text{Phase}\{d_1 - d_2\} - \text{Phase}\{d_1 + d_2\} \quad . \tag{52}$$

The results using a RHCP transmitted wave and a LHCP transmitted wave differ only in the sign of 2θ. The 2θ indicates that the crosspolarized phase is directly dependent upon the canting angle of the raindrops. Thus, canting angle changes translate directly into phase variations in the received signals when circular polarization is used. The direction of the phase change is dependent on the sign of 2θ.

By closely examining the portions of the equations for RHCP and LHCP that are identical, several simplifications can be made.

$$\Delta' = \text{Phase}\{d_1 - d_2\} - \text{Phase}\{d_1 + d_2\}$$

$$= \text{Phase}\left\{\frac{d_1 - d_2}{d_1 + d_2}\right\} *$$

$$= \text{Phase}\left\{\frac{(d_1/d_2) - 1}{(d_1/d_2) + 1}\right\} \quad . \tag{53}$$

Recalling the definitions

$$d_1 = e^{-(\alpha_1 + j\beta_1)L}$$

$$d_2 = e^{-(\alpha_2 + j\beta_2)L} \quad , \tag{54}$$

their ratio is

$$\frac{d_1}{d_2} = \frac{e^{-(\alpha_1 + j\beta_1)L}}{e^{-(\alpha_2 + j\beta_2)L}}$$

$$= e^{-([\alpha_1 - \alpha_2] + j[\beta_1 - \beta_2])L}$$

$$= e^{-(\alpha + j\beta)L} \tag{55}$$

where

$$\alpha = \alpha_1 - \alpha_2$$

$$\beta = \beta_1 - \beta_2 \quad .$$

Substituting the above relations into (53) results in the crosspolarized phase as a function of the differential propagation properties of the medium.

---

* This is a consequence of $(e^{j\theta_1}/e^{j\theta_2}) = e^{j(\theta_1 - \theta_2)}$

$$\Delta' = \text{Phase } \left\{ \frac{(d_{1/d_2}) - 1}{(d_{1/d_2}) + 1} \right\}$$

$$= \text{Phase } \left\{ \frac{e^{-(\alpha + j\beta)L} - 1}{e^{-(\alpha + j\beta)L} + 1} \right\}$$

$$= \text{Phase } \left\{ \frac{e^{-\alpha L}(\cos \beta L - j \sin \beta L) - 1}{e^{-\alpha L}(\cos \beta L - j \sin \beta L) + 1} \right\}$$

$$= \text{Phase } \left\{ \frac{(e^{-\alpha L} \cos \beta L - 1) - j e^{-\alpha L} \sin \beta L}{(e^{-\alpha L} \cos \beta L + 1) - j e^{-\alpha L} \sin \beta L} \right\} \quad . \qquad (56)$$

The numerator and denominator of the expression in brackets may be multiplied by the complex conjugate of the denominator. The resultant in the denominator is a real number which may be neglected with no affect upon the phase angle.

$$\Delta' = \text{Phase}\{[(e^{-\alpha L} \cos \beta L - 1) - j e^{-\alpha L} \sin \beta L]$$

$$\times [(e^{-\alpha L} \cos \beta L + 1) + j e^{-\alpha L} \sin \beta L]\}$$

$$\Delta' = \text{Phase}\{[(e^{-\alpha L} \cos \beta L - 1)(e^{-\alpha L} \cos \beta L + 1) + (e^{-\alpha L} \sin \beta L)^2]$$

$$+ j[e^{-\alpha L} \sin \beta L(e^{-\alpha L} \cos \beta L - 1 - e^{-\alpha L} \cos \beta L - 1)]\}$$

$$\Delta' = \text{Phase}\{[e^{-2\alpha L} \cos^2 \beta L - 1 + e^{-2\alpha L} \sin^2 \beta L]$$

$$+ j[-2 e^{-\alpha L} \sin \beta L]\}$$

$$\Delta' = \text{Phase}\{(e^{-2\alpha L} - 1) - j(2e^{-\alpha L} \sin \beta L)\}$$

$$= \tan^{-1} \left\{ \frac{-2e^{-\alpha L} \sin \beta L}{e^{-2\alpha L} - 1} \right\} \quad . \qquad (57)$$

Considering again the $\pm 2\theta$ term, the complete expression for crosspolarized phase for perfect circularly polarized waves and antennas is

$$\Delta = \pm 2\theta + \tan^{-1} \{\frac{-2 \ e^{-\alpha L} \ \sin \ \beta L}{e^{-2\alpha L} - 1}\} \qquad (58)$$

where

$$\theta = \text{canting angle} \begin{cases} +2\theta \text{ for LHCP transmitter} \\ -2\theta \text{ for RHCP transmitter} \end{cases}$$

α = differential attenuation of the medium in nepers/km

β = differential phase of the medium in degrees/km

L = path length in km .

Predictions based on this equation will be presented and discussed in section 2.5.

2.2.3 Linear Polarization

The procedure used in the preceeding section for circular polarization is essentially duplicated for the case of linearly polarized waves. Nevertheless there are several important differences that warrant briefly proceeding through the steps.

Assume a horizontally polarized transmitting antenna. The vector representation of the wave leaving the transmitter and incident upon the rain medium is

$$E^i = E_x^i \ \hat{x} \qquad (59)$$

and in matrix form it is represented by

$$
\vec{E}^i \equiv \begin{bmatrix} E_x^i \\ \\ E_y^i \end{bmatrix} \propto \begin{bmatrix} 1 \\ \\ 0 \end{bmatrix} . \tag{60}
$$

After propagating through the medium, the wave is given by the product of the transmission matrix and the incident wave matrix. The results of this multiplication are the x and y components of the wave leaving the medium.

$$
\begin{bmatrix} E_x \\ \\ E_y \end{bmatrix} = \begin{bmatrix} d_1 \cos^2\theta + d_2 \sin^2\theta & (d_1 - d_2)\sin\theta\cos\theta \\ \\ (d_1 - d_2)\sin\theta\cos\theta & d_1 \sin^2\theta + d_2 \cos^2\theta \end{bmatrix} \begin{bmatrix} 1 \\ \\ 0 \end{bmatrix}
$$

$$
= \begin{bmatrix} d_1 \cos^2\theta + d_2 \sin^2\theta \\ \\ (d_1 - d_2)\sin\theta\cos\theta \end{bmatrix} . \tag{61}
$$

The copolarized receiving antenna responds to the horizontally polarized wave. This horizontal component of the wave can be extracted by inspection. Because the phasor voltage output of the copolarized antenna is proportional to the horizontal wave component,

$$
\overline{V}_{co} \propto d_1 \cos^2\theta + d_2 \sin^2\theta \tag{62}
$$

and the phase is

$$\phi_{co} = \text{Phase}\{\overline{V}_{co}\} = \text{Phase}\{d_1 \cos^2 \theta + d_2 \sin^2 \theta\}$$
$$= \text{Phase}\{d_1 \cot^2 \theta + d_2\} \quad . \tag{63}$$

The voltage at the output port of the crosspolarized antenna is proportional to the vertical component of the wave

$$\overline{V}_x \propto (d_1 - d_2)\sin \theta \cos \theta \quad . \tag{64}$$

Therefore the phase of the crosspolarized wave is

$$\phi_x = \text{Phase}\{\overline{V}_x\} = \text{Phase}\{(d_1 - d_2)\sin \theta \cos \theta\}$$
$$= \text{Phase}\{d_1 - d_2\} \quad . \tag{65}$$

The crosspolarized phase is by definition

$$\Delta = \phi_x - \phi_{co}$$
$$= \text{Phase}\{d_1 - d_2\} - \text{Phase}\{d_1 \cot^2 \theta + d_2\} \quad . \tag{66}$$

This is remarkably similar to the expression for a circularly polarized wave in (43) and (52).

If a vertically polarized wave were transmitted the wave incident upon the medium is

$$\vec{E}^i = \begin{bmatrix} E_x^i \\ \\ E_y^i \end{bmatrix} \propto \begin{bmatrix} 0 \\ \\ 1 \end{bmatrix} . \tag{67}$$

Multiplication of this by the transmission matrix and reduction to the copolarized and crosspolarized signal phases yields

$$\Delta = \text{Phase}\{d_1 - d_2\} - \text{Phase}\{d_1 \tan^2 \theta + d_2\} \quad . \tag{68}$$

This is an expected result because rotating the transmitted wave polarization by 90° is equivalent to a change in θ of 90° in the opposite direction. Replacing θ in (66) with $\theta \pm 90°$ gives (68). This concept may be extended and any linear polarization can be accounted for by defining the proper $\theta \pm \psi$.

These expressions may be further simplified:

$$\Delta = \text{Phase}\{d_1 - d_2\} - \text{Phase}\{d_1 \cot^2 \theta + d_2\}$$

$$= \text{Phase} \left\{ \frac{d_1 - d_2}{d_1 \cot^2 \theta + d_2} \right\}$$

$$= \text{Phase} \left\{ \frac{(d_{1/d_2}) - 1}{(d_{1/d_2})\cot^2 \theta + 1} \right\} \quad . \tag{69}$$

Using (55),

$$\frac{d_1}{d_2} = e^{-(\alpha + j\beta)L} \quad ,$$

and substituting this into (69) yields

$$\Delta = \text{Phase} \left\{ \frac{e^{-(\alpha + j\beta)L} - 1}{e^{-(\alpha + j\beta)L} \cot^2 \theta + 1} \right\}$$

$$= \text{Phase} \left\{ \frac{(e^{-\alpha L} \cos \beta L - 1) - j\, e^{-\alpha L} \sin \beta L}{(e^{-\alpha L} \cot^2 \theta \cos \beta L + 1) - j\, e^{-\alpha L} \cot^2 \theta \sin \beta L} \right\} \quad . \tag{70}$$

Multiplying the numerator and denominator by the complex conjugate of the denominator, then suppressing the resultant real denominator

gives

$$\Delta = \text{Phase}\{[(e^{-\alpha L} \cos \beta L - 1) - j \, e^{-\alpha L} \sin \beta L]$$
$$\times [e^{-\alpha L} \cot^2 \theta \cos \beta L + 1) + j \, e^{-\alpha L} \cot^2 \theta \sin \beta L]\}$$

$$\Delta = \text{Phase}\{[(e^{-\alpha L} \cos \beta L - 1)(e^{-\alpha L} \cot^2 \theta \cos \beta L + 1)$$
$$+ (e^{-\alpha L} \sin \beta L)(e^{-\alpha L} \cot^2 \theta \sin \beta L)]$$
$$+ j[(e^{-\alpha L} \cos \beta L - 1)(e^{-\alpha L} \cot^2 \theta \sin \beta L)$$
$$- (e^{-\alpha L} \sin \beta L)(e^{-\alpha L} \cot^2 \theta \cos \beta L + 1)]\}$$

$$\Delta = \text{Phase}\{[e^{-2\alpha L} \cot^2 \theta \cos^2 \beta L - e^{-\alpha L} \cot^2 \theta \cos \beta L$$
$$+ e^{-\alpha L} \cos \beta L - 1 + e^{-2\alpha L} \cot^2 \theta \sin^2 \beta L]$$
$$+ j[e^{-\alpha L} \sin \beta L(e^{-\alpha L} \cot^2 \theta \cos \beta L - \cot^2 \theta - e^{-\alpha L} \cot^2 \theta \cos \beta L - 1)]\}$$

$$\Delta = \text{Phase}\{[e^{-2\alpha L} \cot^2 \theta + e^{-\alpha L} \cos \beta L(1 - \cot^2 \theta) - 1]$$
$$+ j[e^{-\alpha L} \sin \beta L(-\cot^2 \theta - 1)]\}$$

$$\Delta = \tan^{-1} \left\{ \frac{-e^{-\alpha L} \sin \beta L(1 + \cot^2 \theta)}{e^{-2\alpha L} \cot^2 \theta + e^{-\alpha L} \cos \beta L(1 - \cot^2 \theta) - 1} \right\} \; . \tag{71}$$

where

θ = canting angle

α = differential attenuation   nepers/km

β = differential phase per km

L = path length   km .

As in the case of circular polarization this equation is a compact expression relating crosspolarized phase directly to the properties of the medium. This equation lends itself very well to computer programming and predictions based on this equation are

presented in section 2.5.

The crosspolarized phase for a linearly polarized incident wave does not exhibit the direct canting angle dependence noted with circular polarization. Although it is not directly apparent from an inspection of the equations, the crosspolarized phase for linearly polarized waves is only slightly affected by θ. This is a strong point in favor of using linear polarization rather than circular when a cancellation system is considered. The θ dependence of phase for both linear polarization and circular polarization will be discussed and illustrated in detail in section 2.5 and in Chapter 4.

2.3 Characteristics of the Crosspolarized Phase

An intermediate result in the derivation of the Δ equations is of significance for both circular polarization and linear polarization. This result, which is in identical form for both polarizations, is

$$\Delta' = \text{Phase}\{d_1 - d_2\} - \text{Phase}\{d_1 + d_2\} \tag{72}$$

For circular polarization, and for linear polarization

$$\Delta = \text{Phase}\{d_1 - d_2\} - \text{Phase}\{d_1 \cot^2 \theta + d_2\} \ . \tag{73}$$

It is recalled that d_1 and d_2 represent the propagation of waves polarized along the major axis and minor axis of the rain-drops, respectively.

$$d_1 = e^{-(\alpha_1 + j\,\beta_1)L}$$

$$d_2 = e^{-(\alpha_2 + j\,\beta_2)L} \qquad . \tag{74}$$

From this consideration

$$|d_1| < |d_2| \tag{75}$$

and

$$\text{angle}\{d_1\} < \text{angle}\{d_2\} \qquad . \tag{76}$$

The quantities d_1 and d_2, being complex numbers, can be represented as phasors or vectors, as indicated in Figure 2-4. Both $\vec{d_1}$ and $\vec{d_2}$ are drawn below the horizontal axis because of the negative sign on the exponent.

The sum and difference vectors are also included in Figure 2-4. The angle between the sum and difference vectors is Δ, the cross-polarized phase.

Decreasing rain rate causes a corresponding decrease in attenuation and phase delay. This is illustrated in the sequence of Figures 2-5a, b, and c. The sum vector always lies between $\vec{d_1}$ and $\vec{d_2}$ and as rain rate approaches zero this vector falls nearly on the horizontal axis. The sum vector represents the copolarized signal phase and the angle of this vector is insignificant at low rain rates.

The difference vector represents the phase of the crosspolarized signal. This vector is very sensitive to $\vec{d_1}$ and $\vec{d_2}$ and its angle
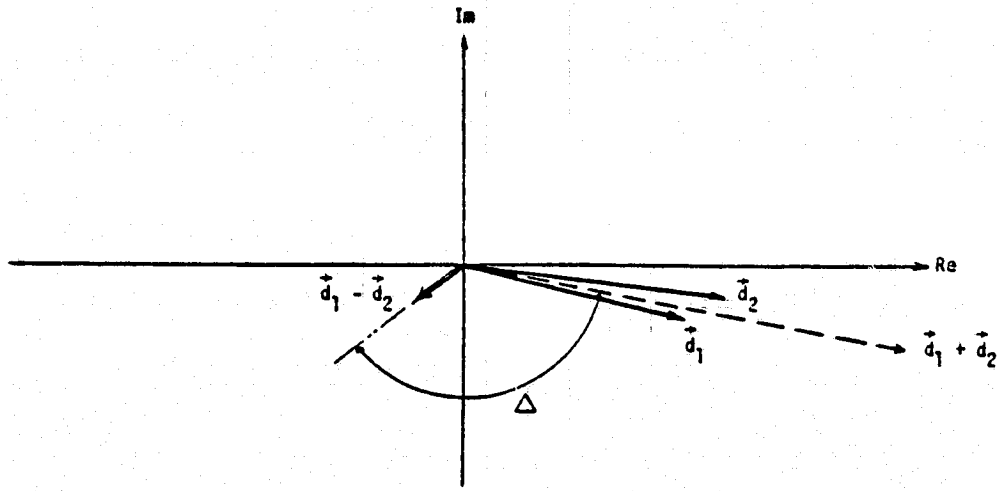
Figure 2-4. Vectors representing the phase of
the copolarized signal and the
phase of the crosspolarized signal.
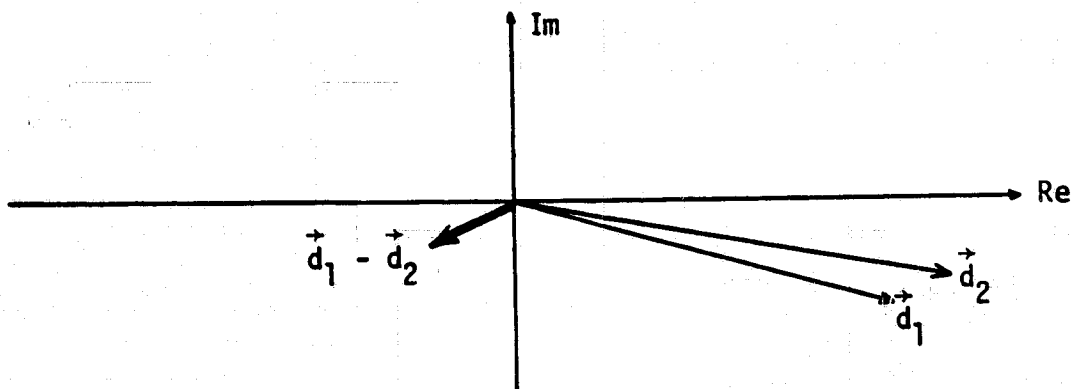
Figure 2-5a. Rainrate = x.
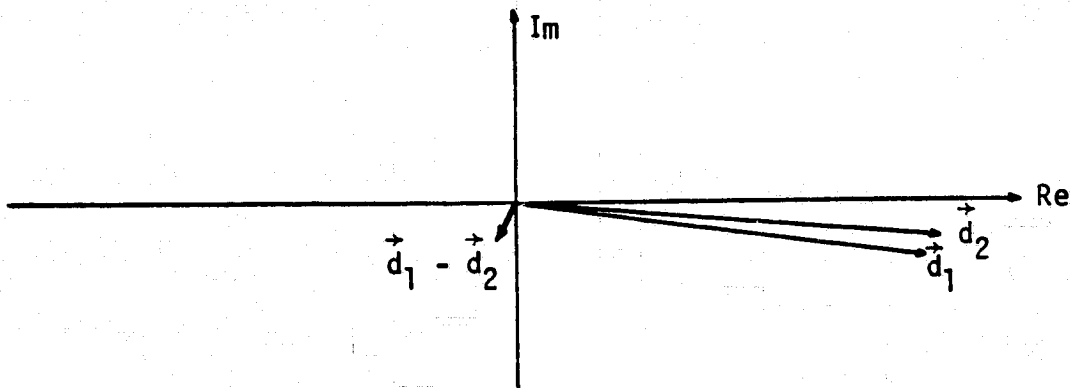
Figure 2-5b. Rainrate = y < x.
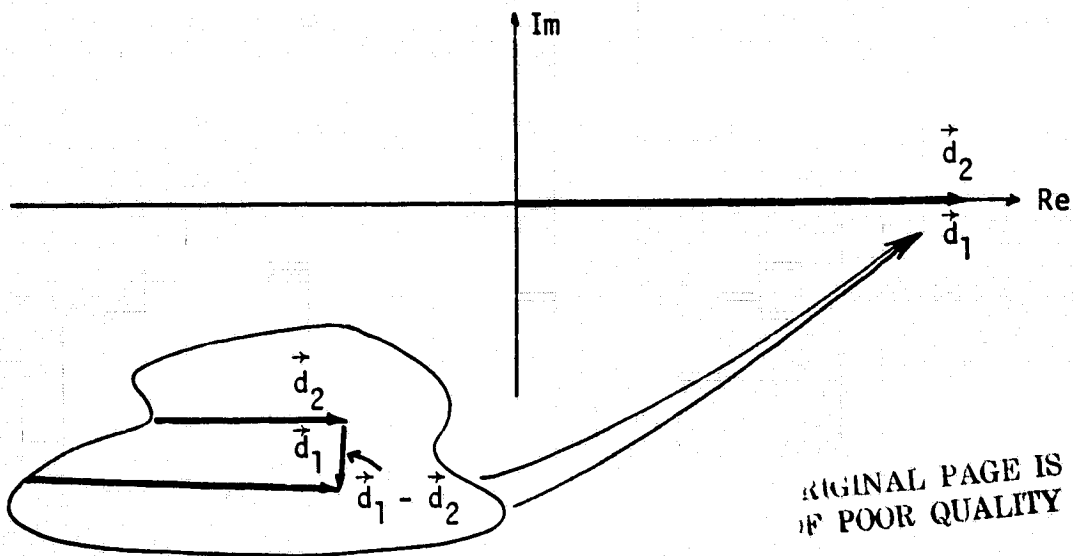
Figure 2-5c. Rainrate = 0^+.

Figure 2-5. Variation of phase angles as a function of rainrate.

can vary widely. Since the angle of the sum vector is negligible at low rain rates

$$\Delta \simeq \text{Phase}\{d_1 - d_2\} \quad . \tag{77}$$

The angle of this difference vector approaches -90° in the limit of zero rain rate as illustrated in the inset of Figure 2-5c. A mathematical analysis of the limit of crosspolarized phase is presented in Appendix 2. McEwan has shown that the phase associated with ice depolarization is ±90° [7]. Ice depolarization is characterized by the lack of both significant attenuation and thus differential attenuation. This corresponds to vectors $\vec{d}_1$ and $\vec{d}_2$ being of equal length, a case which results in a -90° crosspolarized phase. The +90° result is explained by other factors [7].

It is obvious by an inspection of Figure 2-5 (in reverse sequence) that with increasing rain rate the difference vector can rotate only in the negative direction since $|d_1| < |d_2|$. The sum vector also rotates in the negative direction but through a smaller angle than the difference vector. This indicates that the cross-polarized phase must retard with increasing rain rate.

Of course the -90° limit of crosspolarized phase neglects the 2θ term for circular polarization. Any other constant term that might appear in a practical system has been neglected also.

2.4 Phase Predictions

The equations for crosspolarized phase are

$$\Delta = \pm 2\theta + \tan^{-1} \{\frac{-2e^{-\alpha L} \sin \beta L}{e^{-2\alpha L} - 1}\} \qquad (78)$$

for circular polarization, and

$$\Delta = \tan^{-1} \{\frac{-e^{-\alpha L} \sin \beta L(1 + \cot^2 \theta)}{e^{-2\alpha L} \cot^2 \theta + e^{-\alpha L} \cos \beta L(1 - \cot^2 \theta) - 1}\} \qquad (79)$$

for linear polarization. The usefulness of these equations is that changes in the crosspolarized phase Δ can be directly related to the medium properties. In order to use these equations functions relating α and β to a parameter such as rain rate are needed.

Raindrop scattering functions S_1 and S_2 have been computed by Morrison and Cross [8]. The 1 and 2 subscripts indicate orthogonal directions along the axes of a raindrop. By summing the scattered waves from all raindrops in a medium one kilometer thick and using a Laws and Parsons [9] drop size distribution the attenuations α_1 and α_2 and the phase delays β_1 and β_2 may be determined [4]. These results are presented by T. S. Chu in tabular form for rain rates from 0 to 150 mm/hr and for frequencies up to 30 GHz [5]. Chu's tabulated values were used to compute differential attenuation and differential phase according to

$$\alpha = (\alpha_1 - \alpha_2)\cos^2 \gamma$$

and $\hspace{10cm}$ (80)

$$\beta = (\beta_1 - \beta_2)\cos^2 \gamma$$

where

γ = elevation angle to the satellite.

$$= \begin{cases} 33° \text{ CTS (11.7 GHz)} \\ 44° \text{ COMSTAR D-2 (28.56 GHz)} . \end{cases}$$

Polynomial regressions on these points yield equations of differential attenuation and differential phase as functions of rain rate. Plots of the two equations for 11 GHz are shown in Figures 2-6 and 2-7.

When using perfect antennas the reciprocal of the crosspolarization ratio (CPR) is equal to the isolation between the copolarized channel and the crosspolarized channel. Simple relations for CPR as a function of α and β [10] are used to determine isolation,

$$I = 20 \log_{10} \left\{ \frac{\left|1 + e^{-(\alpha + j\beta)L}\right|}{\left|1 - e^{-(\alpha + j\beta)L}\right|} \right\} \quad dB \qquad (81)$$

for circular polarization and

$$I = 20 \log_{10} \left\{ \frac{\left| 1 + e^{-(\alpha + j\beta)L} \tan^2 \theta \right|}{\left|(1 - e^{-(\alpha + j\beta)L}) \tan \theta\right|} \right\} \quad dB \qquad (82)$$

for linear polarization.

These equations, the Δ phase equations, curve fits to differential attenuation and differential phase, and curve fits to effective path length at 11.7 GHz and 28.56 GHz were integrated into a computer routine to provide theoretical phase versus isolation curves. Before presenting these predictions, a consideration of the path length is in order.
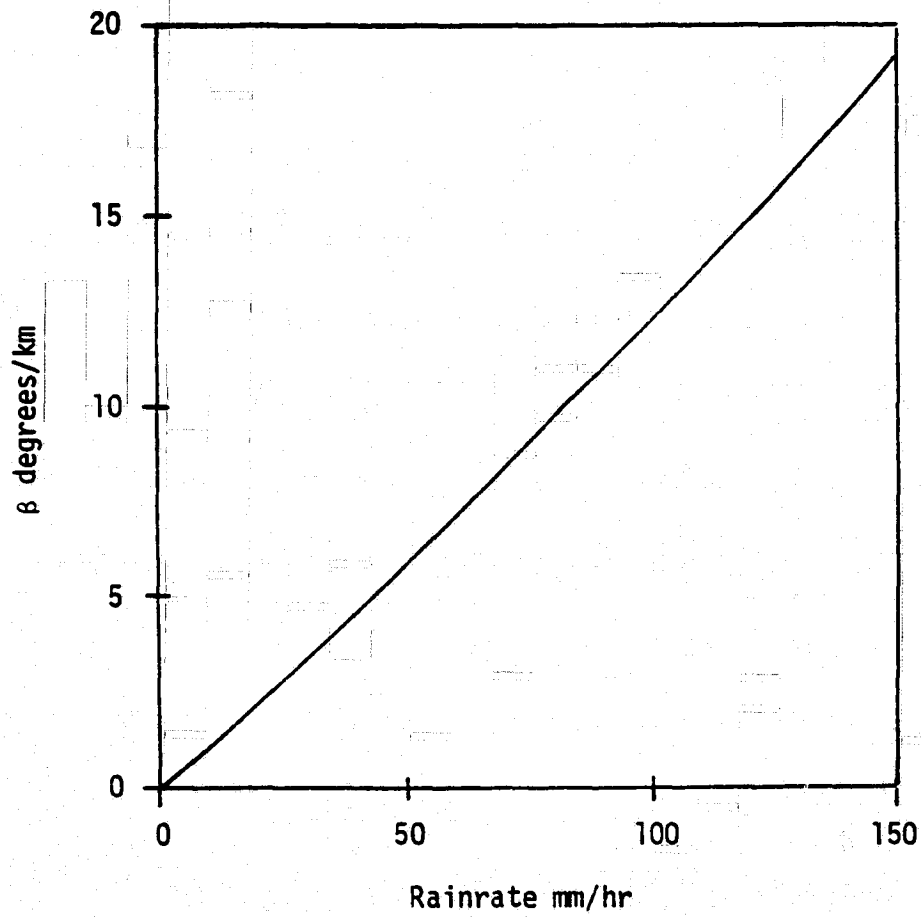
Figure 2-6. Differential phase of a 1 km thick rain medium at 11 GHz.
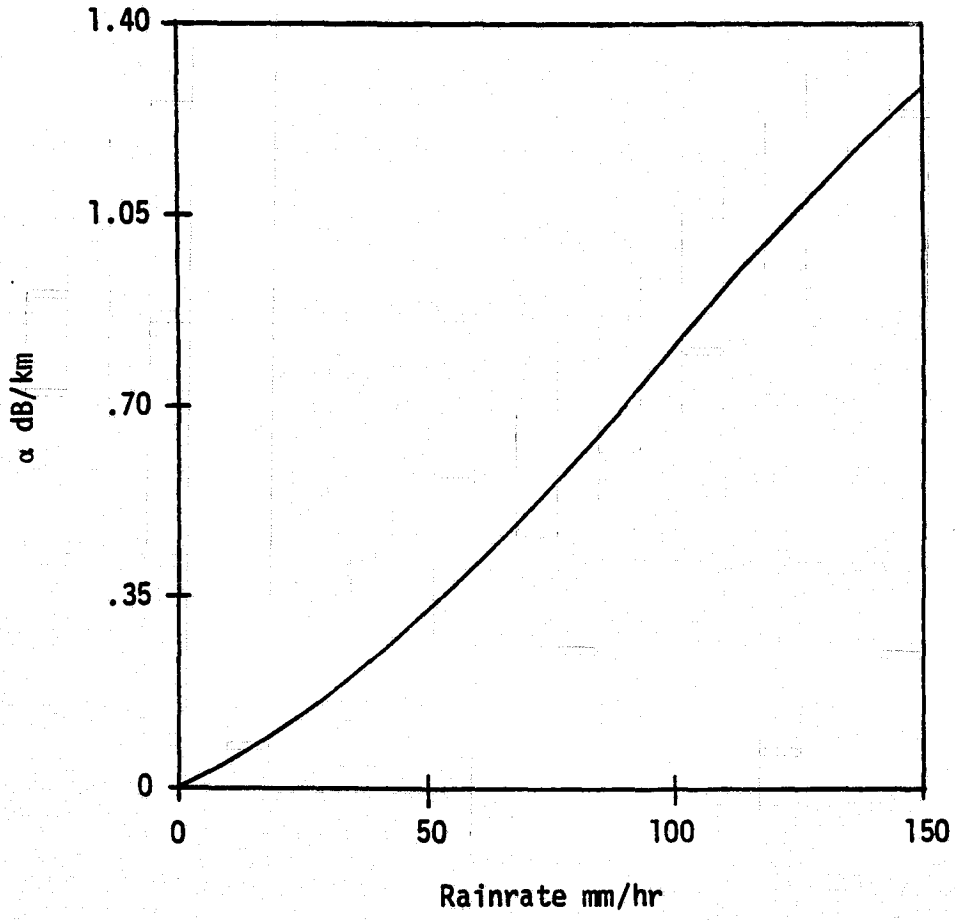
Figure 2-7. Differential attenuation of a 1 km thick rain medium at 11 GHz.

The effective path lengths used in the predictions in this thesis were derived from measured attenuation statistics at 11.7 GHz and 28.56 GHz. Measurements were made over a three month period at the VPI&SU satellite tracking station. Theoretical attenuation values needed to compute effective path length were provided by the VPI&SU Rain Propagation Prediction Model [11].

Computations using the Δ phase equations have shown phase to be very insensitive to path length. This is reasonable, for as illustrated in Figure 2-8 the phase of the crosspolarized signal is primarily dependent on the raindrop scattering functions. All copolarized waves add in phase at the receiver as do all crosspolarized waves. The relative phase between the two waves at the receiver is essentially the same as the relative phase when they leave the raindrop. In the case of linear polarization and a very long path the differential phase of the medium (in some cases) causes the copolarized wave and the crosspolarized wave to experience slightly different delays. Linear polarization at lower frequencies is subject to this differential phase effect more severely than at higher frequencies. This will be illustrated in the phase predictions to be presented in the next section.

2.5 Theoretical Curves

Isolation versus phase curves are presented on polar coordinate axes because phase is an angular variable. Polar axes are established with the high values of isolation (corresponding to low rain rates or
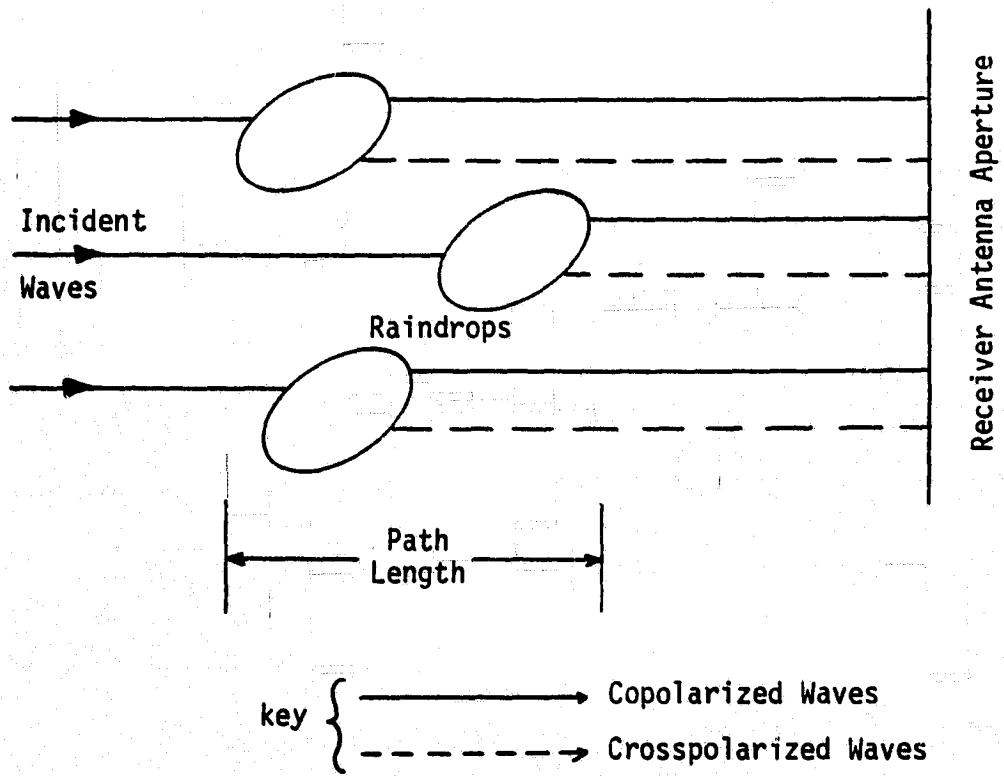
Figure 2-8. Independence of relative phase
upon path length.

clear weather) at the origin. Propagation through rain causes a reduction in isolation which means moving radially outward in the polar coordinate system. Phase variations which occur at low values of isolation appear to be magnified in comparison to the same change at high values of isolation. This is because the transformation from rectangular to polar coordinates is nonlinear. The effect is desirable because the phase variations at low values of isolation are important both in propagation research and to the operation of a cancellation system.

The predictions to follow are based on perfect antennas. Imperfect antennas introduce errors in both isolation and phase, but these errors are small for low values of isolation (again those values of importance). More will be said about antenna effects in the next section.

Figure 2-9 is the polar representation of crosspolarized phase for an 11 GHz circularly polarized wave with a constant canting angle $\theta = 0°$. It should be noted that the limit of phase for high values of isolation (zero rain rate) is near -90° and that the phase retards with decreasing isolation (increasing rain rate). Of course, a practical receiving system will introduce a constant phase value in addition to the variable phase shown in Figure 2-9. As an example, this constant phase value can be introduced by the separate front end amplifiers of a dual-polarized receiver. The constant term can be simulated in the polar plot by simply rotating the plot about its origin.
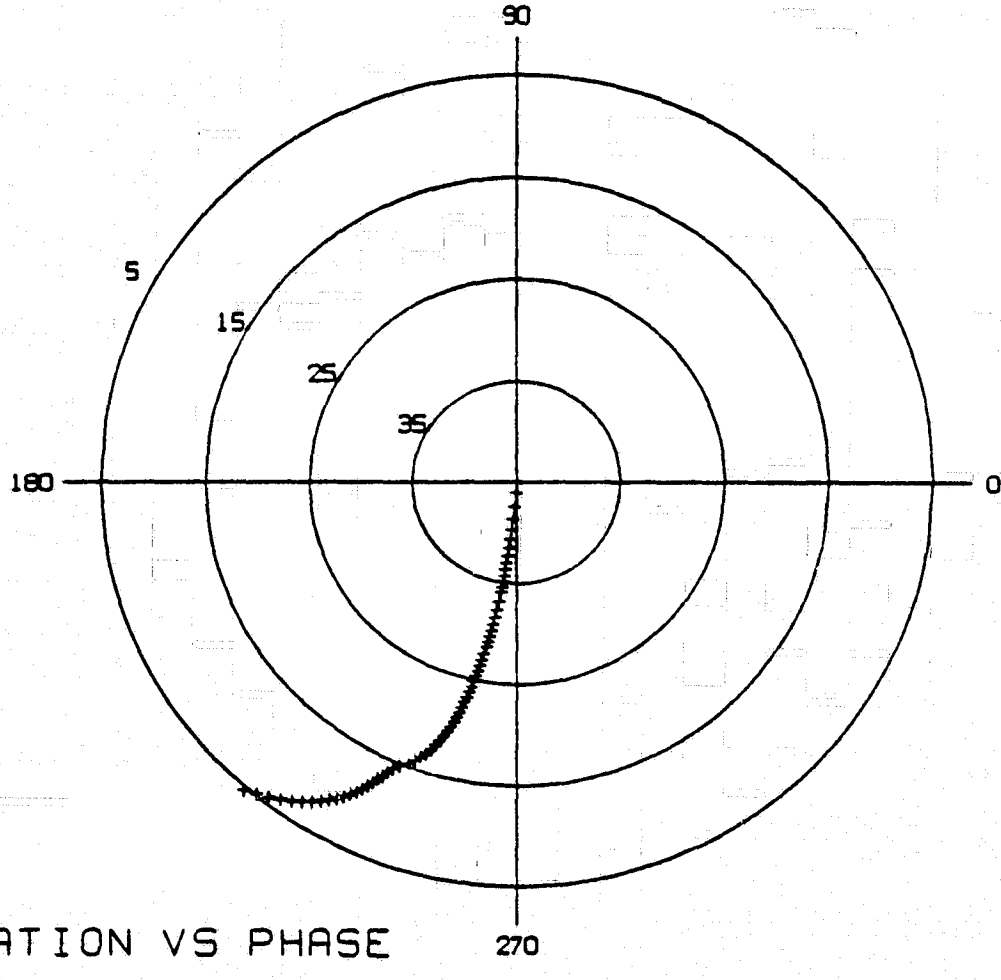
ISOLATION VS PHASE

Figure 2-9. Predicted phase for 11 GHz circular polarization, canting angle $\theta = 0°$.

Figure 2-9 shows isolation decreasing to 5 dB. A more realistic situation is illustrated in Figure 2-10 which assumes the same conditions as before except that isolation is restricted to the range of 35 dB to 15 dB. This range is more typical of measured values seen at the VPI&SU satellite tracking station.

Figure 2-11 illustrates the effect of changes in the canting angle upon a circularly polarized wave. It is seen from (58) that 2θ is a term in the phase expression derived for circular polarization. The figure shows two curves, one for a 0° canting angle and the other for a 20° canting angle. This places bounds on the crosspolarized phase which are separated by 40°. The phase behavior within the bounds depends upon how the canting angle changes. There is evidence that the canting angle can change by as much as 20° either by canting angle oscillations [12] or by an absolute change in the mean canting angle [13].

Figures 2-12 and 2-13 illustrate phase versus isolation predictions for an 11 GHz linearly polarized wave. These plots show phase for a variety of canting angles. For canting angles near 45° the magnitude and direction of phase change are essentially the same as in the case of the crosspolarized phase of a circularly polarized wave. It is immediately obvious, though, that with linear polariza- tion the canting angle variation has very small effect in comparison to its effect upon a circularly polarized wave. Note that Figure 2-12 shows canting angles over a range of 60°. This range translates to a 120° phase variation when considering circular

ISOLATION VS PHASE
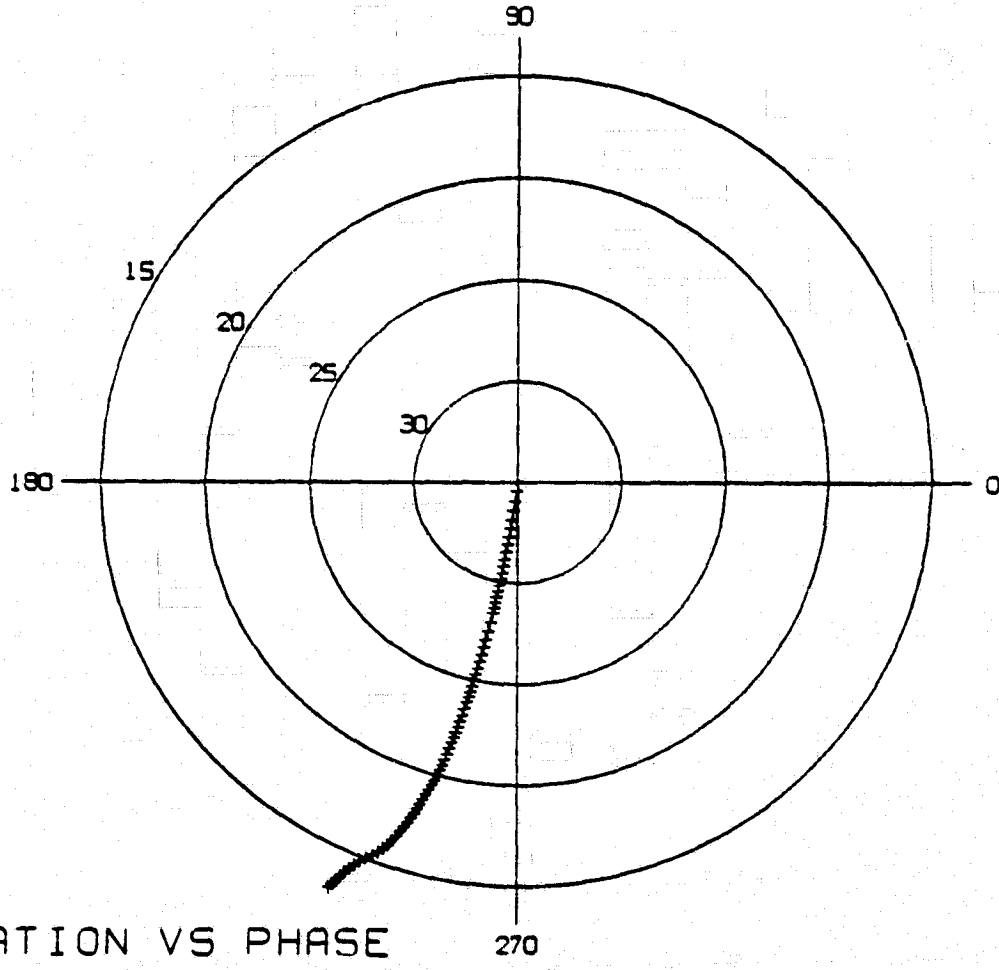
Figure 2-10. Predicted phase for 11 GHz circular
polarization, canting angle θ = 0°.

ISOLATION VS PHASE
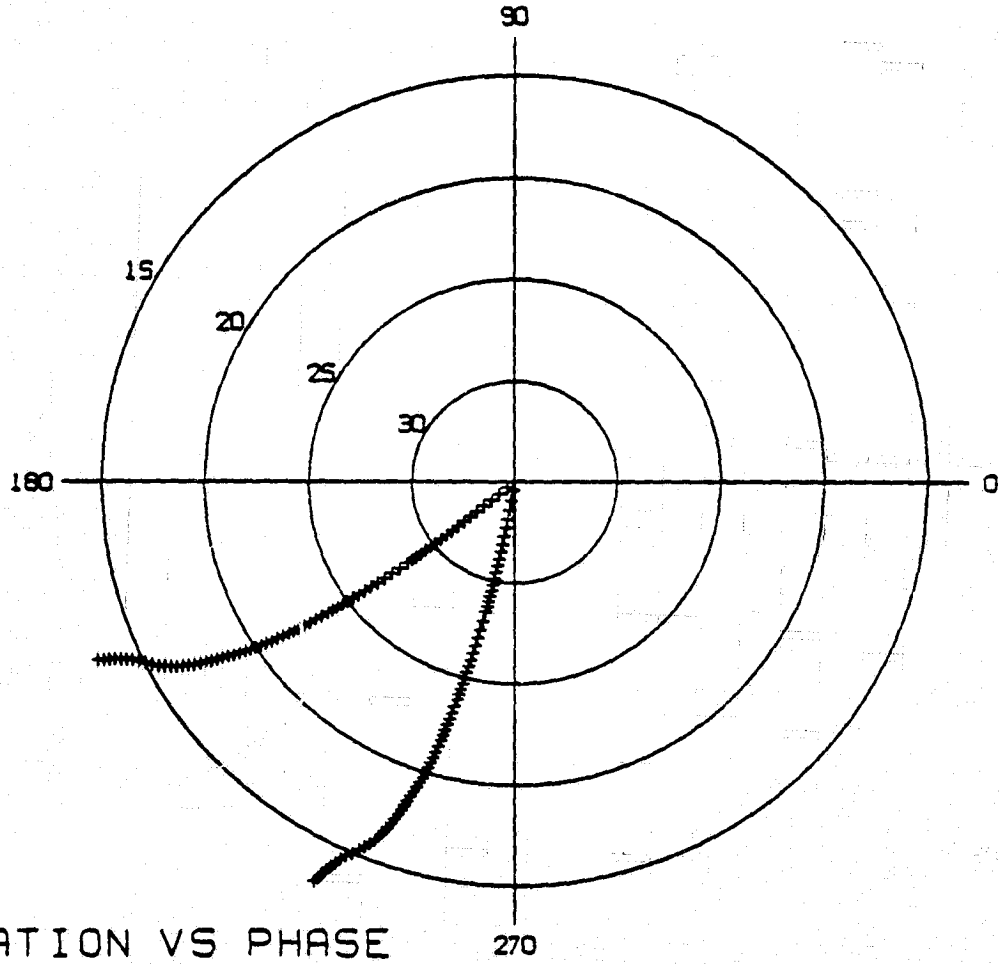
Figure 2-11.   Predicted phase for 11 GHz circular
polarization showing the effect of a
20° canting angle change.
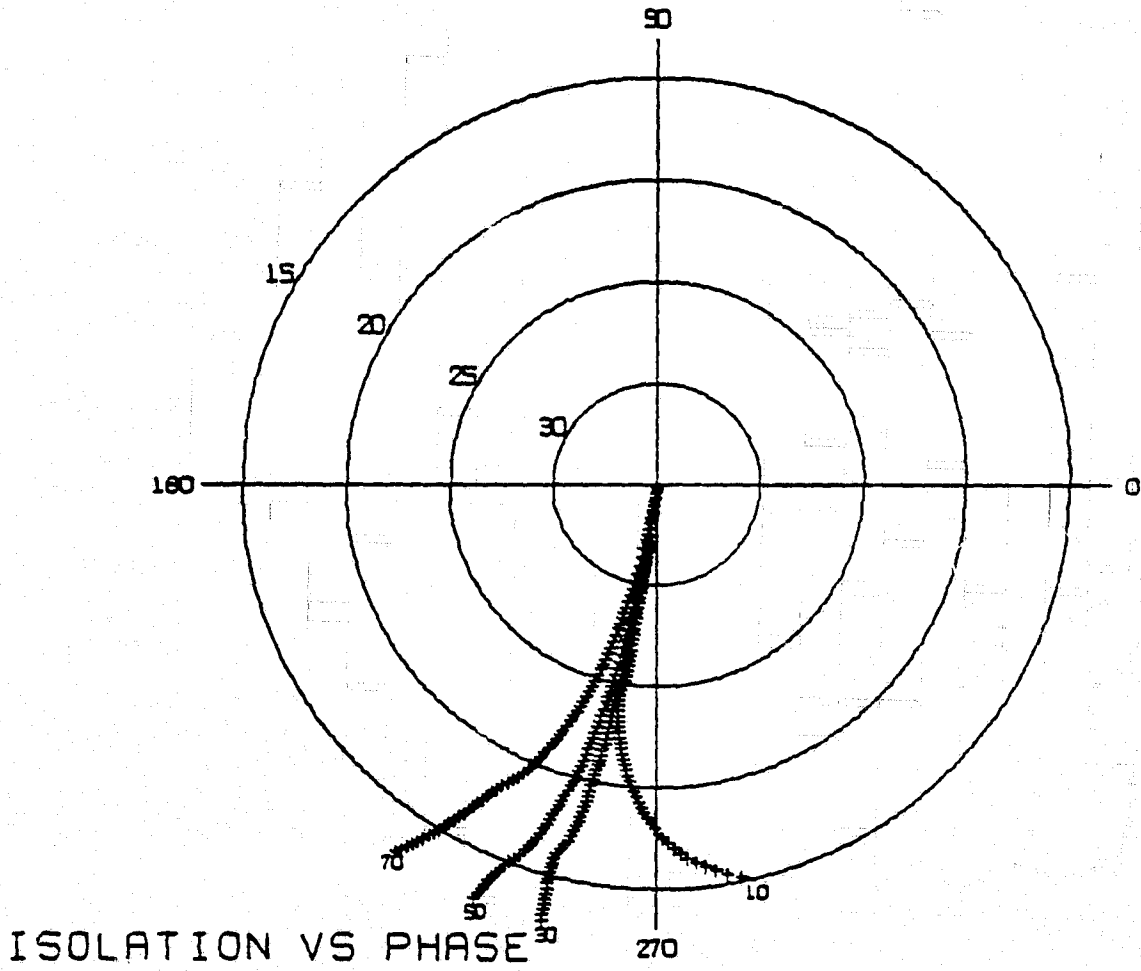
Figure 2-12.   Predicted phase for 11 GHz linear
polarization, canting angle
θ = 10°, 30°, 50°, and 70°.

ISOLATION VS PHASE
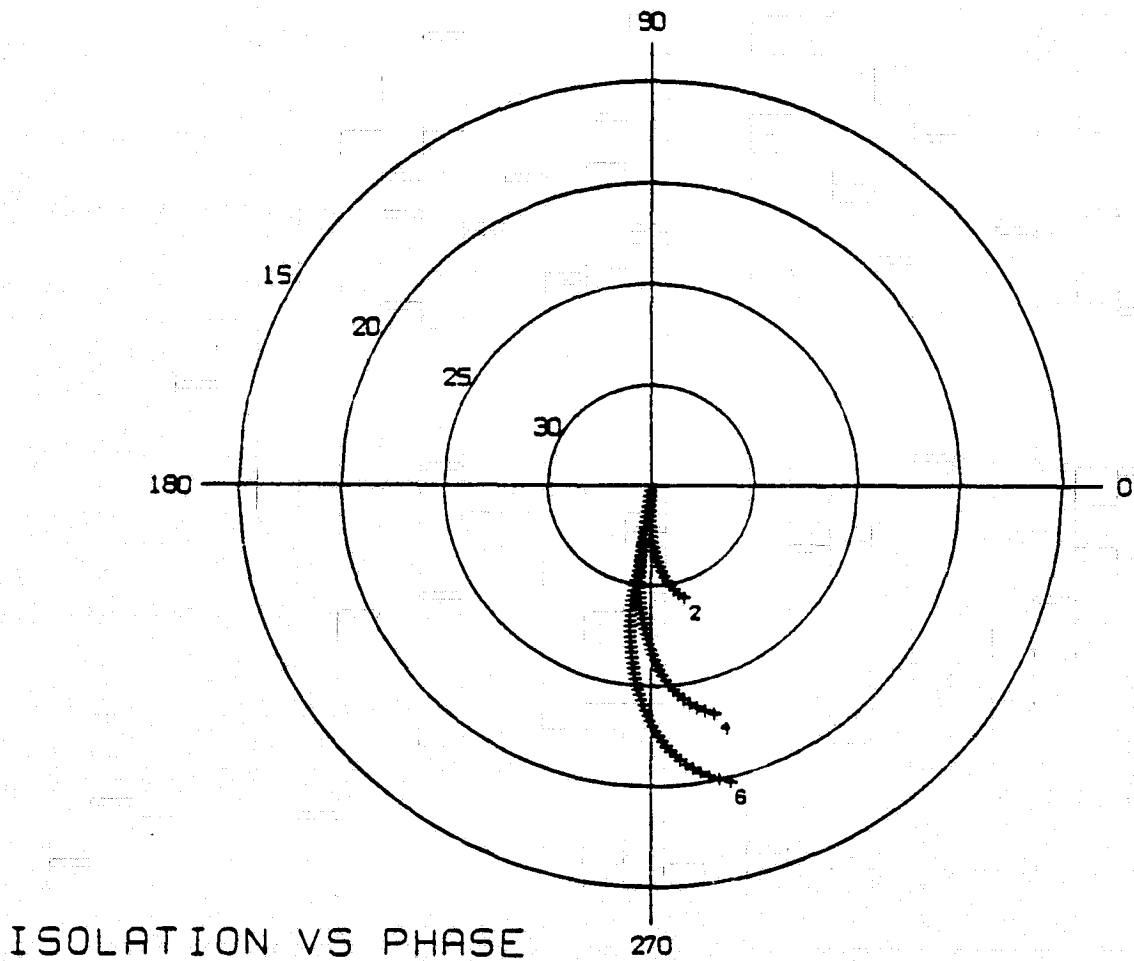
Figure 2-13. Predicted phase for 11 GHz linear
polarization, canting angle
θ = 2°, 4°, and 6°.

polarization.

These linear polarization predictions assume a horizontally polarized wave. The canting angle as defined here is actually the angle between the major axis of the raindrop and the polarization direction. This fact can be used to obtain predictions for waves polarized other than horizontally.

The unusual behavior of the phase at small canting angles can be explained by considering the properties of the medium. Recall that the crosspolarized phase starts at -90° and retards with increasing rain rate. This is the case in Figures 2-12 and 2-13 but at higher rain rates some curves diverge and begin to advance in phase. This is because of the differential phase of the medium. The differential phase causes the horizontal wave component to be delayed more than the vertical component. For small angles θ the horizontal component is approximately the copolarized wave and the situation exists where the copolarized wave is retarding faster than the crosspolarized wave. This is equivalent to an advance in the relative phase. In other words, for small θ and high rain rate the differential phase of the medium dominates the phase of the rain-induced crosspolarized wave. This condition requires the effects of the differential phase of the medium to be relatively large compared to the effects of the differential attenuation. This is the case at frequencies below approximately 15 GHz. The phase predictions for 28 GHz do not show this behavior.

Figures 2-14 and 2-15 show crosspolarized phase versus isolation

ISOLATION VS PHASE
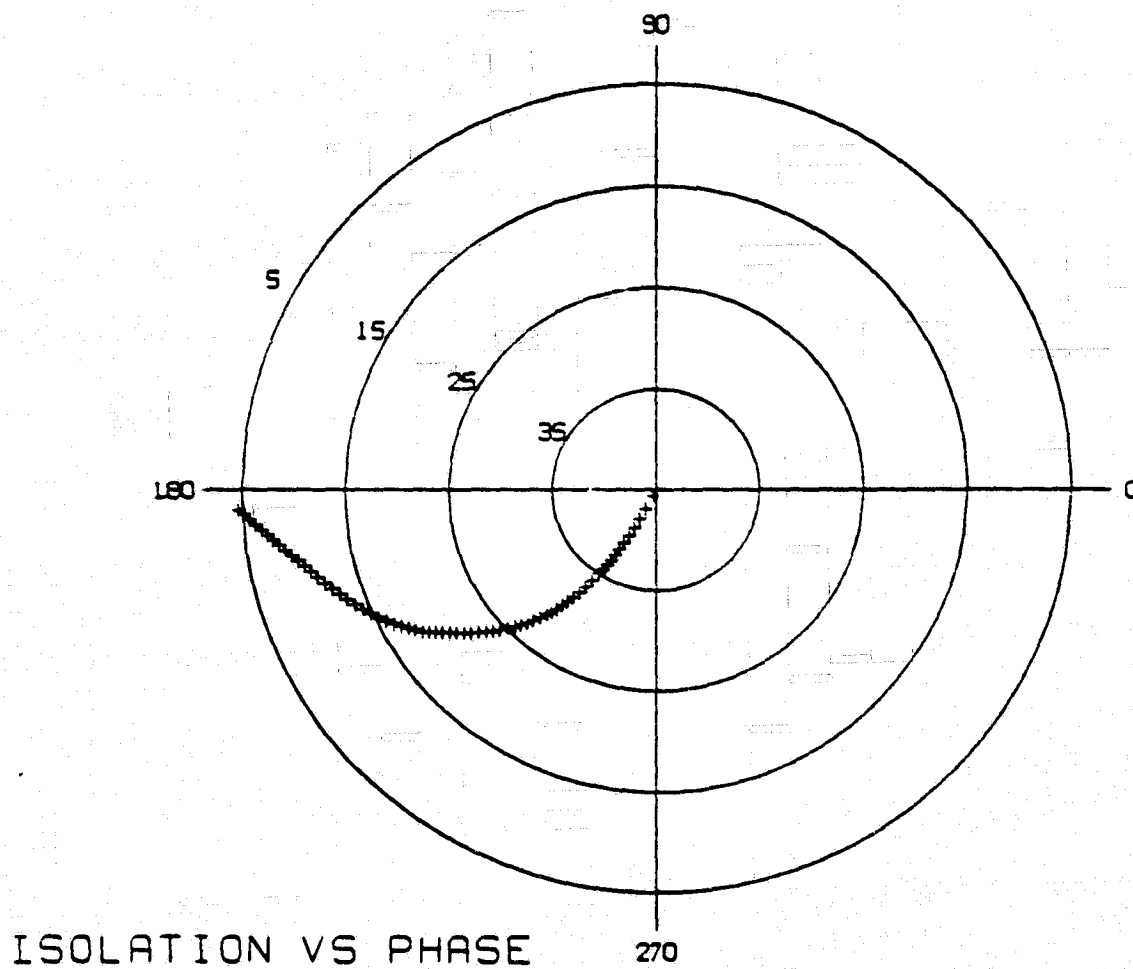
Figure 2-14. Predicted phase for 28 GHz circular
polarization, canting angle θ = 0°.

ISOLATION VS PHASE
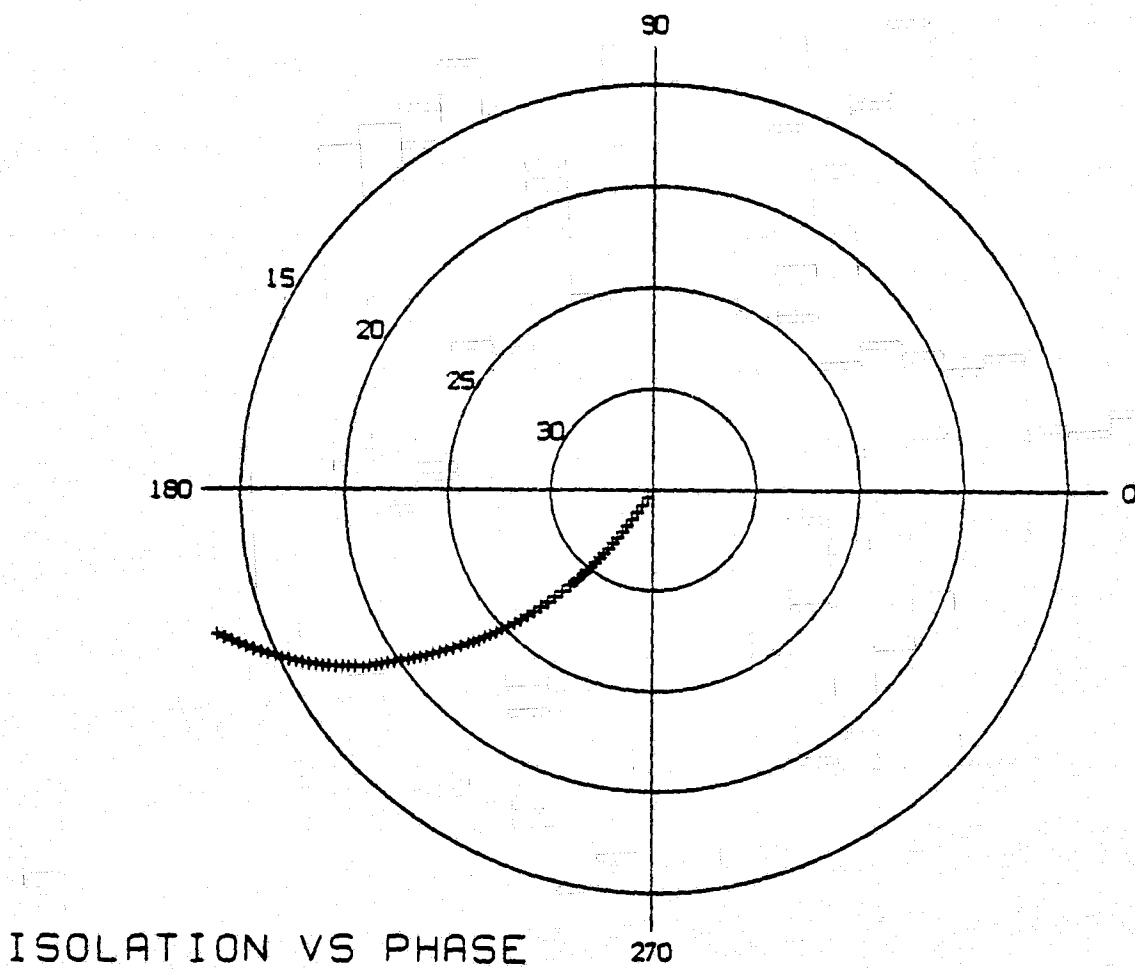
Figure 2-15.   Predicted phase for 28 GHz circular
              polarization, canting angle θ = 0°.

for 28 GHz circular polarization. A larger absolute phase change occurs at 28 GHz than at 11 GHz but a comparison of Figure 2-14 (28 GHz) and Figure 2-9 (11 GHz) shows that most of this change occurs at high isolations corresponding to very low rain rates. Differential phase values at 28 GHz and 11 GHz differ by a factor of approximately two. Differential attenuation values (measured in dB) at 28 GHz and 11 GHz differ by a factor of about three except at very low rain rates where the 28 GHz differential attenuation is almost an order of magnitude larger than the differential attenuation at 11 GHz. This relatively large differential attenuation at low rain rates for a frequency of 28 GHz causes the initial large crosspolarized phase change.

Figures 2-16 and 2-17 illustrate crosspolarized phase for 28 GHz linear polarization. These curves exhibit the same initial phase jump at low rain rates. As with 11 GHz linear polarization, canting angle variations have little effect on the crosspolarized phase. Note that the phase advance seen in the 11 GHz linear polarization curves does not appear in the 28 GHz curves. This is because of the smaller differential phase of the medium at higher frequencies.

2.6 Ground Station Antenna Effects

All of the mathematics and discussions up to this point have assumed perfect antennas for both transmitting and receiving. This section will examine the errors that may have been introduced by this
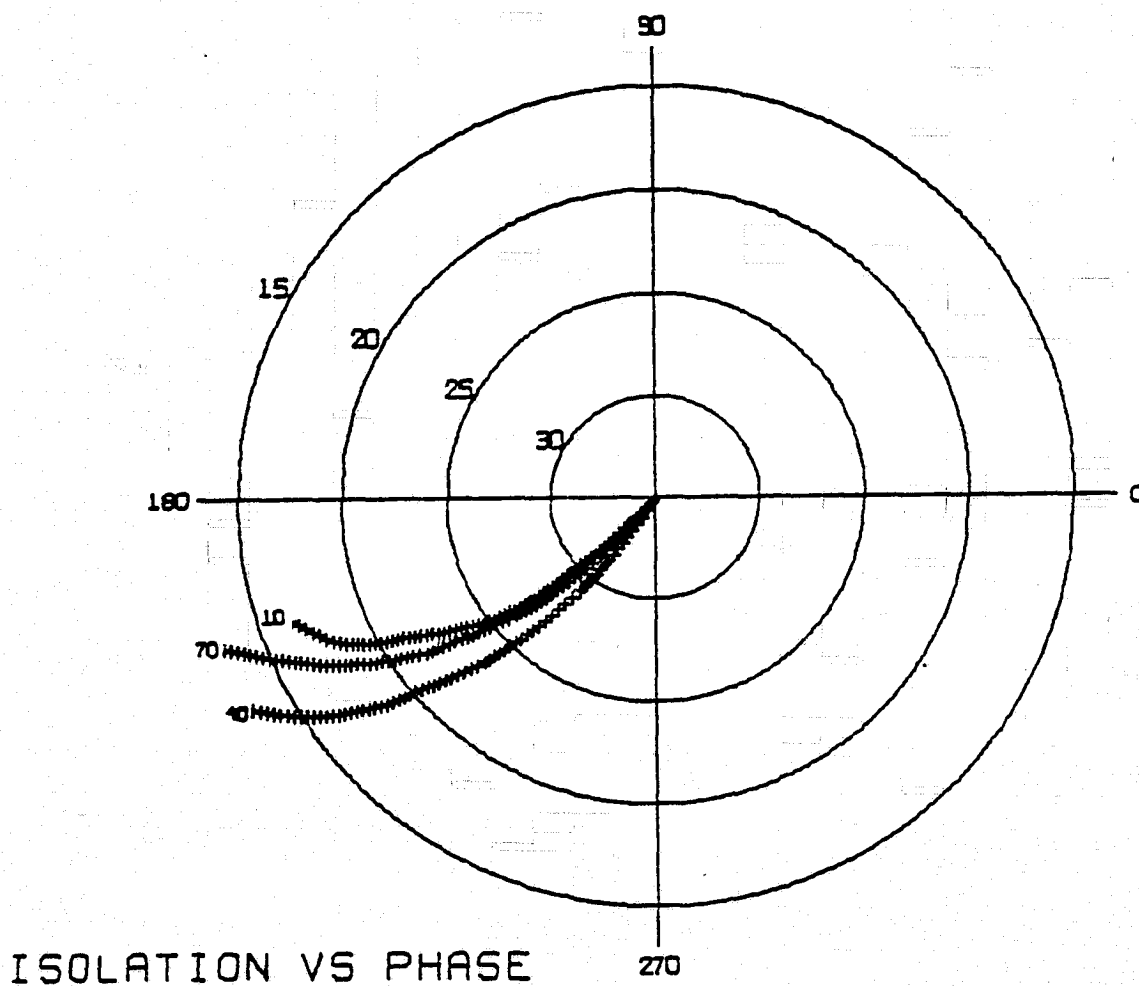
ISOLATION VS PHASE

Figure 2-16. Predicted phase for 28 GHz linear
polarization, canting angle
$\theta = 10°$, $40°$, and $70°$. Note that
the curves cross each other and
that at lcw isolations the $70°$
curve lies between the ones for
$10°$ and $40°$.

ISOLATION VS PHASE
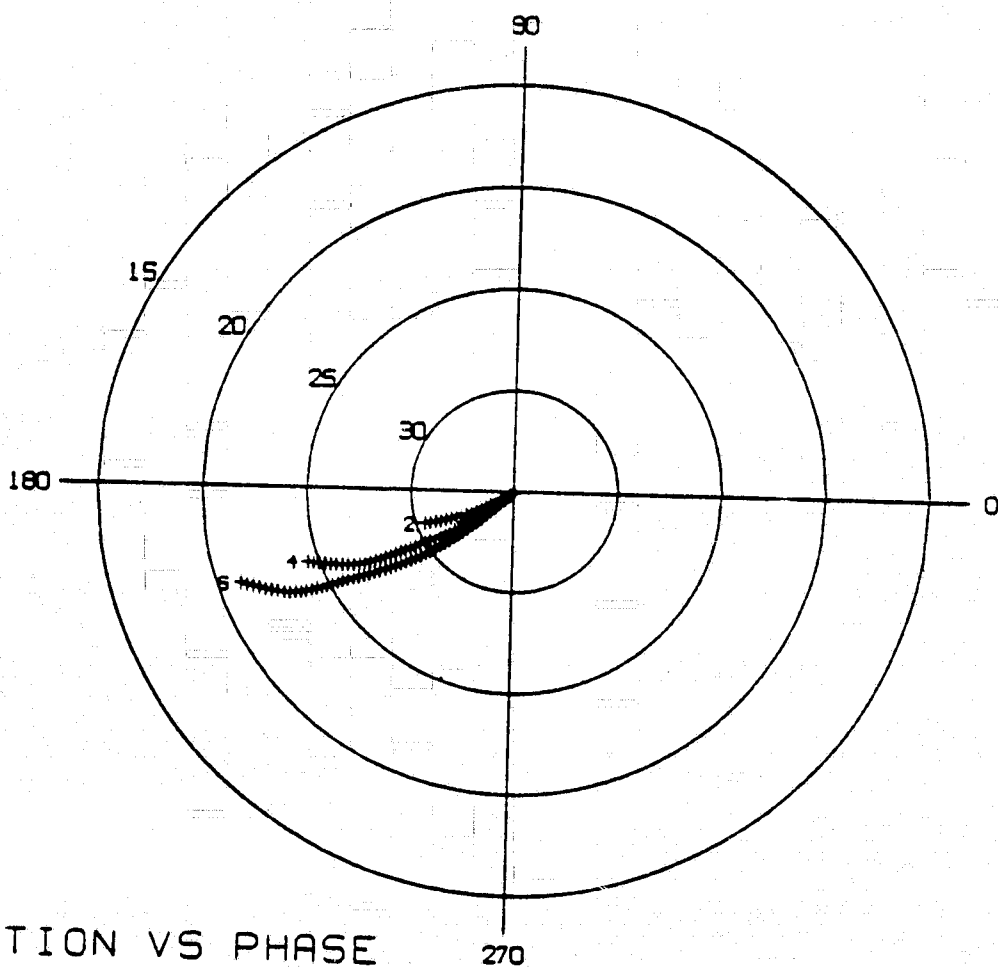
Figure 2-17.   Predicted phase for 28 GHz linear
polarization, canting angle
$\theta = 2°$, $4°$, and $6°$.

assumption.

Given a real antenna, what is the maximum deviation in phase from the predictions based on perfect antennas? Consider for now the case of circular polarization. The transmitted wave is assumed to be RHCP and the depolarized wave leaving a rain-filled medium is RHEP (right-hand elliptically polarized). This wave can be considered to be composed of a RHCP wave and a LHCP wave. The crosspolarization ratio (CPR) of the wave is defined as the ratio of these two components.

$$CPR_W(dB) = 20 \ \log_{10} \frac{|E_{LHCP}|}{|E_{RHCP}|} \qquad (83)$$

where

$|E_{RHCP}|$ = magnitude of the RHCP wave (assumed to be the copolarized wave)

$|E_{LHCP}|$ = magnitude of the LHCP wave .

Therefore if

$$|E_{RHCP}| = A$$

then $\qquad (84)$

$$|E_{LHCP}| = 10^{CPR_W(dB)/20} A .$$

An imperfect antenna may be considered to be an array composed of two elements. One element is a perfect RHCP antenna and the other is a perfect LHCP antenna. The relative magnitude of the

response of these two elements to equal amplitude RHCP and LHCP waves respectively is the CPR of the antenna.

$$CPR_A = \frac{|e_{LHCP}|}{|e_{RHCP}|} \tag{85}$$

where e_{LHCP} and e_{RHCP} represent the antenna responses. The CPR is related to the axial ratio of the antenna by [14]

$$CPR_A = \frac{|AR_A| - 1}{|AR_A| + 1} \quad . \tag{86}$$

The antenna parameter ε is also related to the axial ratio by

$$\varepsilon = \cot^{-1} AR_A \quad . \tag{87}$$

From these equations the relative contribution of the component elements is

$$\frac{|e_{LHCP}|}{|e_{RHCP}|} = \frac{|AR_A| - 1}{|AR_A| + 1} = \frac{|\cot \varepsilon| - 1}{|\cot \varepsilon| + 1} \quad . \tag{88}$$

The antenna has been assumed to be RHEP (i.e. the copolarized antenna, dominantly RHCP). Therefore if

$$|e_{RHCP}^{co}| = B$$

then

$$|e_{LHCP}^{co}| = \frac{|\cot \varepsilon_{co}| - 1}{|\cot \varepsilon_{co}| + 1} B \quad . \tag{89}$$

The voltage output from the imperfect antenna is the phasor sum of the response of the copolarized antenna RHCP element to the RHCP component of the wave and the response of the copolarized antenna

LHCP element to the LHCP component wave. The output of the RHCP element is proportional to

$$|E_{RHCP}||e_{RHCP}^{CO}| = AB \tag{90}$$

and the output of the LHCP element is proportional to

$$|E_{LHCP}||e_{LHCP}^{CO}| = (10^{CPR_W(dB)/20})(\frac{|\cot \epsilon_{co}| - 1}{|\cot \epsilon_{co}| + 1})AB \quad . \tag{91}$$

For a CPR_W of -20 dB and a copolarized antenna ϵ of 40° ($|AR_A| \approx 1.5$ dB) this latter output is less than 1% of the former output and is considered negligible.

The crosspolarized antenna is more severely affected by imperfections. An imperfect crosspolarized antenna may respond to the strong copolarized wave with an output comparable in magnitude to its response to the weaker crosspolarized wave.

Again the relative response of the antenna to equal magnitude RHCP and LHCP waves is related to the antenna parameters by

$$\frac{|e_{RHCP}^{X}|}{|e_{LHCP}^{X}|} = \frac{|AR_x| - 1}{|AR_x| + 1} = \frac{|\cot \epsilon_x| - 1}{|\cot \epsilon_x| + 1} \tag{92}$$

where $|e_{LHCP}^{X}|$ is now the larger quantity. Therefore if

$$|e_{LHCP}^{X}| = C$$

then

$$|e_{RHCP}^{X}| = \frac{|\cot \epsilon_x| - 1}{|\cot \epsilon_x| + 1} C \quad . \tag{93}$$

The output voltage from the crosspolarized antenna LHCP element is proportional to

$$|E_{LHCP}||e^x_{LHCP}| = 10^{CPR_W(dB)/20} AC \qquad (94)$$

which is the desired response of the antenna. The output of the RHCP element is proportional to

$$|E_{RHCP}||e^x_{RHCP}| = \frac{|\cot \varepsilon_x| - 1}{|\cot \varepsilon_x| + 1} AC \quad . \qquad (95)$$

This quantity represents the error due to an imperfect antenna. The phasor addition of this to the desired response yields the antenna output. This is illustrated in Figure 2-18 where $\vec{D}$ is the desired response and $\vec{U}$ is the undesired response. The angles of the two phasors are arbitrary and the tip of $\vec{U}$ can lie anywhere on the circle with radius $|\vec{U}|$.

The maximum phase error is η as indicated in the figure. Therefore

$$\eta = \sin^{-1} |\vec{U}|/|\vec{D}|$$

$$= \sin^{-1} \left[\frac{\dfrac{|\cot \varepsilon_x| - 1}{|\cot \varepsilon_x| + 1} AC}{10^{CPR_W(dB)/20} AC} \right]$$

$$= \sin^{-1} \left[\frac{\dfrac{|\cot \varepsilon_x| - 1}{|\cot \varepsilon_x| + 1}}{10^{CPR_W(dB)/20}} \right] \quad . \qquad (96)$$

The angle ε of a perfect circularly polarized antenna is $\pm 45°$. Let ε_d represent the deviation from this perfect value; then
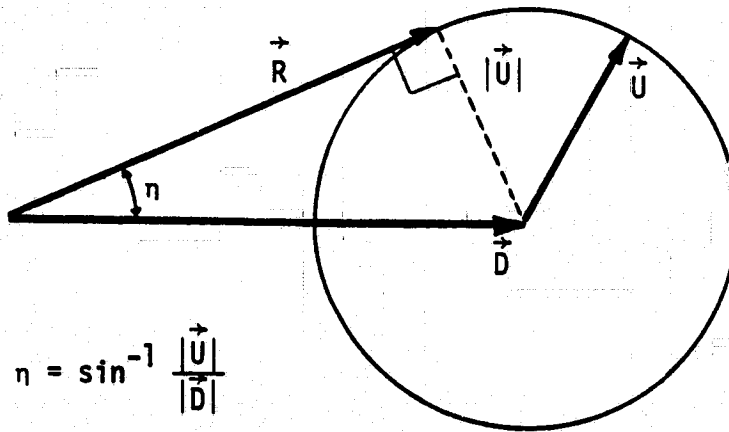
$$\eta = \sin^{-1} \frac{|\vec{U}|}{|\vec{D}|}$$

Figure 2-18. The phasor addition of desired and undesired antenna responses.

$$|\epsilon_x| = 45° - \epsilon_d \quad . \tag{97}$$

Using this, $\cot |\epsilon_x| = |\cot \epsilon_x|$ for $-45° \leq \epsilon_x \leq 45°$, and the trigono-metric identity

$$\cot(A - B) = \frac{\cot B \cot A + 1}{\cot B - \cot A} \tag{98}$$

a simplified equation results.

$$\eta = \sin^{-1} \{\frac{\tan \epsilon_d}{10^{CPR_W(dB)/20}}\} \quad . \tag{99}$$

A typical antenna with a CPR_A of 30 dB ($\epsilon \approx 43.2°$, $|AR_A| \approx$ 1.065 → .55 dB) receiving a wave with $CPR_W = -20$ dB can generate a maximum phase error of 18°.

Isolation is defined as the ratio of the <u>measured</u> copolarized signal magnitude to the measured crosspolarized signal magnitude. Figure 2-18 illustrates that the measured crosspolarized signal amplitude associated with the maximum phase error is

$$R = |\vec{D}| \cos \eta \quad , \quad \eta < 90° \quad , \tag{100}$$

thus large phase errors η are accompanied by an improvement in the isolation.

In the case of a perfect antenna isolation and CPR_W are related by

$$I = \frac{1}{CPR_W}$$

or

$$I(dB) = - CPR_W(dB) \quad . \tag{101}$$

The improvement in isolation is expressed as

$$I = -CPR_W - 20 \log_{10}(\cos \eta) \ dB \quad . \tag{102}$$

This improvement amounts to only 0.4 dB in the preceeding example.

The analysis of antenna phase errors for linear polarization proceeds in a similar fashion but now the polarization parameter of interest is γ rather than ε, where

$$\gamma = \tan^{-1} \frac{|E_V|}{|E_H|} \tag{103}$$

where

$|E_V|$ = magnitude of vertical wave component

$|E_H|$ = magnitude of horizontal wave component .

A horizontally polarized wave becomes an elliptically polarized wave upon propagation through a depolarizing medium. This elliptical wave can be decomposed into a horizontally polarized component and a vertically polarized component. Again CPR_W is defined as the ratio of these components,

$$CPR_W(dB) = 20 \log_{10} \frac{|E_V|}{|E_H|} \quad . \tag{104}$$

Therefore if

$$|E_H| = A$$

then

$$|E_V| = 10^{CPR_W(dB)/20} A \quad . \tag{105}$$

The imperfect copolarized (dominantly horizontal) antenna may be decomposed into a horizontally polarized element and a vertically polarized element. As was the case with circularly polarized waves and antennas the undesired output component from the copolarized antenna is negligible.

The imperfect crosspolarized antenna is also decomposed into a horizontally polarized element and a vertically polarized element. Figure 2-19 illustrates a possible polarization ellipse of the crosspolarized antenna. The quantities e_H and e_V are the responses of the component elements to equal magnitude horizontally polarized and vertically polarized waves respectively. It is seen that

$$\frac{|e_V|}{|e_H|} = \tan \gamma_x \quad . \tag{106}$$

Therefore the two components can be expressed as

$$|e_V| = C \qquad |e_H| = \cot \gamma_x C \quad . \tag{107}$$

The output voltage from the vertically polarized element is proportional to

$$|E_V||e_V| = 10^{CPR_W(dB)/20} AC \tag{108}$$

and the output of the horizontally polarized element is proportional to
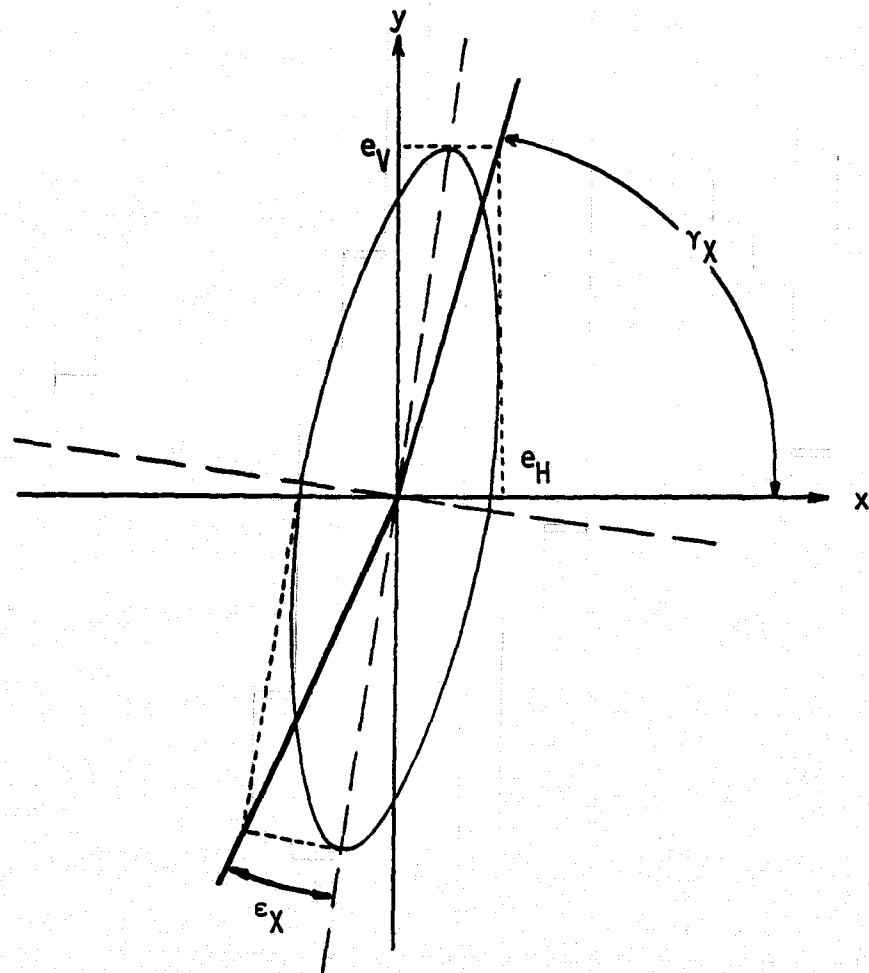
Figure 2-19. Possible polarization ellipse
of an imperfect linearly
polarized antenna.

$$|E_H||e_H| = \cot \gamma_x \; AC \quad . \tag{109}$$

The phasor sum of these voltages yields the true output from the imperfect crosspolarized antenna. The angle between the phasors is arbitrary therefore the worst case phase error is

$$\eta = \sin^{-1}\left[\frac{\cot \gamma_x}{10^{CPR_W(dB)/20}}\right] \quad . \tag{110}$$

A relatively good vertically polarized antenna will have a large axial ratio and a tilt angle very close to 90°. Referring to Figure 2-19 it can be seen that

$$\varepsilon_x \approx 90° - \gamma_x \tag{111}$$

and that as the tilt angle approaches 90° this approximation becomes an equality.

With relatively good antennas, the replacement of γ_x with 90° - ε_x is justified, and

$$\eta = \sin^{-1}\left[\frac{\tan \varepsilon_x}{10^{CPR_W(dB)/20}}\right] \quad . \tag{112}$$

A perfect linarly polarized antenna has $\varepsilon = 0°$ and its deviation from perfect is

$$\varepsilon_d = \varepsilon_x \quad , \tag{113}$$

therefore

$$\eta = \sin^{-1}\left[\frac{\tan \varepsilon_d}{10^{CPR_W(dB)/20}}\right] \quad . \tag{114}$$

This is identical to the results obtained with circularly polarized antennas.

Figures 2-20 and 2-21 are polar-plot representations of cross-polarized phase for 11 GHz circular polarization and 28 GHz linear polarization. Also included on these plots are maximum phase error bounds η for an antenna with $\varepsilon_x = 43.7°$ corresponding to an axial ratio of 1.047 or 0.4 dB. The CPR of this antenna is -33 dB. These values were chosen because they closely approximate the 11.7 GHz antenna at the VPI&SU tracking station.

The solid lines in Figures 2-20 and 2-21 represent calculated values of η. The broken portion of the line represents an approximation to the error. When the desired and undesired antenna responses become equal in magnitude the inverse sine equations, (99) and (114), become invalid and the crosspolarized phase error can be as much as 360°. The wave CPR at which this situation occurs is easily determined by solving for CPR with the argument of the inverse sine set equal to one. This value is approximately 33 dB and the broken line indicates a maximum phase error of 360° for isolations greater than 33 dB. This is a very conservative estimate because large phase errors such as this are accompanied with a substantial increase in isolation. The actual error bound will be smaller than that indicated.

The VPI&SU 11.7 GHz system uses a 12 foot diameter prime focus-fed parabolic reflector antenna. Manufacturer's measurements on this antenna include axial ratio on boresight and at the -10 dB
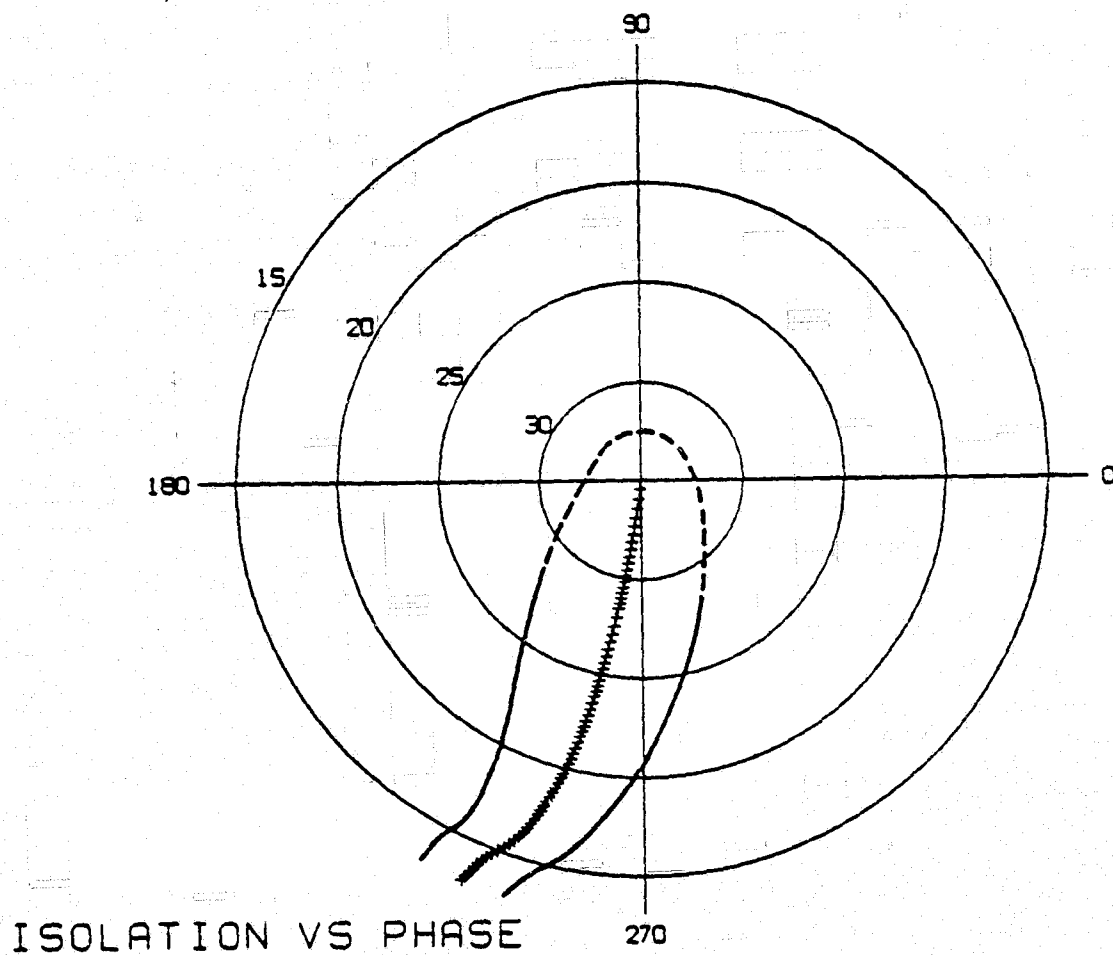
ISOLATION VS PHASE

Figure 2-20. Predicted phase for 11 GHz circular
polarization with maximum imperfect
antenna error bounds. The antenna
axial ratio is 0.4 dB.
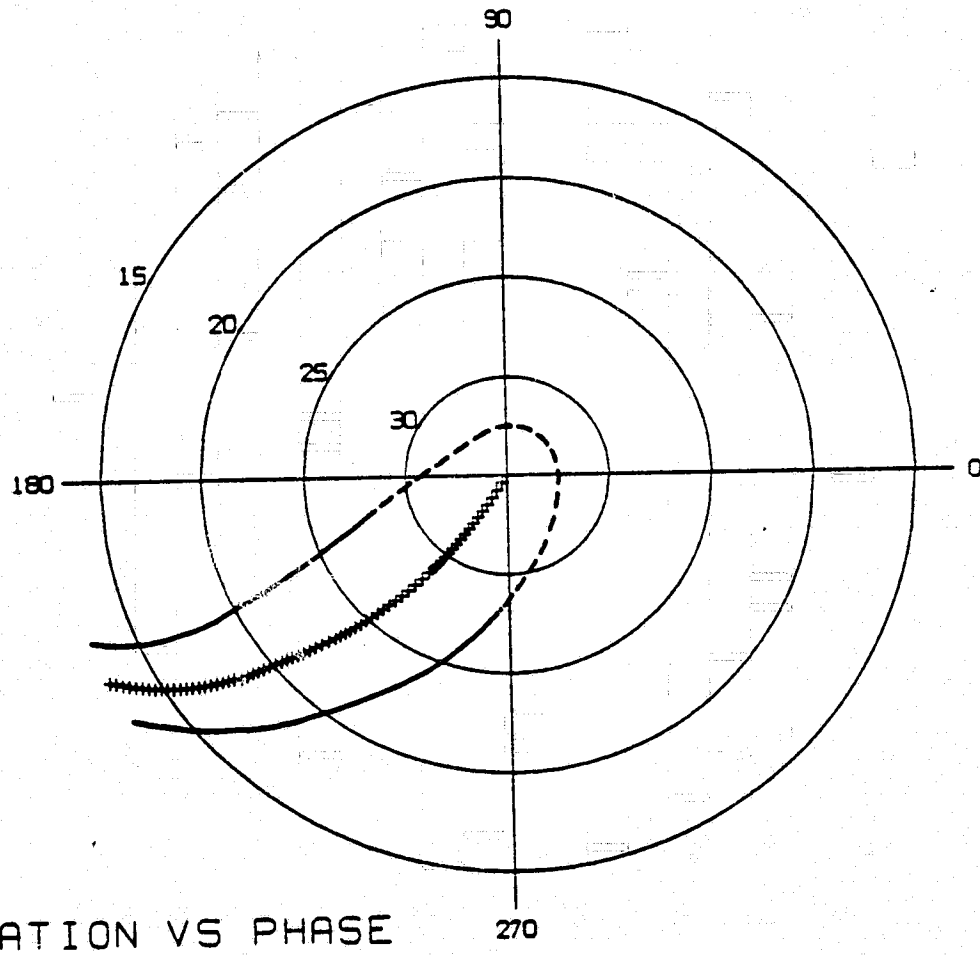
ISOLATION VS PHASE

Figure 2-21. Predicted phase for 28 GHz linear
polarization with maximum imperfect antenna
error bounds. The antenna CPR is -33 dB.

point. These values are tabulated in Table 2-1. It is noted that off axis pointing causes a rapid degradation of axial ratio which correspondingly increases the maximum phase error. The -10 dB point is approximately 0.5° from boresight.

Antenna pattern measurements are performed on the 11.7 GHz antenna by adjusting antenna pointing to scan the mainbeam across a satellite beacon. This scan is performed in both the elevation and azimuth planes while received signal amplitude and phase are recorded. The results of the phase measurements are plotted in Figure 2-22. Note that large phase variations occur off axis.

This particular exercise was performed during clear weather conditions when the system was operating with a high on-axis isolation. This corresponds to the area near the origin of Figure 2-20. Phase errors during a depolarizing event will be substantially less than those measured during clear weather. This discussion serves only to illustrate potential problems involved with antenna pointing.

2.7 Satellite Antenna Effects

The discussion in the previous section neglected the effects of an imperfect transmitting antenna. This approach is probably justified because in some cases much is known about the earth station antenna but little is known about the spacecraft antenna and, as will be seen, the effects of an imperfect transmitting antenna can act to cancel errors caused by an imperfect receiving antenna. This is a

Table 2-1. Axial ratio of VPI&SU 11.7 GHz
parabolic reflector antenna.

	On Axis	-10 dB Point
$|AR|$ (dB)	.27	2.0
ε degrees	44.11°	38.46°

LHCP 11.7 GHz
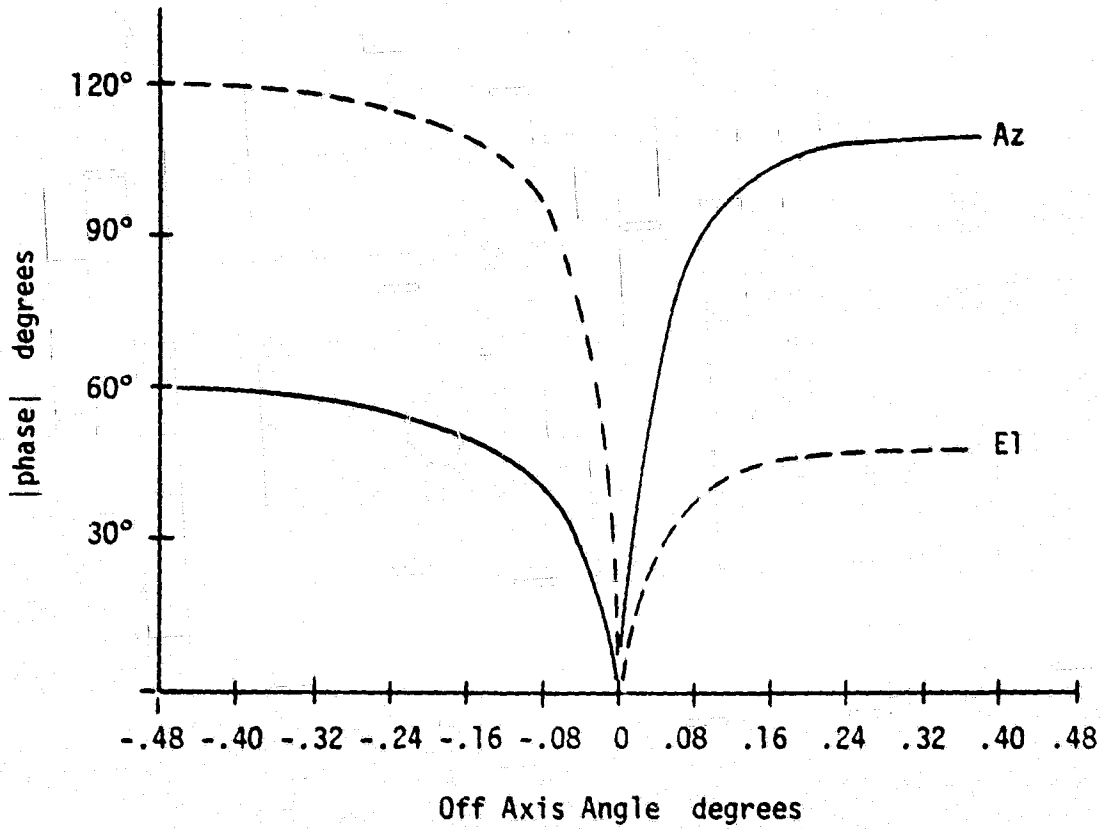
Figure 2-22. Clear weather phase measurement of the 11.7 GHz VPI&SU Earth Station antenna.

statement that two elliptically polarized antennas may be matched in polarization better than an elliptically polarized antenna and a circularly polarized antenna.

The spacecraft antenna polarization can be decomposed into two orthogonal elements, one desired and one undesired. The relative magnitude of these components is set by the antenna parameters ε and γ as in the previous discussion. The undesired transmitted wave is represented by a vector, $\vec{U}_2$, which is included in the vector diagram of the receive antenna output voltage along with the vectors $\vec{D}$ and $\vec{U}$. This is shown in Figure 2-23a.

For circular polarization a further simplification can be made. Most earth station antennas are operated such that their polarization tilt angle is aligned with the polarization tilt angle of the satellite antenna (i.e., the polarization tilt angle of the incoming wave in clear weather). If the crosspolarized receiving antenna is indeed orthogonal to the copolarized receiving antenna its tilt angle will be 90° from that of the satellite antenna.

When the copolarized wave is RHCP, the crosspolarized receiving antenna responds to the RHCP wave with a voltage $|\vec{U}|$ at an angle of, say, zero degrees. Define the tilt angle of the crosspolarized antenna as zero degrees. This sets the tilt angle of the satellite antenna to be ±90°. Therefore, the LHCP wave component leaving the satellite must be 180° out of phase with the RHCP transmitted wave. The crosspolarized antenna responds to this with a voltage $|\vec{U}_2|$ at an angle of 180°. Therefore, $\vec{U}_2$ is displaced from U by 180° and
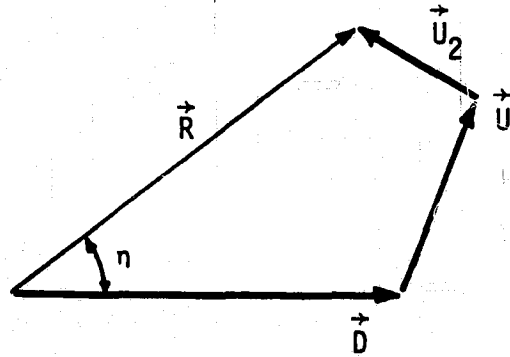
Figure 2-23a.   General case.
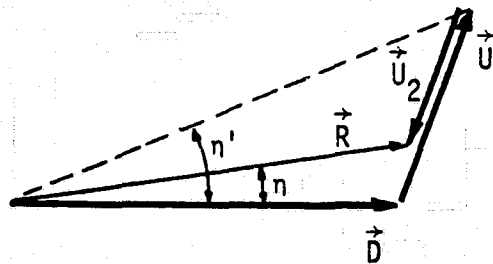
Figure 2-23b.   Transmit and receive antennas
with aligned tilt angles.

Figure 2-23.   The phasor addition of desired and
undesired antenna responses including
an imperfect transmitting antenna.

cancellation occurs. This is illustrated in Figure 2-23b where it is seen that η is substantially less than the phase error for perfect transmitting antennas (η' in Figure 2-23b).

The process of rotating the receiving antenna during clear weather for the maximum isolation is a procedure used to force the 180° difference in $\vec{U}$ and $\vec{U}_2$. The vector $\vec{D}$ does not exist in clear weather conditions therefore the mangitude of the resultant $\vec{U} + \vec{U}_2$ is inversely proportional to clear weather isolation.

This argument indicates that η used in plotting Figures 2-20 and 2-21 is larger than the error that will be seen in a practical system. Again this shows that Figures 2-20 and 2-21 illustrate the worst possible case.

The situation presented by linearly polarized systems is more difficult to visualize because the angle between $\vec{U}$ and $\vec{U}_2$ is determined by the δ's of the antennas rather than the physical tilt angles of the antennas. However, if the receive antennas are truely orthogonal the process of maximizing the clear weather isolation is equivalent to minimizing the resultant of $\vec{U}$ and $\vec{U}_2$, thus reducing phase errors.

CHAPTER 3

THE VPI&SU RECEIVING SYSTEMS

3.1 The Experiment

The VPI&SU satellite communications experiment is a research project within the Department of Electrical Engineering and is jointly funded by the National Aeronautics and Space Administration, the Defense Communications Agency, and the U. S. Army Research Office. The purpose of the project is (1) to collect rain attenuation, rain depolarization, and weather data, (2) to correlate these data with each other, (3) to produce statistics, and (4) to develop theoretical models to explain and predict weather-related propagation phenomena.

The satellite tracking station located adjacent to the Virginia Tech campus houses three dual-polarized receiving systems. The Communications Technology Satellite (CTS) circularly polarized beacon is received at 11.7 GHz and the Comstar D-2 linearly polarized beacons are received at 19.04 and 28.56 GHz. The diversity of frequencies and polarizations provides a unique opportunity for conducting milli-meter wave propagation research.

The three receivers, a variety of weather instruments, and a weather radar are interfaced with a Digital Equipment Corporation PDP-11/10 computer. The computer continuously monitors the status of the experiment, points the 11 GHz antenna, and records data from all devices.

An IBM 370/158 VM facility is available for processing the data

recorded by the experiment. A statistical software package is used to reduce data taken over long periods of time and a computer graphics package is provided for displaying data on a storm-by-storm basis. The graphics package is of particular interest because of its ability to display phase data for a given propagation event.

Of the three systems only the 19 GHz beacon is alternately switched between two polarization states. It was for this reason and because of the similarity of the 11.7 GHz and 28 GHz systems that a decision was made to present only 11.7 GHz and 28 GHz phase data in this thesis. A detailed description of the 11.7 and 28 GHz receiving system follows.

3.2 The Receivers

3.2.1 General Discussion

The 11.7 GHz receiver and the 28 GHz receiver are identical with the exception of a parametric amplifier in the crosspolarized channel of the 11.7 GHz system. A detailed discussion of the operation of only the 11.7 GHz system will be presented for this reason.

Considerable care has been taken in the design, analysis, and calibration of the receivers to insure the accuracy of the phase measurements. Of particular concern are nonlinear devices which can introduce a phase inversion. A phase inversion is characterized by an actual phase advance being translated into an apparent phase retardation. A phase inversion is equivalent to a sideband inversion

of the type which occurs when a signal frequency is subtracted from the local oscillator frequency by the action of a nonlinear mixer.

One situation responsible for a phase inversion is illustrated in Figure 3-1 where two mixers are shown. The input to the mixers is at frequency ω_s and at phase $+\phi$. Local oscillator frequencies ω_{lo} and ω_{hi} are selected such that $\omega_s - \omega_{lo}$ and $\omega_{hi} - \omega_s$ are both equal to the IF frequency. In mixer A the local oscillator frequency is subtracted from the signal frequency. Mathematically the mixer is a multiplier and its operation is expressed by

$$\sin(\omega_s t + \phi) \cos(\omega_{lo}t)$$
$$= \frac{1}{2}[\sin([\omega_s - \omega_{lo}]t + \phi) + \sin([\omega_s + \omega_{lo}]t + \phi)] \quad .$$

Filtering out the sum component yields the mixer output

$$\frac{1}{2} \sin([\omega_s - \omega_{lo}]t + \phi) \quad . \tag{115}$$

The function of mixer B is to subtract the signal frequency from the local oscillator frequency,

$$\sin(\omega_s t + \phi) \cos(\omega_{hi}t)$$
$$= -\frac{1}{2}[\sin([\omega_{hi} - \omega_s]t - \phi) - \sin([\omega_{hi} + \omega_s]t + \phi)]$$

which yields upon filtering

$$\frac{1}{2} \sin([\omega_{hi} - \omega_s]t - \phi) \quad . \tag{116}$$

The $-\phi$ and $-\omega_s$ in the case of mixer B represents the phase and side-band inversion.
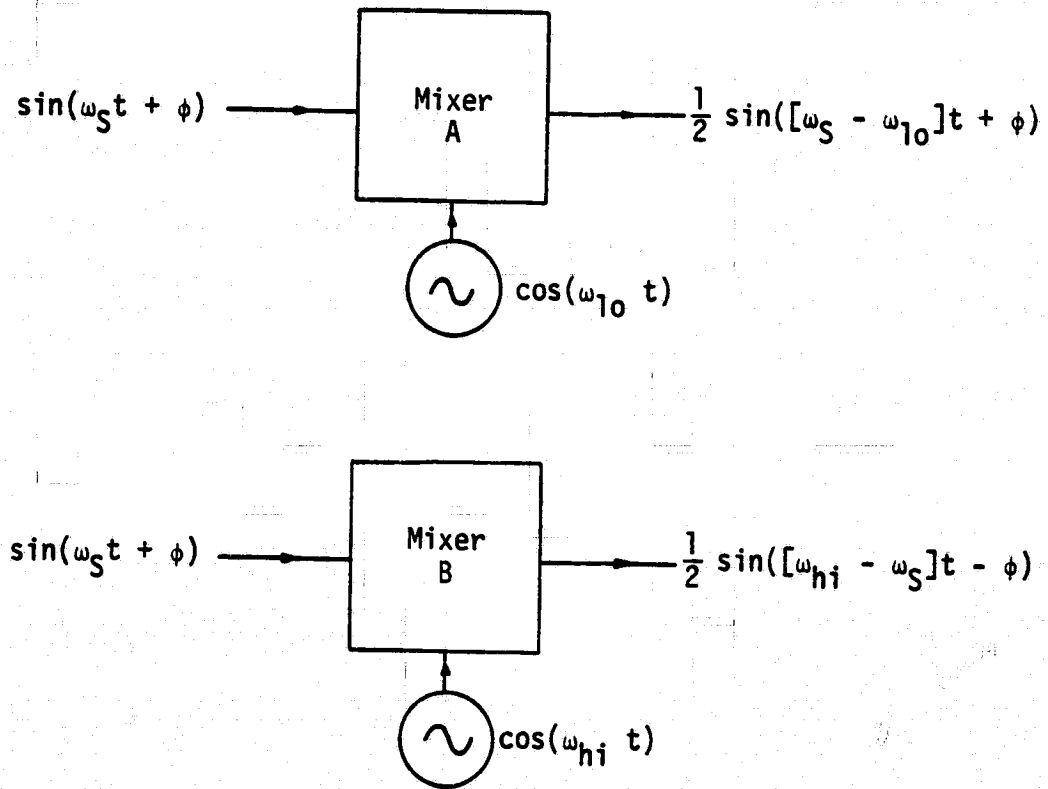
Figure 3-1. A phase inversion introduced by the nonlinear action of a mixer.

A phase inversion should not be confused with a 180° phase reversal. A phase reversal only introduces a constant term in the relative phase of two signals.

In a dual-polarized receiver the copolarized signal provides the reference phase. A phase inversaion in either one or both of the channels would invalidate the phase data.

Other sources of potential problems are amplitude-dependent phase variations and frequency-dependent phase variations. Practical circuits exhibit amplitude-dependent phase distortion but these effects are usually negligible. All resonant circuits exhibit a frequency-dependent phase characteristic, but as will be shown, this is not a factor in the equipment used in this experiment.

A discussion of the individual components forming the 11.7 GHz receiving system follows. Each component will be analyzed in terms of its phase characteristics. Figures 3-2 and 3-3 are simplified block diagrams of the system.

3.2.2 The Antenna

The 11.7 GHz antenna is a prime focus-fed parabolic reflector antenna 12 feet in diameter. The feed horn is supported by the waveguide and there are no supporting spars to generate cross-polarization. The antenna is program pointed by the station computer using orbital elements provided by NASA. Possible phase effects that might be caused by improper antenna pointing have already been discussed. The computer continuously monitors the status of the
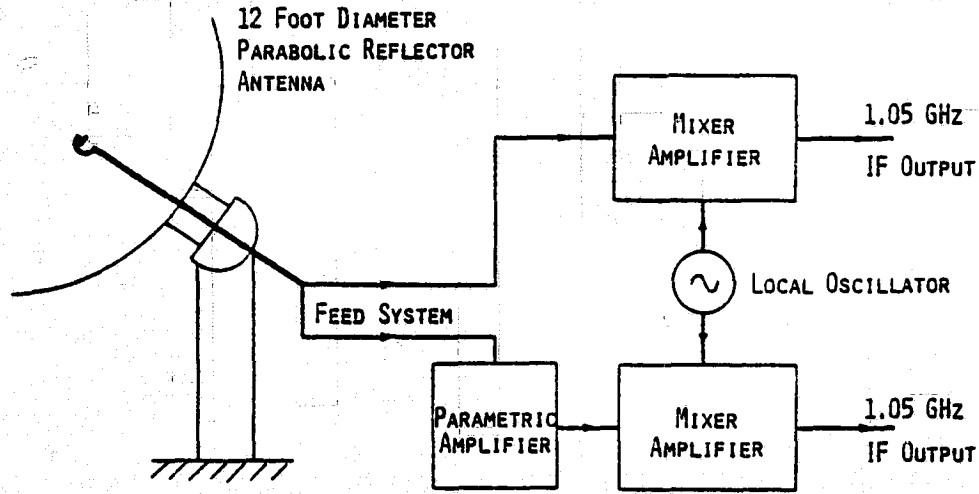
Figure 3-2.   The 11.7 GHz antenna and RF components.

- 85 -
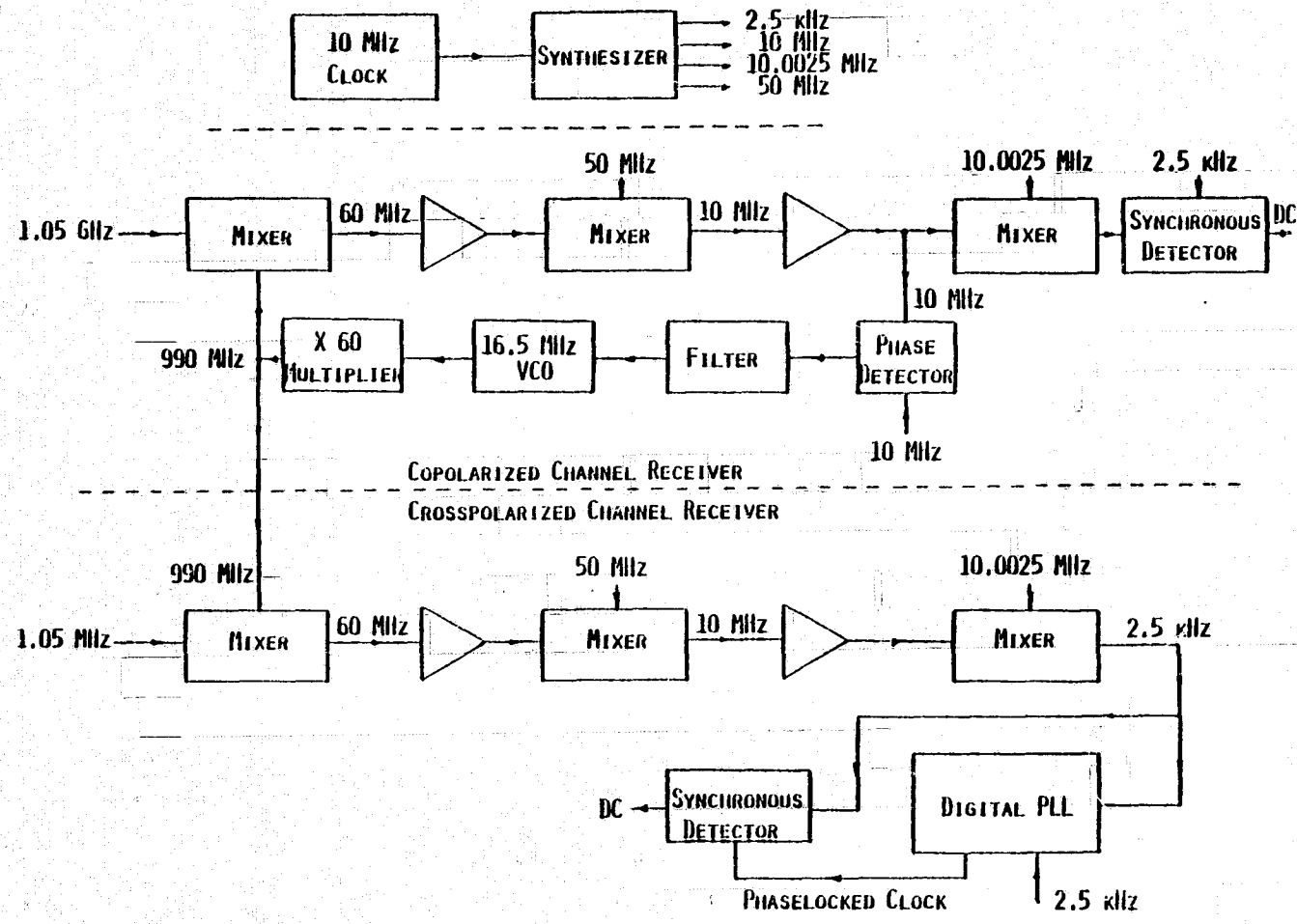
Figure 3-3. The 1.05 GHz IF receiver.

antenna pointing mechanism and if wind or some other factor causes a
pointing error the computer stops data collection until correct
pointing is resumed.

The prime focus feed was chosen rather than a Cassegrain feed
in order to reduce problems associated with water on (or in) the
feed horn. Wet antenna and wet feed tests have been performend and
the resulting phase effects were negligible. Careful analysis of
data from this system has shown that many phase events occur before
the onset of local rainfall, this further eliminates wet antenna
phase effects.

The incoming RHCP wave becomes a LHCP wave upon reflection from
the metal surface of the antenna. Thus the feed horn "sees" a LHCP
wave instead of a RHCP wave in the copolarized channel. The same
reversal occurs on the crosspolarized wave. No problems are
introduced since the antenna waveguide ports are labled to account
for this change. Even though the reflection at the antenna surface
changes the sense of the wave, it can in no way alter the phase
relationship of the copolarized and crosspolarized waves.

The orthomode transducer and other waveguide hardware are
linear devices and therefore exhibit linear phase characteristics.

3.2.3 The R.F. Section (11.7 GHz → 1.05 GHz)

Figure 3-2 shows a block diagram of the 11.7 GHz front end.
The copolarized channel first mixer and the crosspolarized channel
first mixer are driven by the same local oscillator. The oscillator

frequency is 10.65 GHz and is subtracted from the signal frequency to arrive at an IF frequency of 1.05 GHz. Therefore no phase inversion occurs.

A parametric amplifier in the crosspolarized channel is pumped by a 55 GHz source. Currents flow in the amplifier circuitry at the difference frequency $\omega_{pump} - \omega_s$ but, in the final analysis, the parametric amplifier is a linear device and introduces no phase inversion.

The input to the parametric amplifier is represented by

$$v_s(t) = V_s \sin(\omega_s t + \phi) \tag{117}$$

and the pump is represented by

$$v_p(t) = V_p \sin(\omega_p t) \quad . \tag{118}$$

A current flows at a frequency which is equal to the signal frequency subtracted from the pump frequency. This is termed the idler frequency. The idler current is

$$i_i(t) = I_i \sin([\omega_p - \omega_s]t - \phi) \quad . \tag{119}$$

A current also flows at a frequency equal to the idler frequency subtracted from the pump frequency

$$\begin{aligned}
i_0(t) &= I_0 \sin([\omega_p - \omega_i]t) \\
&= I_0 \sin([\omega_p - (\omega_p - \omega_s)]t - [-\phi]) \\
&= I_0 \sin(\omega_s t + \phi) \quad .
\end{aligned} \tag{120}$$

This current represents the amplified version of the input signal. Two phase inversions are indicated by this analysis and their effects cancel. No net phase inversion results. The manufacturer of the parametric amplifier [15] confirmed the above conclusion.

3.2.4 The I.F. Receiver

All local oscillators in the 1.05 GHz IF receiver are phase referenced to each other and to the signal voltages by virtue of the action of the phaselock loops. All local oscillators are common to both the copolarized channel and the crosspolarized channel.

Figure 3.3 is a simplified block diagram of the IF receiver. Three frequency conversions occur in the receiver and one of the conversions subtracts the signal frequency from the local oscillator frequency. This introduces one phase inversion, but this phase inversion is nullified later in the receiver chain.

Frequency changes within a filter passband can cause phase changes. Resonant circuits are integral parts of the amplifiers in the receiver, and several crystal filters (not shown) with narrow passbands are included in the signal path. All local oscillators in the receiver and all of the IF signals are ultimately frequency referenced to a highly stable 10 MHz master oscillator. This assures that all circuits and filters are operated at a constant point on their frequency-phase characteristic.

Possible sources of amplitude dependent phase variations are the two phaselock loops in the receiver because all phaselock loops

exhibit some phase change with varying input signal levels. Several safeguards have been provided to eliminate this effect in the receiver. The dynamic ranges of the phaselock loops have been measured at approximately 40 dB. Most of the propagation events (and, except where noted, all of those presented in this thesis) are associated with signal fades well within the dynamic range of the receiver, therefore the loops are operating with ample input signal levels. Phaselock detection circuits are provided in both phaselock loops. The status of phaselock is monitored by the computer and data will not be recorded unless both loops are phaselocked.

3.2.5 The Digital PLL

A unique feature of this receiver is the digital phaselock loop which was designed by P. H. Wiley and E. A. Manus of the VPI&SU Electrical Engineering Department [16]. This phaselock loop requires that the main phaselock loop in the copolarized channel establish frequency lock before it can perform its function.

The phaselock loop in the copolarized channel brings the 10 MHz IF signal into phaselock with the 10 MHz master clock in the receiver. Since the 10.0025 MHz and 2.5 kHz local oscillators are derived from the 10 MHz clock the resultant 2.5 kHz IF signal is phaselocked to the 2.5 kHz clock. The 2.5 kHz clock waveform is a 5 volt square wave which drives a synchronous detector.

Because there is a phase difference between the copolarized and crosspolarized waves at 11.7 GHz there will also be a phase difference

between the 2.5 kHz IF signals in the copolarized and crosspolarized channels of the receiver. Because all local oscillators are common to both channels the relative phase at 2.5 kHz is identical to that at 11.7 GHz.

This phase difference changes with propagation conditions. Therefore the crosspolarized channel 2.5 kHz IF signal is not phase-locked to the 2.5 kHz receiver clock. In order to use a synchronous detector in the crosspolarized channel the digital phaselock loop generates a new 2.5 kHz clock which is phaselocked to the cross-polarized IF. This is illustrated in Figure 3-4.

Figure 3-5 presents a simplified block diagram of the digital phaselock loop. The modulo-1000 counter commences counting at a 2.5 MHz rate upon the rise of the 2.5 kHz copolarized channel clock. When its count equals that of the up/down counter the digital comparator instructs a multivibrator to generate a 200 μ sec. pulse ($\frac{1}{2}$ cycle of a 2.5 kHz square wave). The analog comparator determines whether this pulse leads or lags the 2.5 kHz crosspolarized IF signal and instructs the up/down counter to compensate accordingly. After several iterations the new 2.5 kHz reference will be in phase with the crosspolarized IF signal.

The two phaselocked 2.5 kHz clocks drive their respective synchronous detectors. An added benefit of this system is that it provides two stable, noisefree TTL level signals which are in phase with the copolarized wave and the crosspolarized wave respectively. These signals are fed to the phase detector.

2.5 kHz Signal

```
┌──────────────────────┐        ┌──────────────────────┐
│                      │        │                      │
│     Digital PLL      │        │                      │
│                      │        │     Synchronous      │
│   (generates new     │        │      Detector        │───▶ VDC
│  phaselocked clock)  │        │                      │
│                      │        │                      │
│                      │        │                      │
└──────────────────────┘        └──────────────────────┘
```

2.5 kHz
reference
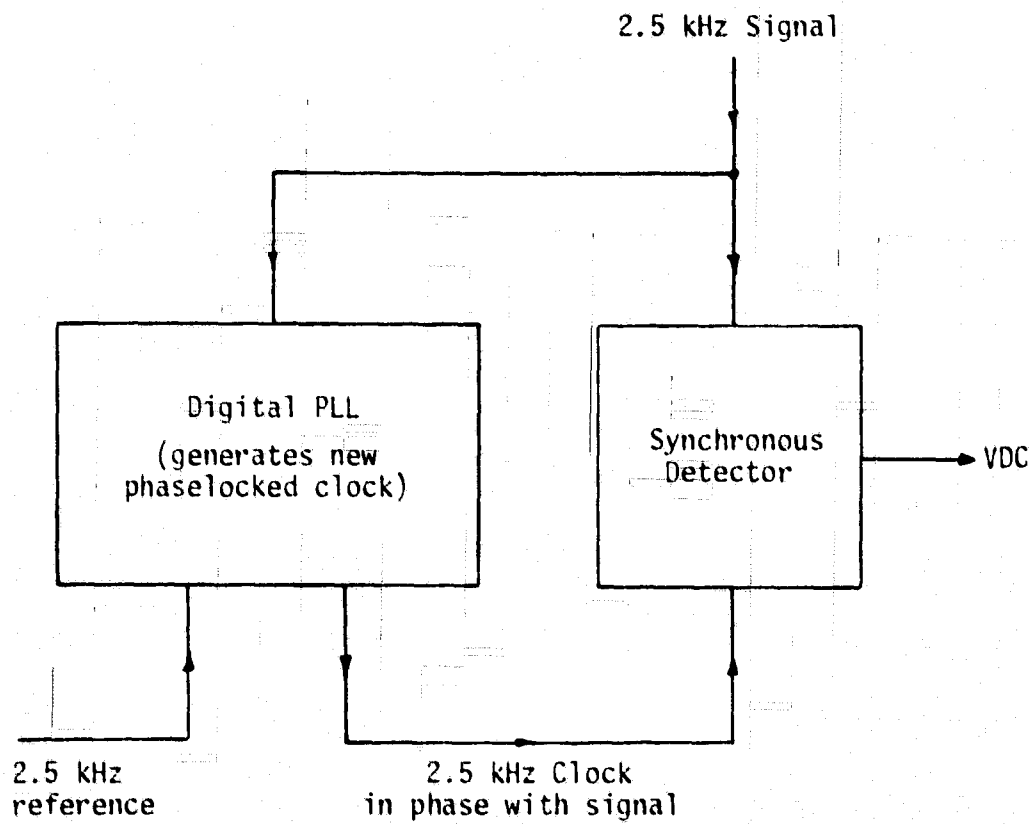
2.5 kHz Clock
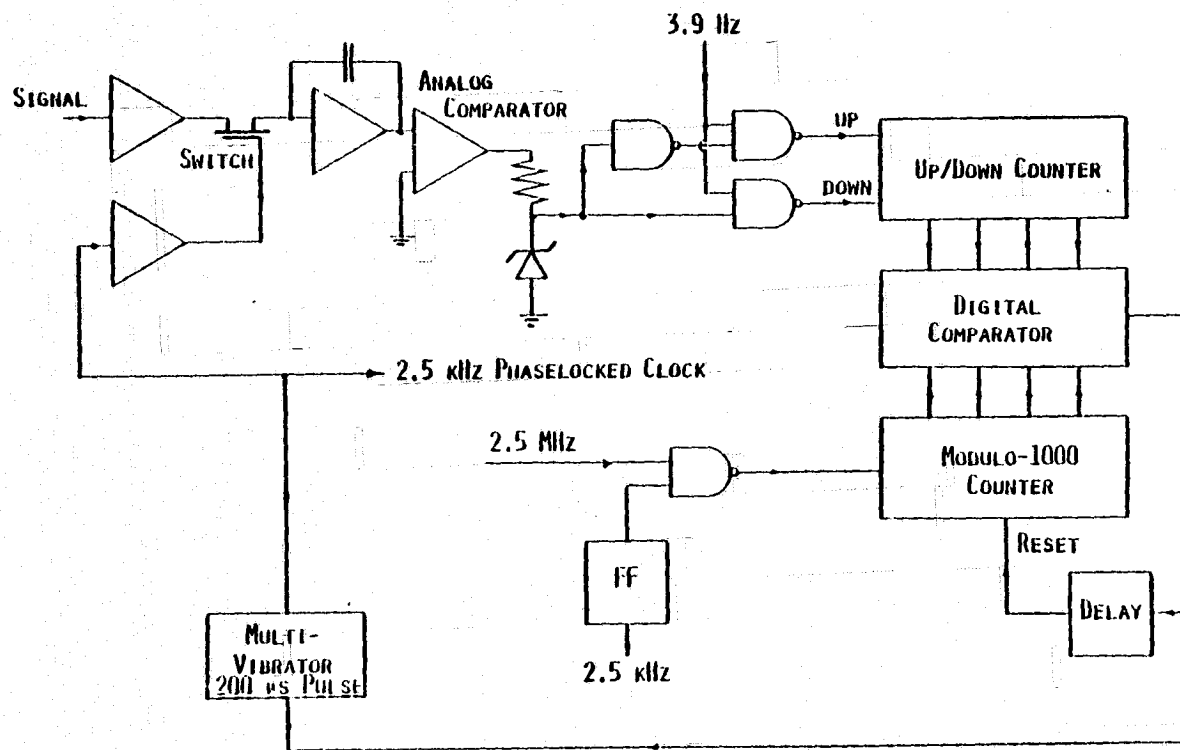in phase with signal

Figure 3-4. The digital phaselock loop.

Figure 3-5. The 2.5 kHz digital phaselock loop.

3.2.6 The Four-Quadrant Phase Detector

The standard $\pm 90°$ phase detector offers at best the triangular characteristic shown in Figure 3-6a. All phase changes greater than 180° are invalid, and should operation occur on the negative sloped portion of the curve an apparent phase inversion exists.

A four-quadrant phase detector, developed by P. H. Wiley and E. A. Manus [17], overcomes these problems. The phase-output voltage characteristic is shown in Figure 3-6b and the circuit diagram is shown in Figure 3-7. The rise of input 1 turns the flip flop on and the rise of input 2 turns it off. The duration of the pulse generated by the flip flop is proportional to the relative phase of inputs 1 and 2. The pulse area is integrated by the operational amplifier circuit giving an output of 0 to 5 volts corresponding to 0° to 360°.

Inputs 1 and 2 are selected in order to give an output of $\Delta = \phi_x - \phi_{co}$. The inputs have been arranged to account for the phase inversion introduced by mixer number four.

3.2.7 Data Collection

The zero to five volt output from the phase detector is routed through coaxial cable to an analog-to-digital converter in the experiment controller. The output of the A/D converter is a binary word ranging between 0 and 255. This value is checked by the computer to assure that (1) the phase is not slewing faster than
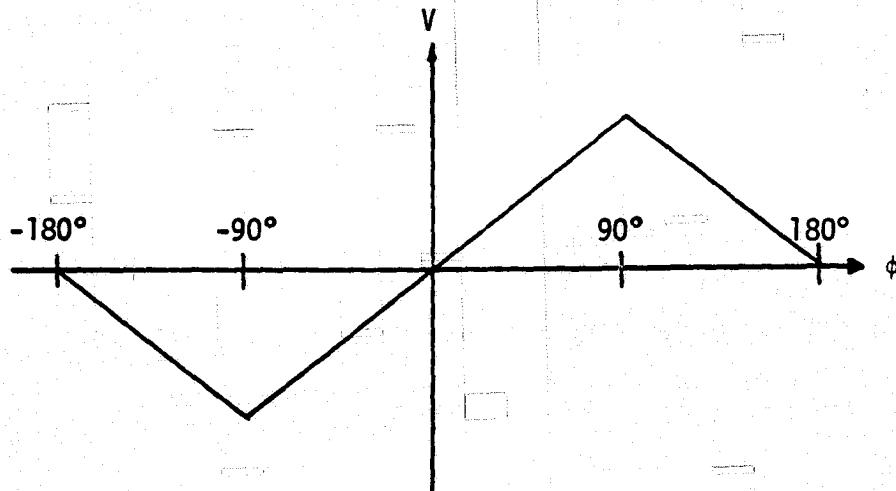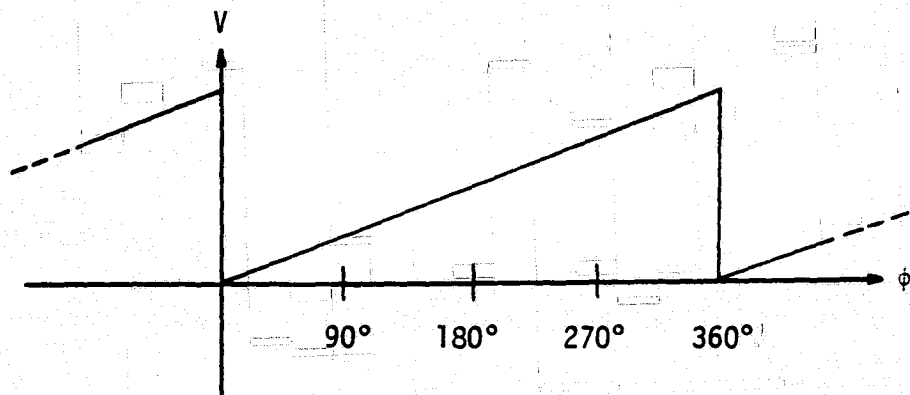
Figure 3-6a. ±90° phase detector.

Figure 3-6b. Four-quadrant phase detector.

Figure 3-6. Output voltage - input phase characteristics
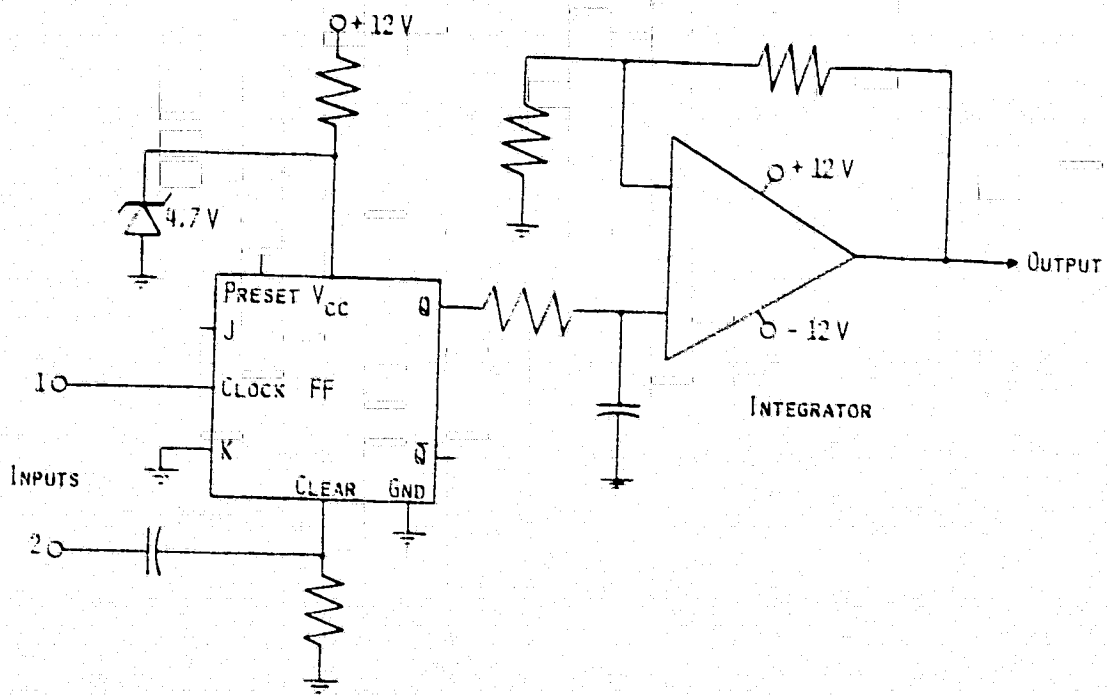   of two phase detectors.

Figure 3-7. Circuit diagram of the four-quadrant
phase detector.

the phaselock loops can follow and (2) that the phase detector output is not oscillating about the 360° - 0° discontinuity in its characteristic. If these checks indicate valid data, and if the receiver phaselock loop indicators show phaselock, and if the antenna is pointed correctly, then the data value is compared to the last stored value. If the difference is greater than 10.7° a new point is recorded on the computer's magnetic disk.

3.2.8 Data Reduction

Periodically the data are moved from the PDP-11 disk to magnetic tape. During this process a scale factor is applied to the binary word to convert it into a number from 0 to 999. This scale factor is a positive number thus no inversion is inserted. The magnetic tape stores data for phase, signal levels, status indicators, weather, and time.

The tape is transferred to the IBM-370/158 where further processing is applied to put the data in a more useable form. Again only positive scale factors are applied to the phase data. The final form of the bulk data is stored on magnetic disk in the IBM-370.

The plotting software accesses this disk and reads data values directly in time sequence. The phase data may be displayed as it is stored or it may be converted along with isolation data into a polar coordinate form. The polar coordinate transformation is

$$x = (C - I)\cos \Delta$$

$$y = (C - I)\sin \Delta$$

(121)

where

I = isolation in dB

$\Delta = \phi_x - \phi_{co}$

C = maximum isolation value in dB .

This transformation creates no phase discrepancies.

3.2.9 Calibration of the System

Signal level calibrations are periodically performed on the receiving systems to assure their accuracy. A phase calibration has been performed on the 11.7 GHz system by using an 11.7 GHz calibration source and monitoring results through to final stage of data reduction. A phase calibration has been performed on the 28 GHz system at the 60 MHz IF frequency.

The 11.7 GHz phase calibration procedure will be described. A stable calibration source was placed on a hilltop approximately 2 miles from the receiving antenna. Precautions were taken to prevent signal leakage directly from the source. A linearly polarized horn was used to transmit because a linearly polarized wave can be considered to be composed of a RHCP wave and a LHCP wave with their relative phase determining the tilt angle of the linear wave. By rotating the linear transmitting horn (i.e. rotating the tilt angle)

the relative phase of the RHCP and LHCP components can be varied; a counterclockwise rotation (wave approaching) of the linearly polarized wave corresponds to a phase delay of the LHCP wave. Measured values of phase shift corresponded to those introduced by rotating the horn.

3.2.10 Data Display

Figure 3-8a through 3-8e illustrate the capabilities of the 11.7 GHz receiver and the data reduction system. The first four figures are time histories of a late August, 1977 storm which occurred at about nine PM (local time) in the evening. This was a relatively severe storm as indicated by the large peak rain rate and the 12 dB fade at 11.7 GHz. The dynamic range of the receiver is in excess of 35 dB, thus the receiver was operating well within its optimum range. Figure 3-8c shows isolation versus time and illustrates a characteristic increase in isolation at the beginning of a storm. This isolation enhancement is due to antenna effects. Figure 3-8d shows a 40° phase change at the time of the isolation increase, but a much larger phase change occurs during the period of isolation degradation. A phase versus isolation polar plot covering the same period as the time histories is presented in Figure 3-8e.

ORIGINAL PAGE IS
OF POOR QUALITY
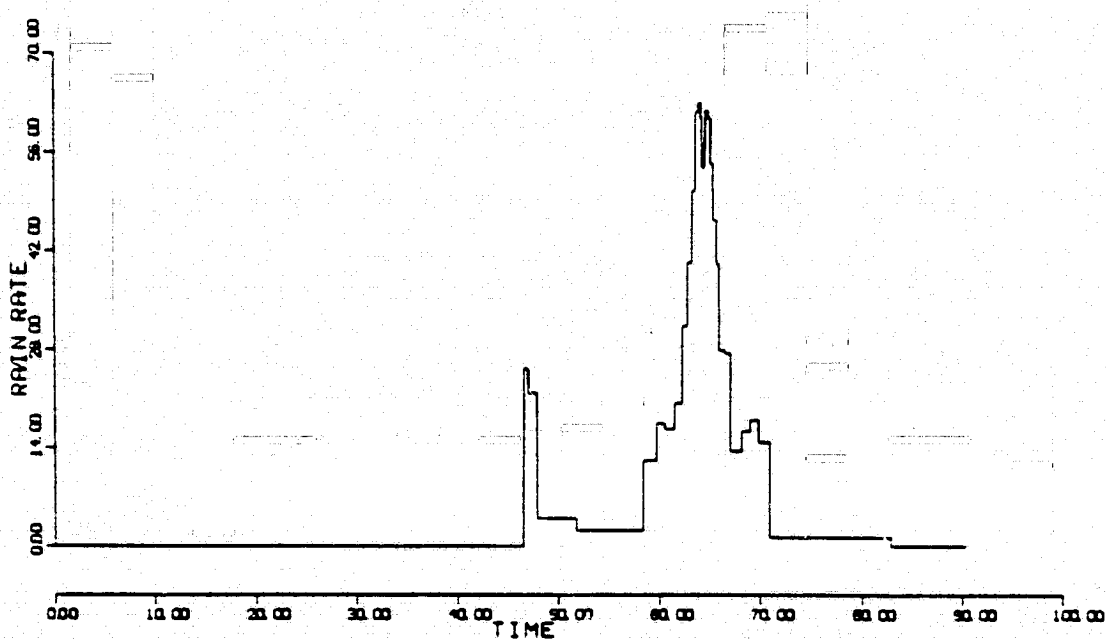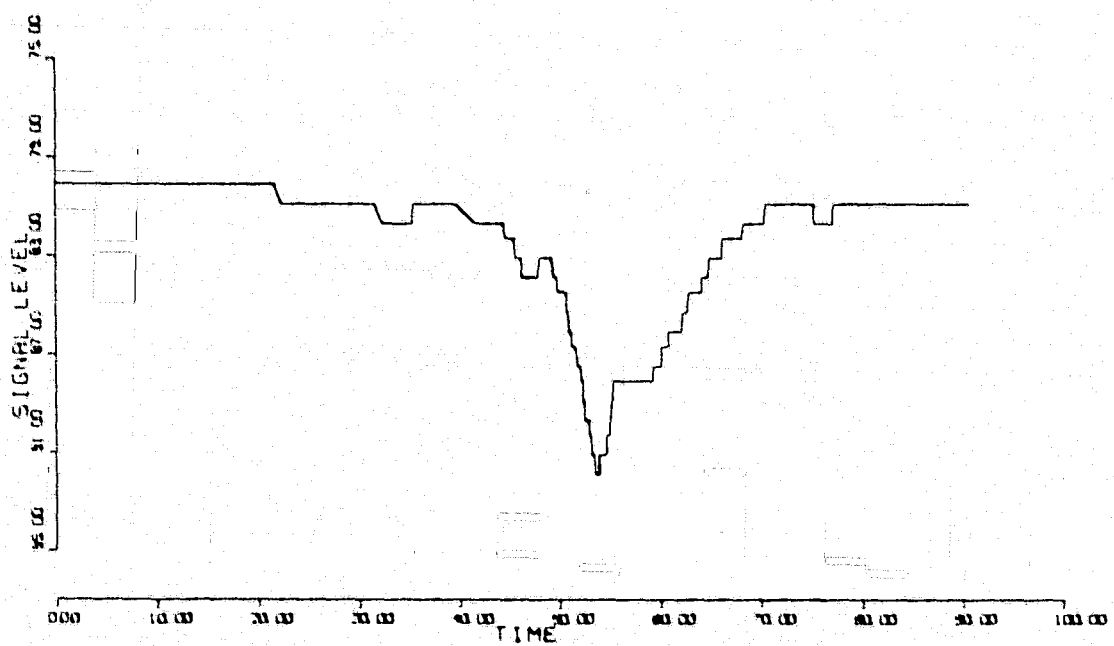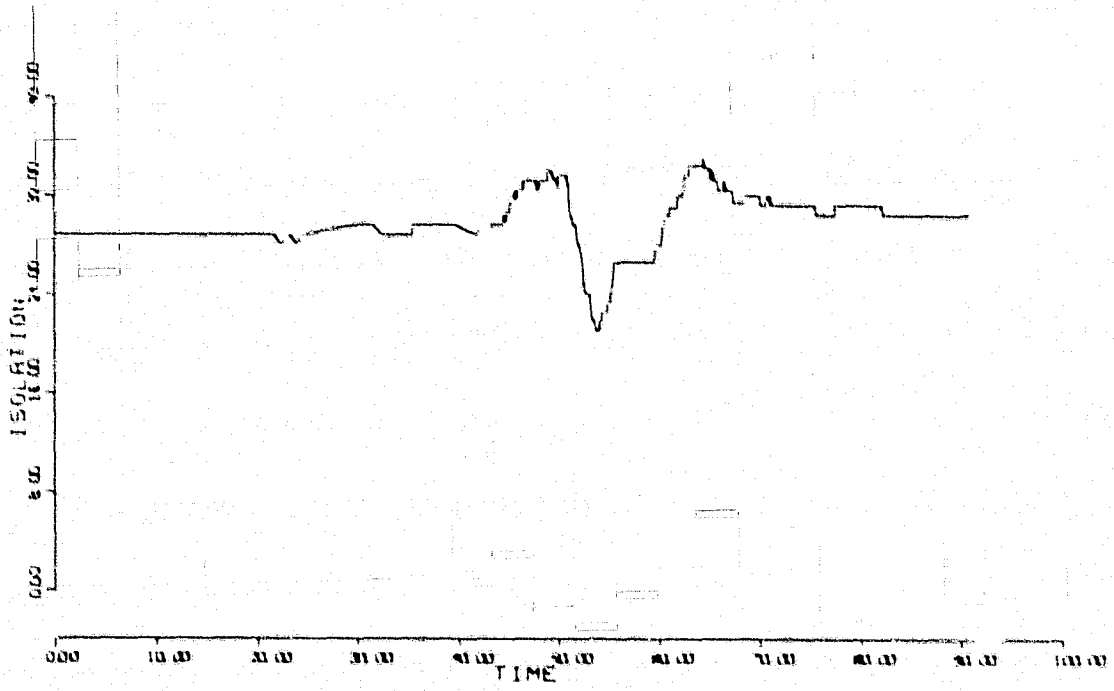

Figure 3-8a. Rain rate.

Figure 3-8b.   Copolarized signal level.

Figure 3-8c.   System isolation.

ORIGINAL PAGE IS
OF POOR QUALITY

Figure 3-8d. Phase versus time.
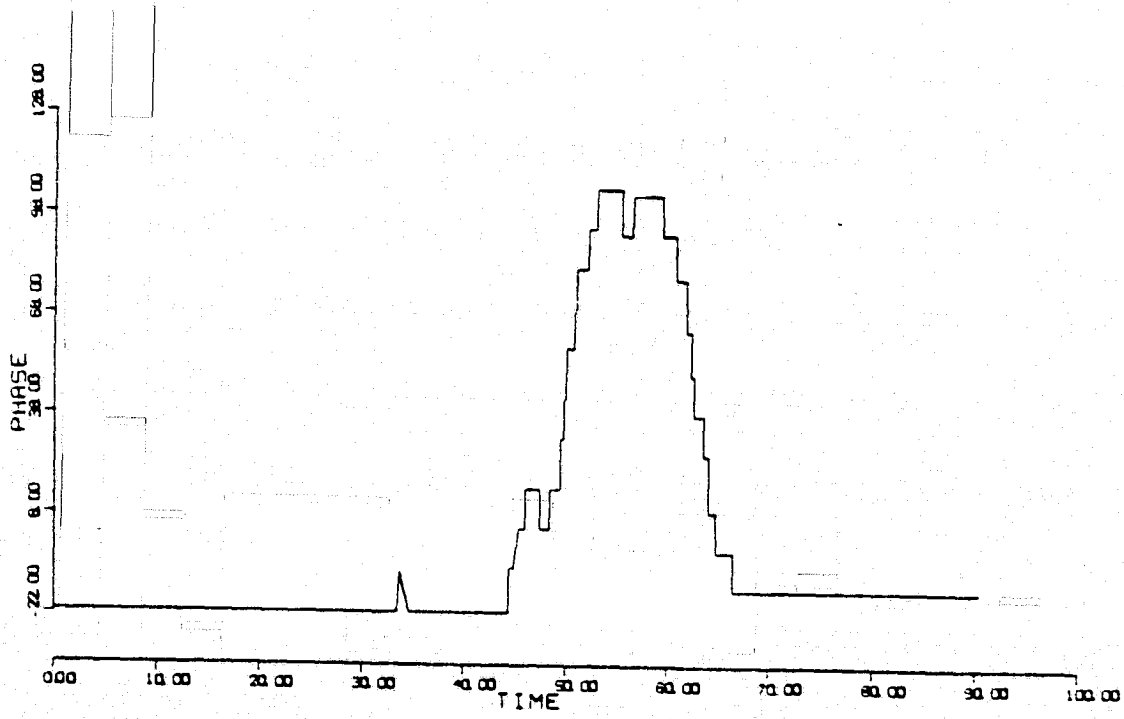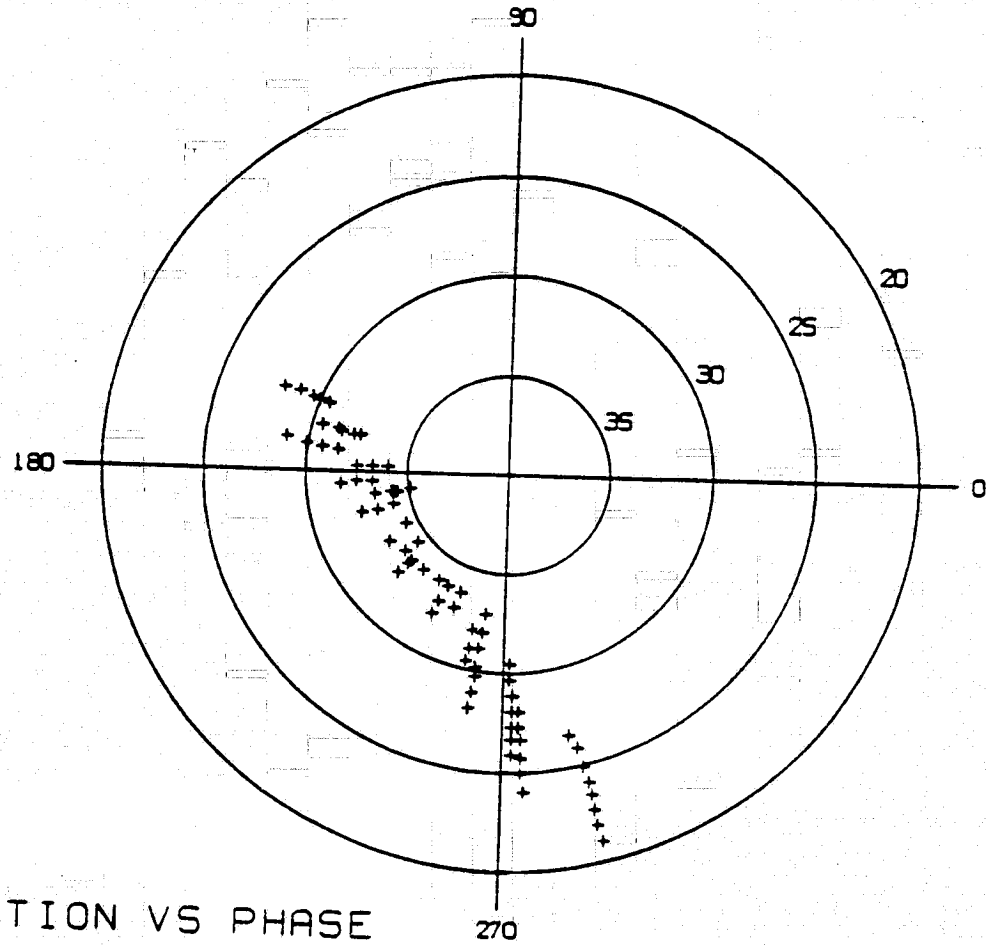
ISOLATION VS PHASE

Figure 3-8e.   Phase "scatter plot".

Figure 3-8.   Data presentation from VPI&SU 11.7 GHz
satellite receiving system. The storm
occurred at 1930 EST August 29, 1977.

CHAPTER 4

COMPARISON OF THEORY AND DATA

4.1 11.7 GHz Circular Polarization

The polar plot presentation of phase and isolation is most indicative of the overall operation of a dual-polarized receiving system because the variables displayed are derived from the magnitude and phase of both the copolarized and crosspolarized signals. The isolation versus phase plot shown in the last chapter is representative of many 11.7 GHz propagation events seen during the summer and autumn of 1977. Figures 4-1 through 4-7 illustrate four propagation events associated with moderately high rain rates and fades between 8 and 13 dB. Figures 4-2 through 4-4 illustrate rain rate, attenuation, and phase for the event depicted in the polar plot of Figure 4-1. The correspondence between rain rate, fade, and phase are obvious from these plots. Close inspection shows that the propagation effects occurred as much as 30 minutes before any ground rainfall was recorded.

Immediately apparent in the polar plots are the wide scatter of data, the large absolute phase change, and the spiral effect caused by a phase advance with decreasing isolation. Canting angle changes and antenna effects are almost certainly factors in the phase changes observed, but neither one taken separately (nor possibly both together) can totally explain the observations.

Figures 4-8 and 4-9 are reproductions of two of the events
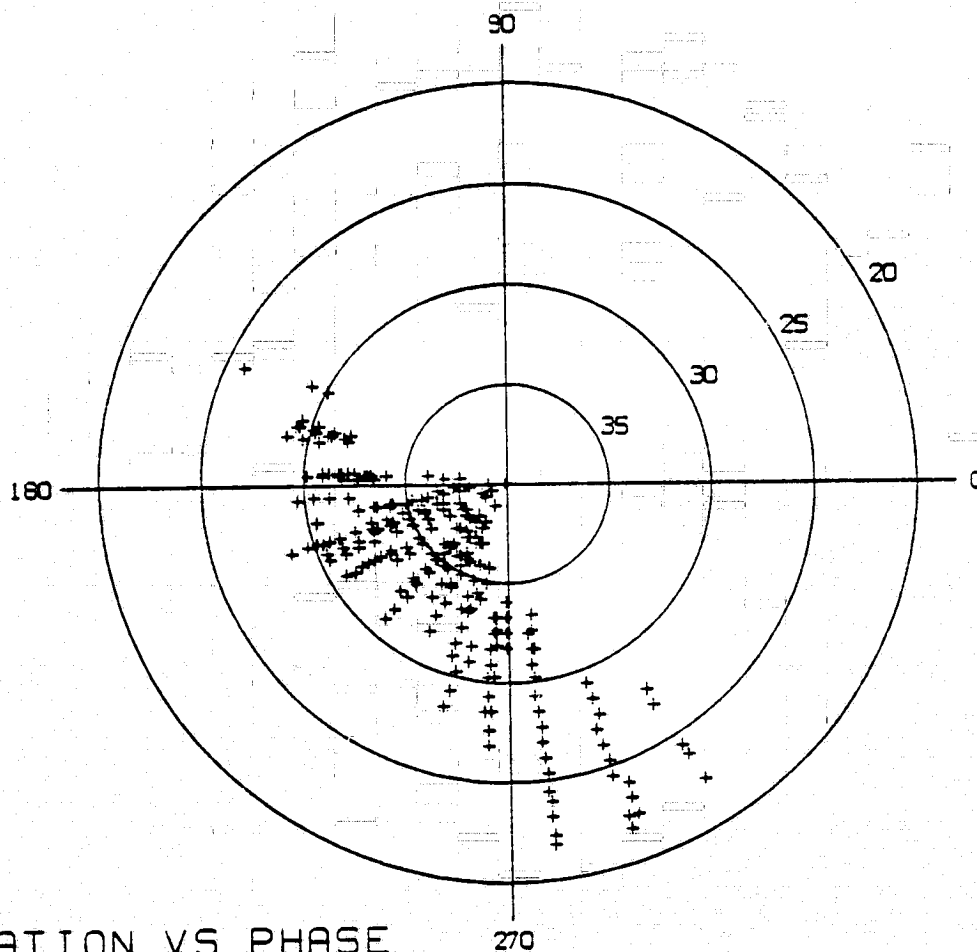
ISOLATION VS PHASE

Figure 4-1.   11.7 GHz phase data showing
characteristic spiral effect.
The storm occurred at 1300 EST
August 13, 1977.
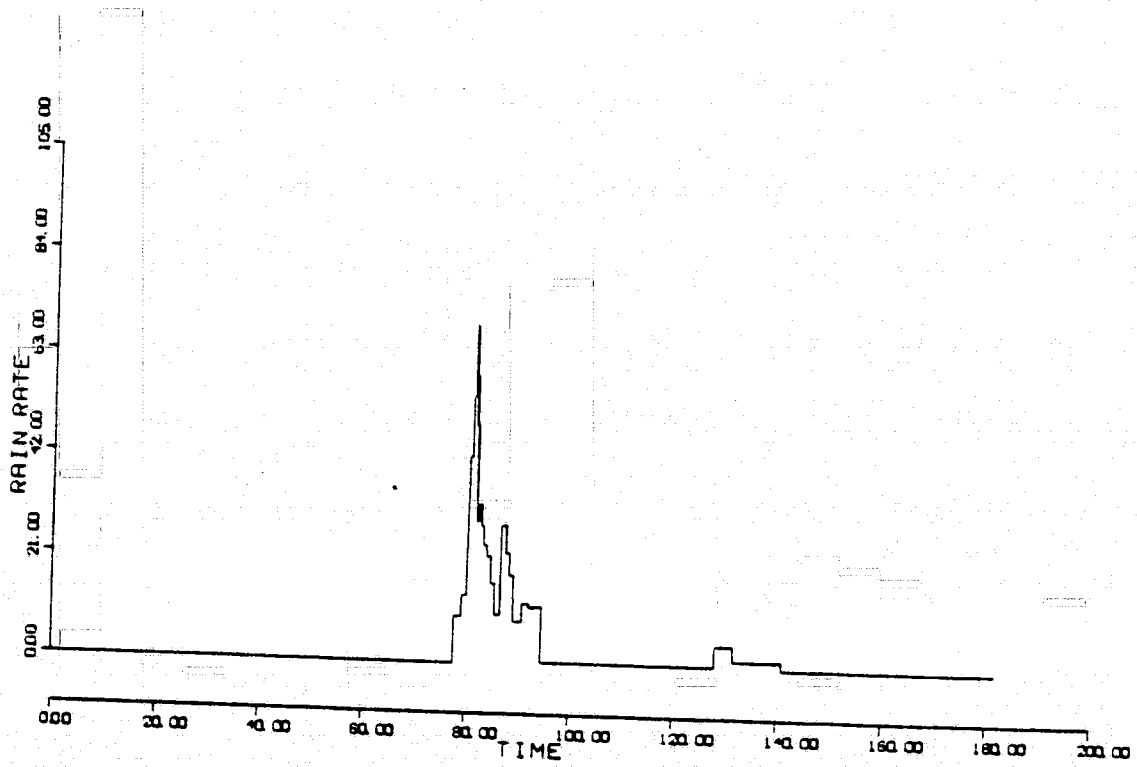
Figure 4-2. Rain rate time history for storm presented in Figures 4-1 through 4-4.

ORIGINAL PAGE IS
OF POOR QUALITY
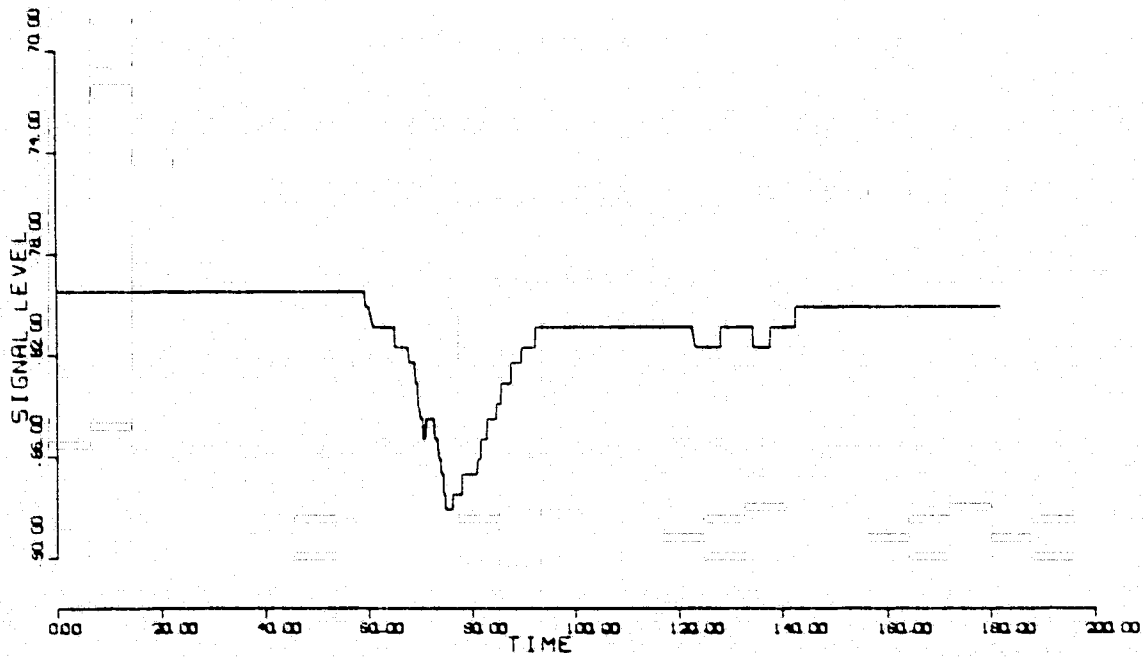
Figure 4-3. Copolarized signal level time history for storm presented in Figures 4-1 through 4-4.
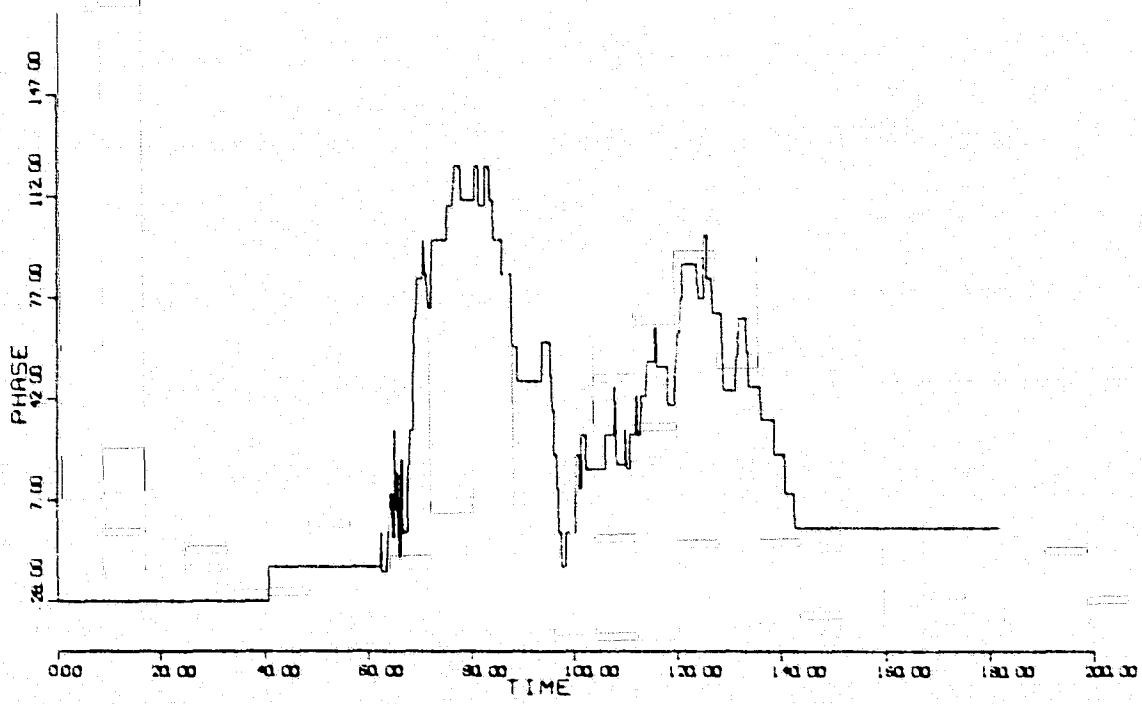
Figure 4-4. Phase time history for storm presented in Figures 4-1 through 4-3.
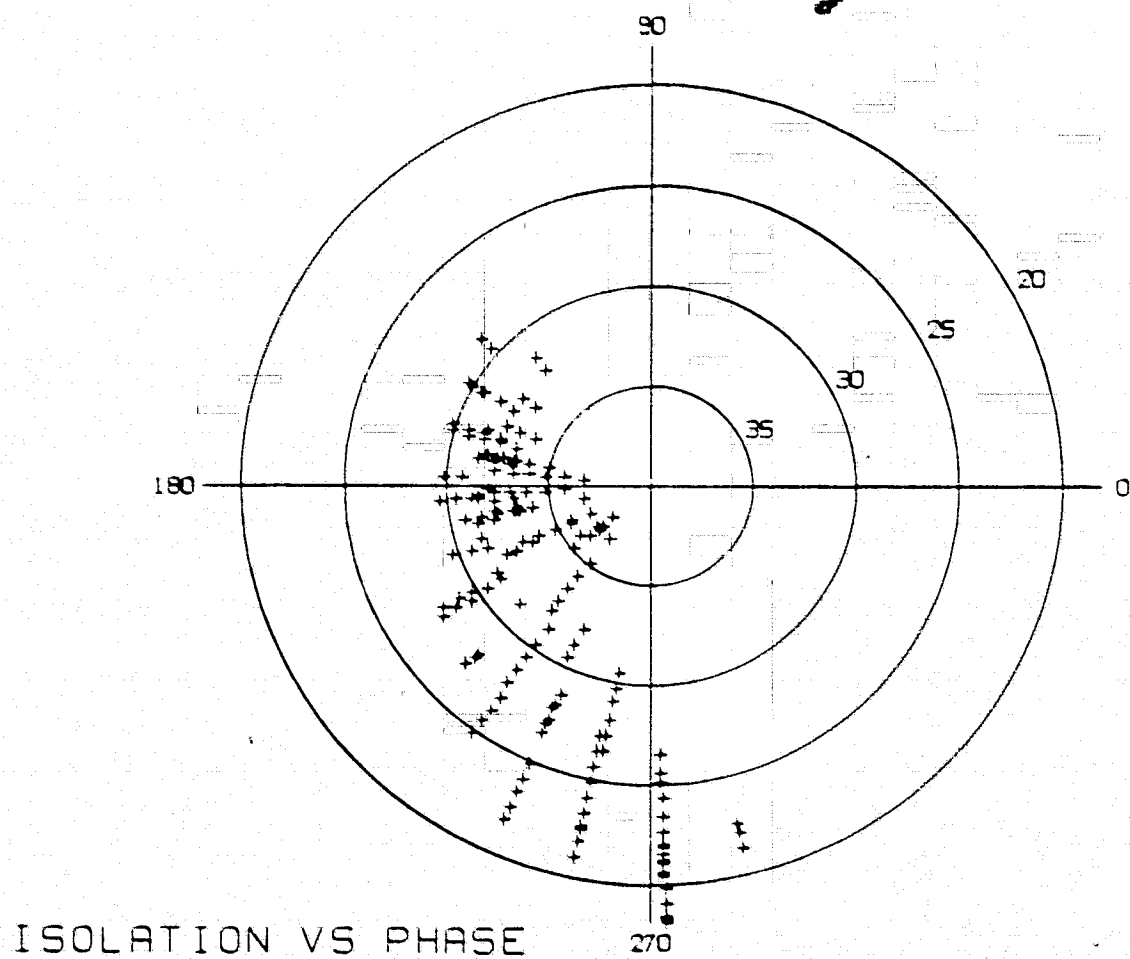
ISOLATION VS PHASE

Figure 4-5. 11.7 GHz phase data. The storm occurred
at 1800 EST August 9, 1977.
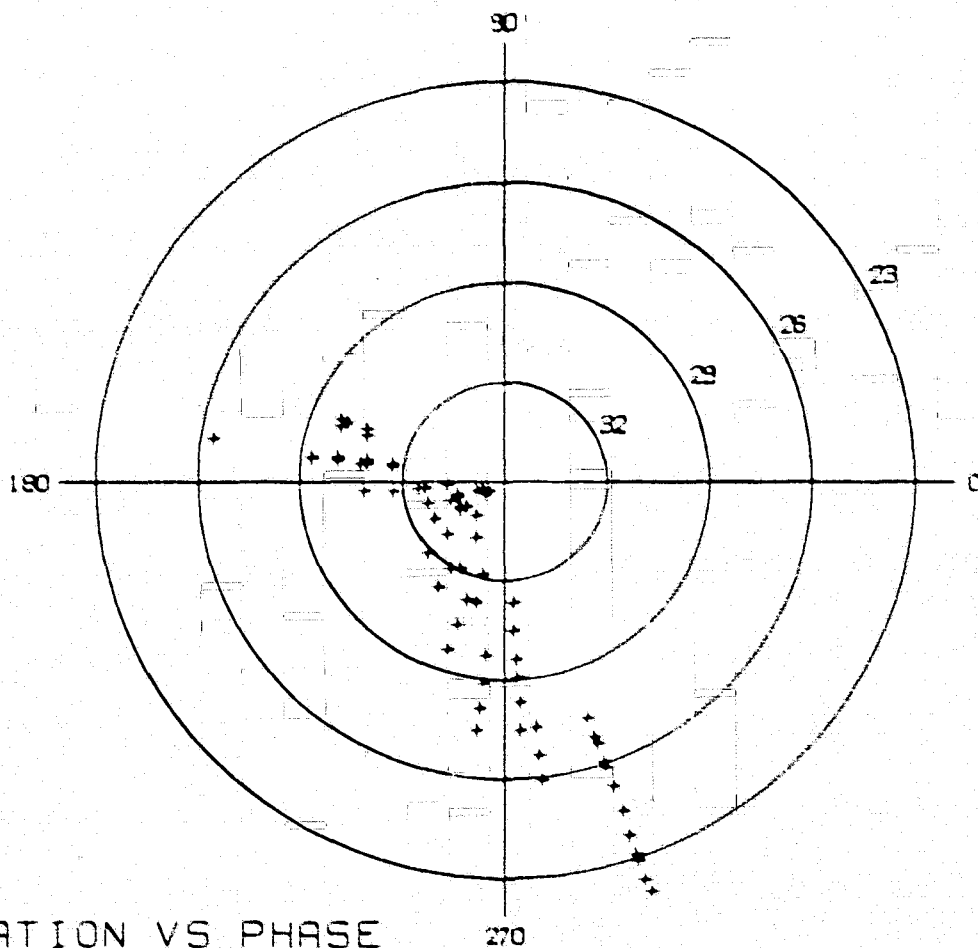
ISOLATION VS PHASE

Figure 4-6. 11.7 GHz phase data. The storm occurred at 1130 EST August 14, 1977.
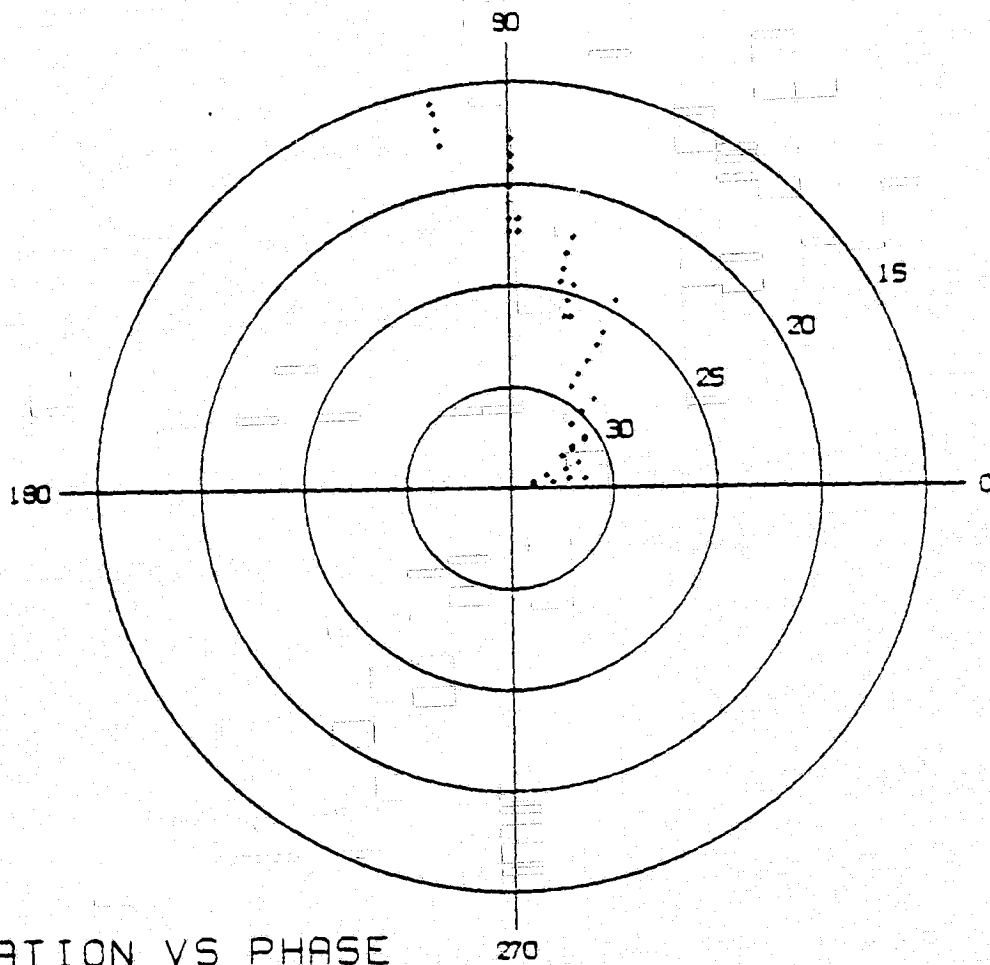
ISOLATION VS PHASE

Figure 4-7. 11.7 GHz phase data. The storm occurred
at 1900 EST December 13, 1977.
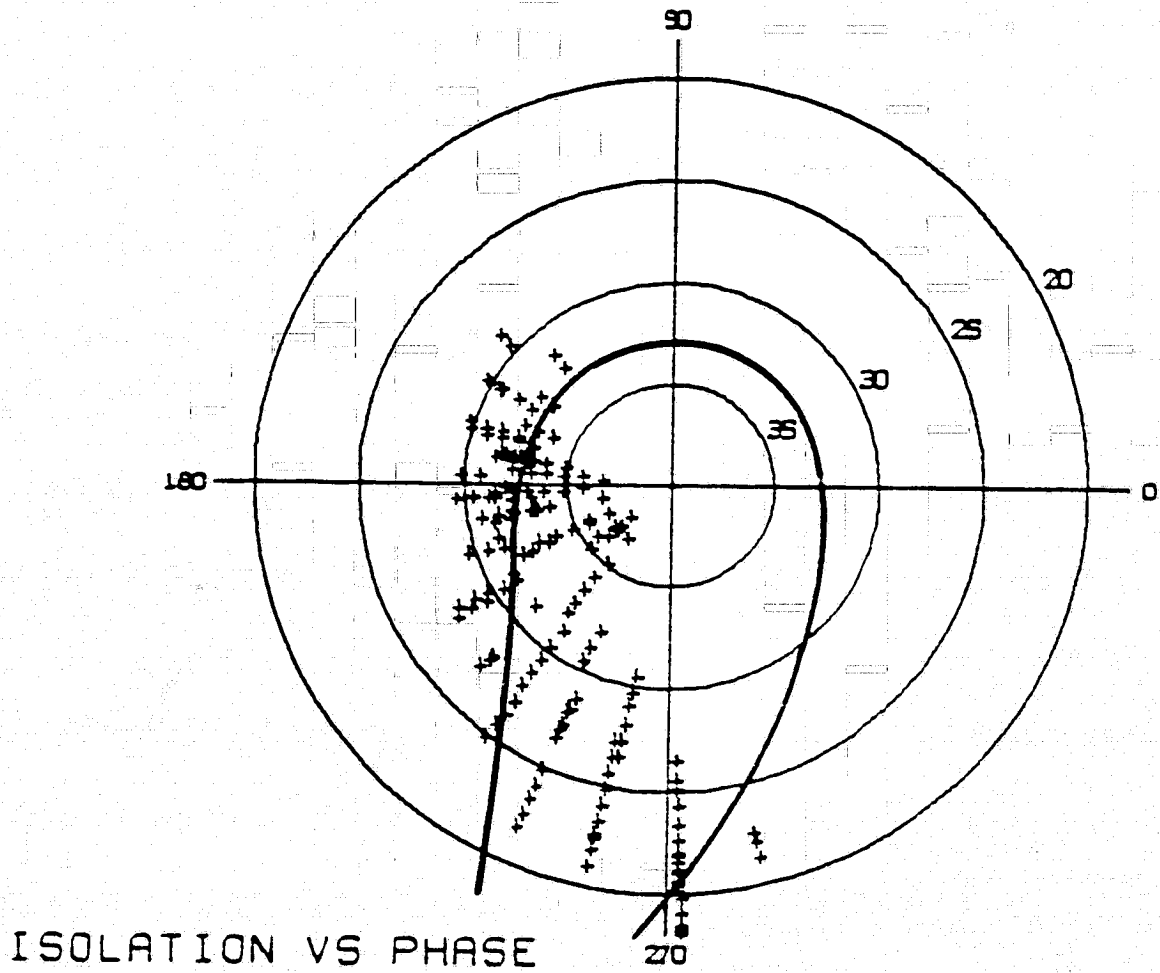
ISOLATION VS PHASE

Figure 4-8. Typical 11.7 GHz phase data with
maximum theoretical prediction
bounds.
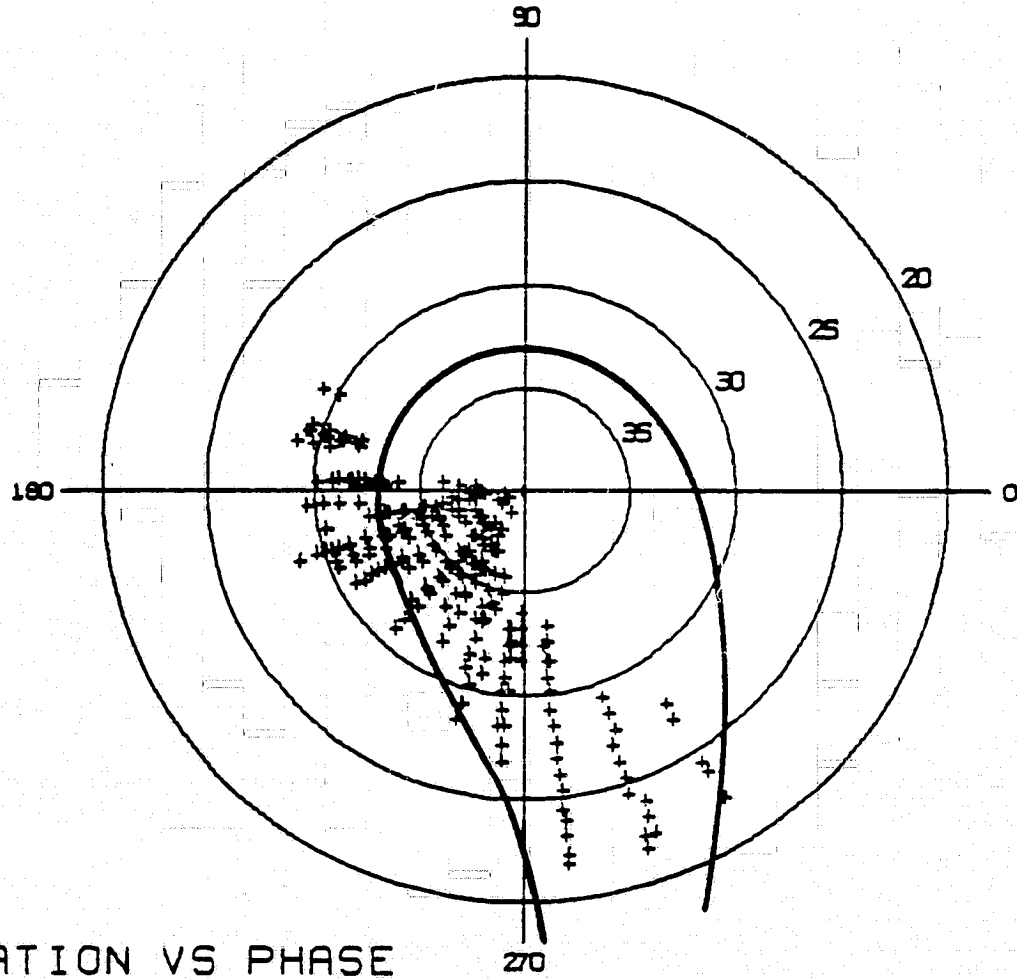
ISOLATION VS PHASE

Figure 4-9.   Typical 11.7 GHz phase data with maximum
theoretical prediction bounds.

already shown, but the maximum bounds on imperfect antenna effects
are included. An antenna axial ratio of .4 dB (representing a
conservative interpretation of the manufacturer's measurements) was
used to compute the bounds. The bounds were drawn at an angle
(representing the system constant phase difference) in order to
include as many data points as possible. These error bounds look
different than those shown earlier because of the difference in
scales.

As previously stated these bounds are for the worst possible
case, it is likely that the bounds for a practical system would be
reduced because the transmit and receive antennas will have matched
tilt angles. Furthermore because the antenna error depends upon
the relative angle of the vectors $\vec{D}$ and $\vec{U}$ in Figure 2-18 and because
these vectors are slowly varying either the positive error bound or
the negative error bound should be used, but not both. Therefore
it is necessary to account for the large scatter in the data by some
other factor.

Recalling the theoretical expression for crosspolarized phase

$$\Delta = \pm 2\theta + \tan^{-1}\left[\frac{-2e^{-\alpha L} \sin \beta L}{e^{-2\alpha L} - 1}\right] \tag{122}$$

and recalling that the inverse tangent term is affected only
slightly by the propagation parameters, it is therefore very likely
that the $\pm 2\theta$ term accounts for the wide scatter in the phase data.
It has been shown that the canting angle oscillates about a mean and
that an oscillation of up to 20° is likely [11]. This will account

for the 40° phase scatter in the 25-30 dB isolation range of Figures 4-8 and 4-9.

It should be emphasized that the actual error bounds of the system are unknown, only the maximum bounds are known. It is possible for the errors in the system to be very small in which case another explanation for the large phase changes (in an opposite direction to that predicted) must be posed. Again the $\pm 2\sigma$ term is a candidate. An absolute canting angle change with some time dependence (or dependence on some other factor) can be made to explain the data.

A cluster of points to the left of the error bounds and in the vacinity of 30 dB isolation is seen in Figures 4-8 and 4-9. This is also illustrated by the data between points A and B in Figure 4-10. The phase of these points is substantially different from the bulk of points in the data. Several explanations for this observation will now be posed.

When this particular plot is viewed on a video graphics display unit the time sequence of the data may be determined. The points in the cluster near A appear at the very beginning of the storm. As time progresses the isolation increases to point B then decreases along the "spiral" toward point C. This isolation increase is also indicated in the isolation time history presented in the previous chapter, Figure 3-8c. This isolation increase is caused by the depolarization of the incoming wave. In this case the depolarized wave is more closely matched to the receiving antenna thus increasing isolation. Figure 4-11 is an attenuation versus phase polar plot

ISOLATION VS PHASE
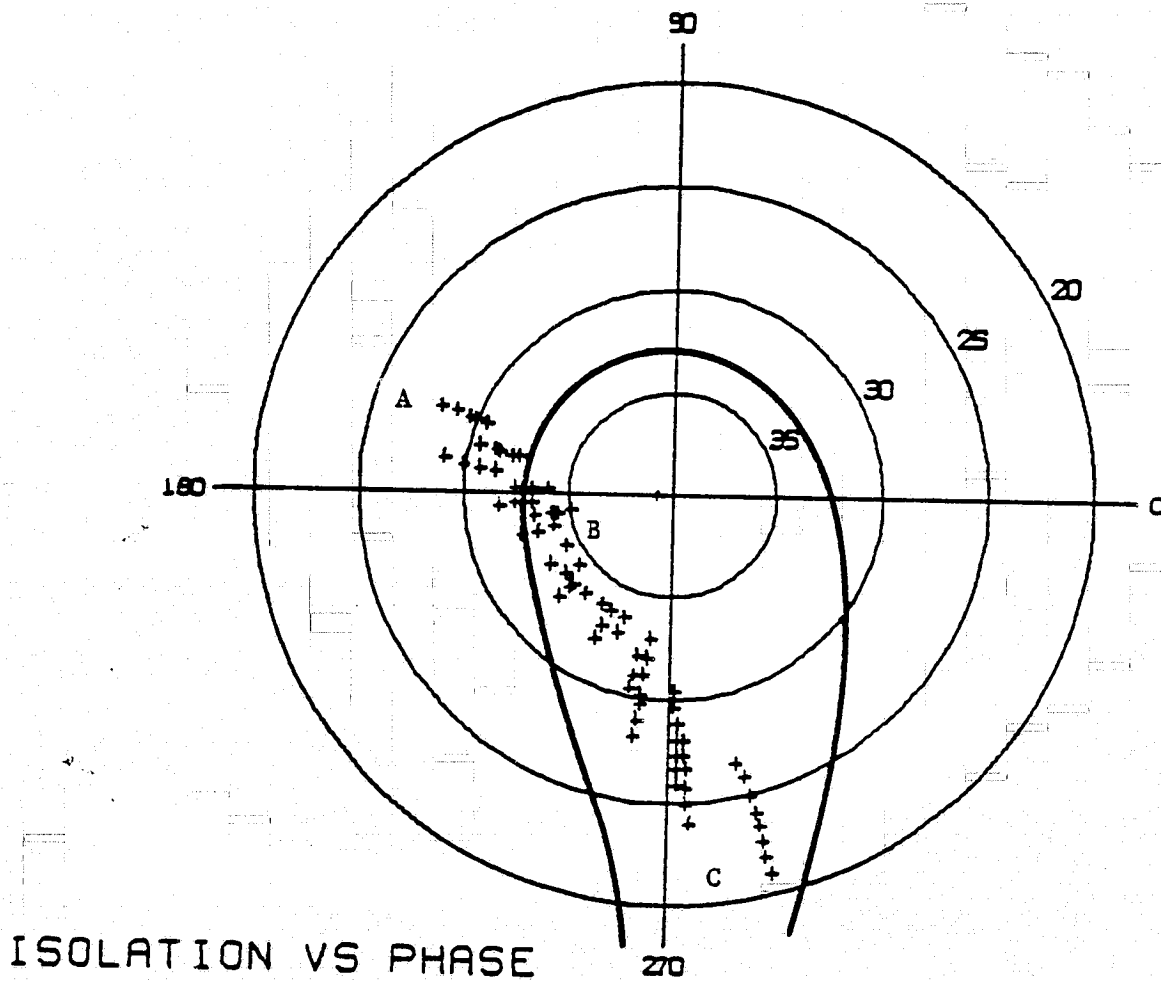
Figure 4-10. 11.7 GHz phase data with antenna error
bounds showing cluster of points near A
which lies outside the bound.

ATTENUATION VS PHASE
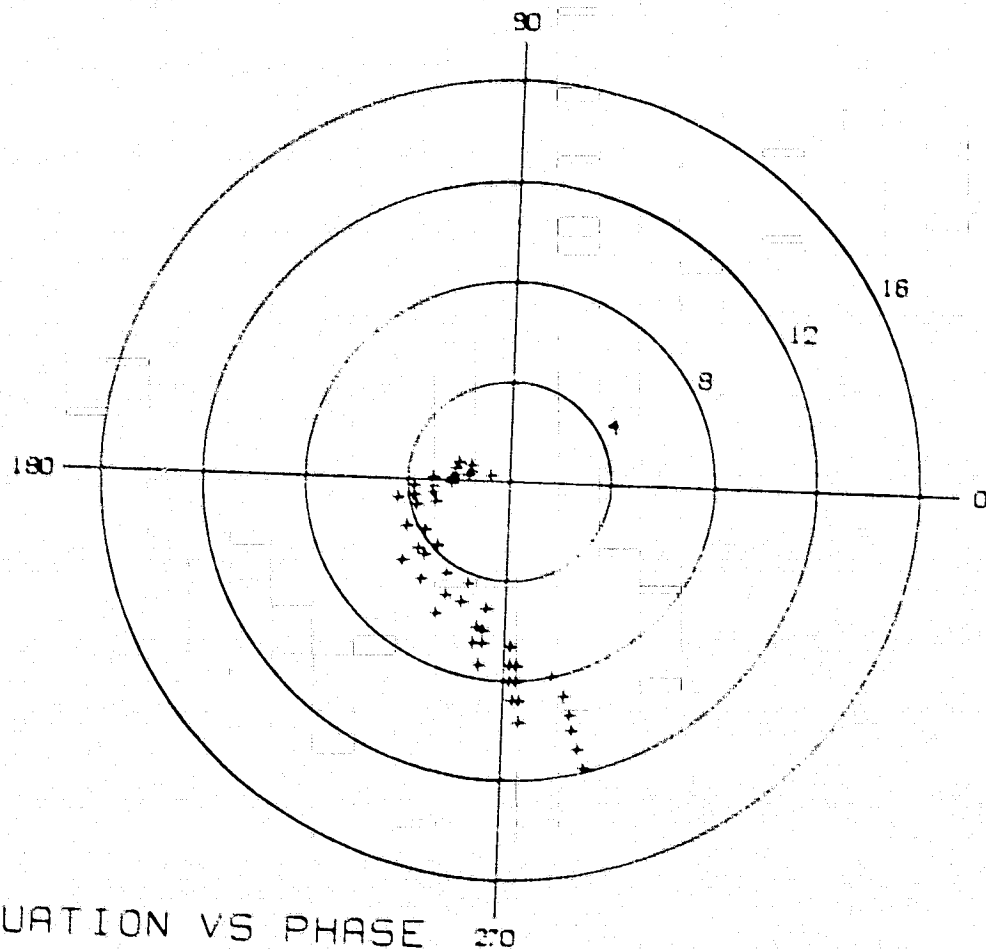
Figure 4-11.   Attenuation and phase data covering the same
time period as Figure 4-10. This shows the
small attenuation experienced during the
initial depolarization.

covering the same time period as that of Figure 4-10. It is seen
that a relatively low attenuation of 1 to 3 dB occurs during this
period of depolarization. Ice crystals in the path can account for
this type of behavior [7].

Storms typically traverse the 11.7 GHz path perpendicularly.
Many of the more severe summer storms are characterized by a large
expanse of clouds at a high altitude. This is illustrated in Figure
4-12. This high altitude portion of the storm possibly contains ice
and as the storm progresses, the path intersects this portion of the
storm first causing the observed data. Later in time the rain
dominates the propagation and the large decrease in isolation is seen
along with an additional phase change.

A variation of this concept assumes no ice. Brussaard [13] has
stated that the raindrop canting angle is dependent on the vertical
wind gradient and that the raindrop canting angle can change by
almost 20° in its last 200 meters of fall. Assume that at the
beginning of a rain event the satellite-earth station path inter-
sects the high altitude portion of the storm where raindrops are
only slightly canted. Later, as ground rainfall begins, the drops
through which propagation occurs are more severely canted due to low
altitude wind gradients. A 20 ° change in canting angle could account
for the 40° change in phase from points A to B in Figure 4-11. Low
altitude rainfall propagation effects later dominate causing the
data from B to C. Figure 4-12 also illustrates this effect.

Typically, ground rainfall begins a substantial amount of time
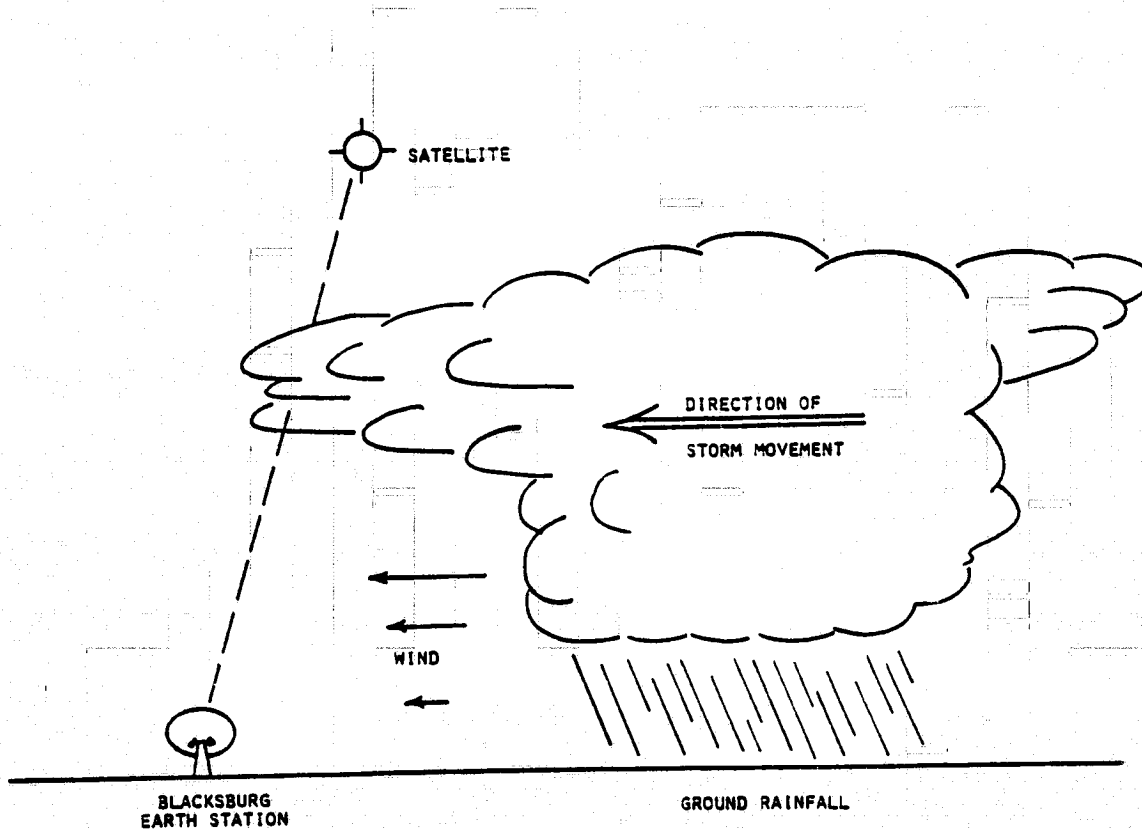
Figure 4-12. A typical rain storm at the
VPI&SU earth station.

after an isolation-attenuation event commences. This would tend to substantiate the above arguments.

The satellite transmits a RHCP wave which means the 2θ term in the Δ phase equation (122) carries a negative sign. In order for the phase to advance the canting angle must move in a negative direction. Assuming a zero canting angle at high altitudes the prevailing winds in Blacksburg are from the direction required to force a negative canting angle at low altitudes, again substantiating the above arguments.

Figures 4-13 and 4-14 show some unusual propagation events that were observed with the 11.7 GHz system. Figure 4-13 shows an event in which the phase appears to spiral in the predicted direction. Close inspection of the data indicates that the corresponding fade was only 2 dB, thus the polar plot probably covers just the beginning of a typical summer storm that did not materialize. This plot represents only the "cluster" of points discussed previously.

Figure 4-14 illustrates the effects of snow. This plot covers a five hour period of relatively heavy snowfall in January. It is not certain whether there was snow accumulation on the antenna at this time but the data does not show the typical characteristic of snow accumulation.

The most outstanding characteristic seen in all of the 11.7 GHz circularly polarized propagation data is the wide scatter of the data. This is largely due to canting angle changes, either absolute changes or oscillations. The exact nature of the change is less
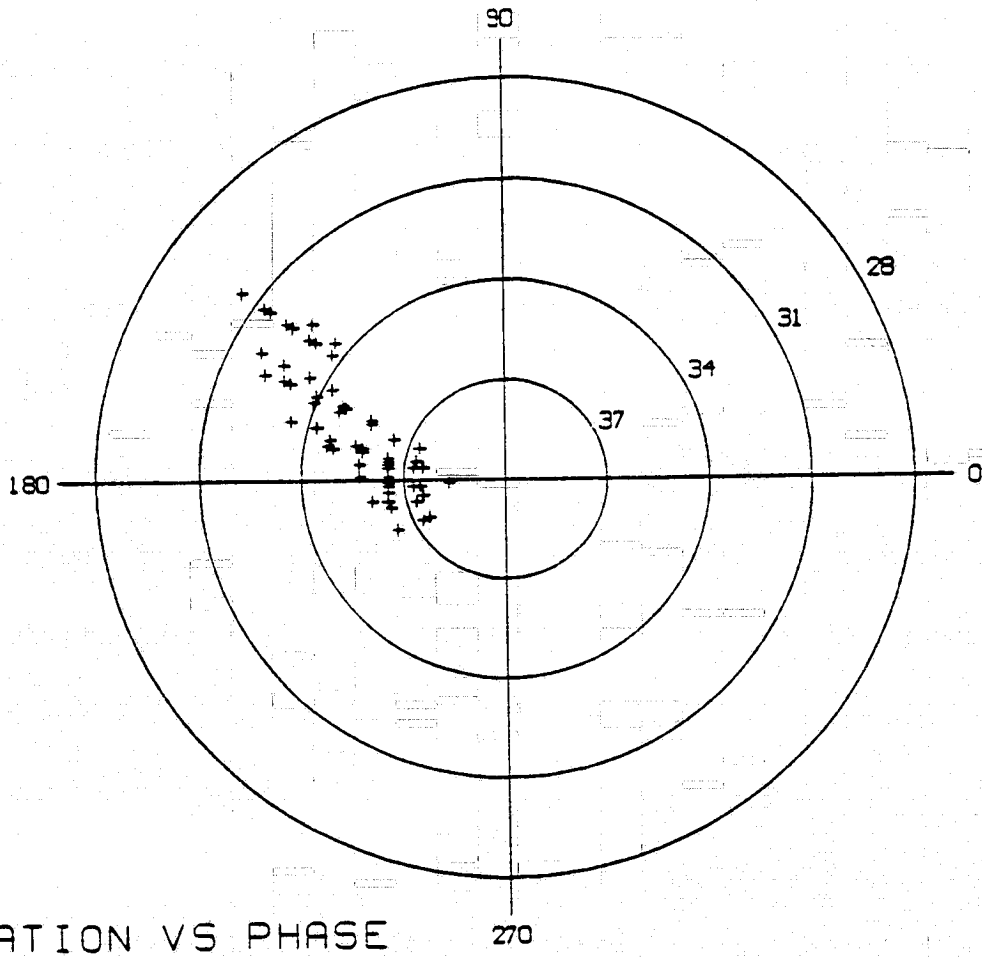
ISOLATION VS PHASE

Figure 4-13. 11.7 GHz phase data associated with a
2 dB fade. The storm occurred at
1100 EST July 24, 1977.

ISOLATION VS PHASE
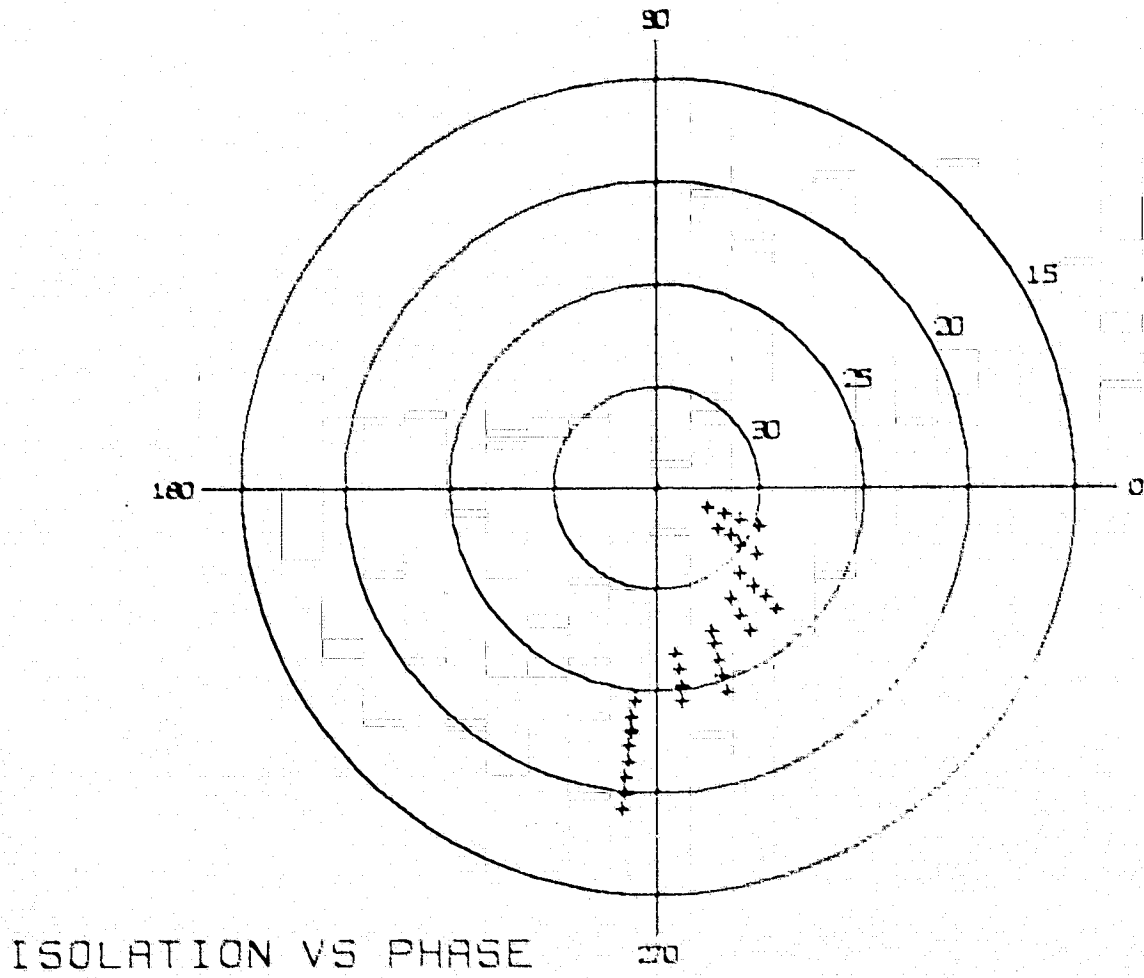
Figure 4-14. 11." GHz phase data taken during a January
snowstorm. The storm occurred at 1800 EST
January 12, 1978.

important than the 2θ phase change that occurs.

A cancellation system which relies on an unchanging phase is adversely affected by the variability of the phase of a circularly polarized wave. It is for this reason (among others) that linear polarization should be favored for satellite communications systems.

4.2   28.56 GHz Linear Polarization

This section presents and briefly discusses phase and isolation data observed using the 28 GHz linearly polarized system. As with the 11.7 GHz data, the 28 GHz data presented exhibits a particular characteristic that is common to a large percent of the individual events. The characteristic is due more to the polarization than frequency, though.

Figure 4-15 is a polar plot of isolation versus phase for an event which occurred late one evening in August. The particular phase behavior seen here is representative of the bulk of propagation events. This was a severe storm as evidenced by the 25 dB fade shown in the storm time history, Figure 4-16. It should be noted that the receiver did not loose lock during this storm. Loss of lock would be indicated by a gap in the time plot.

The computer software used to control the experiment requires that a 10.7° phase change occur in order to record a new data value.* This causes the recorded data to assume positions along a nearly straight line. If all phase changes were recorded the data points would show slightly increased scatter but would be centered about

---

* This is necessary to keep small phase changes from rapidly filling up the computer memory.

ISOLATION VS PHASE
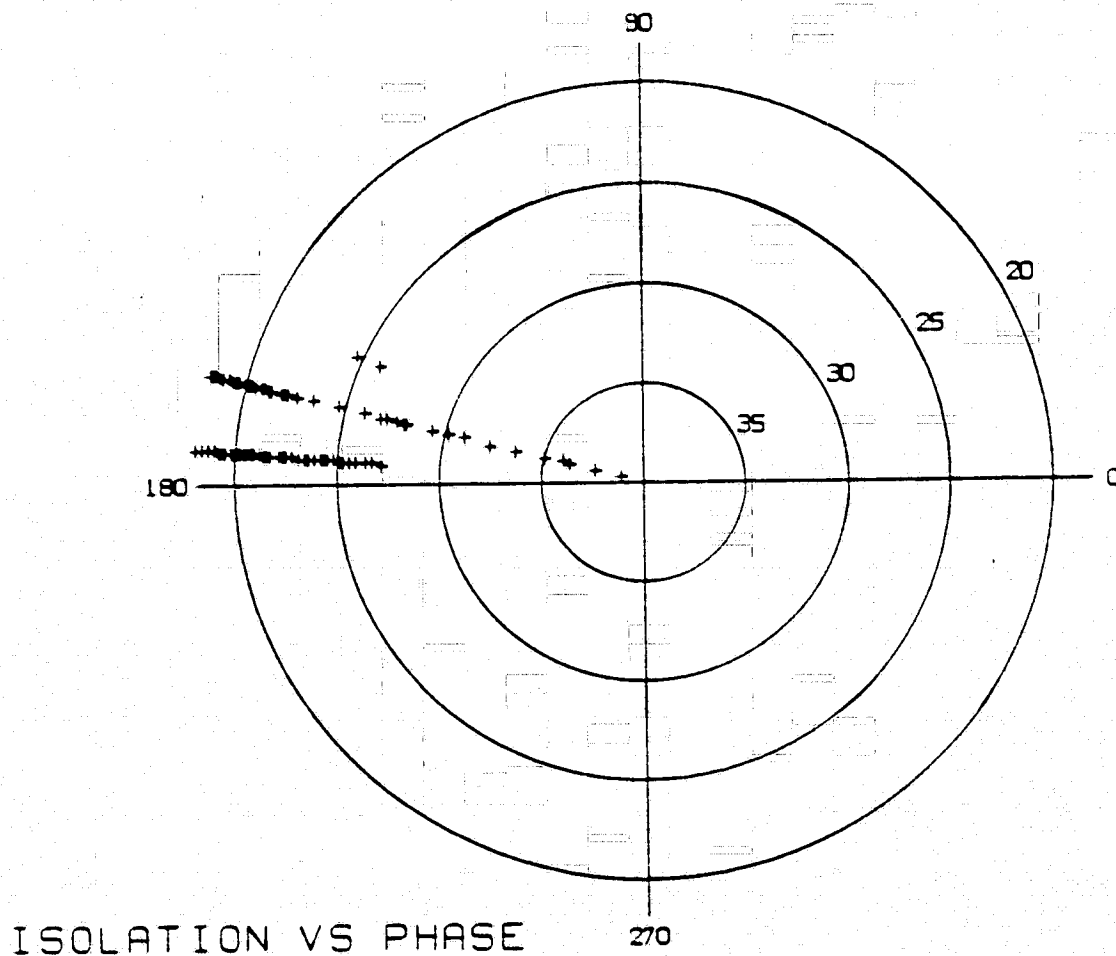
Figure 4-15.   28.56 GHz phase data showing a characteristic
small phase change.   The straight line
effect is because of the method of computer
data storage.   The storm occurred at
1430 EST August 21, 1977.
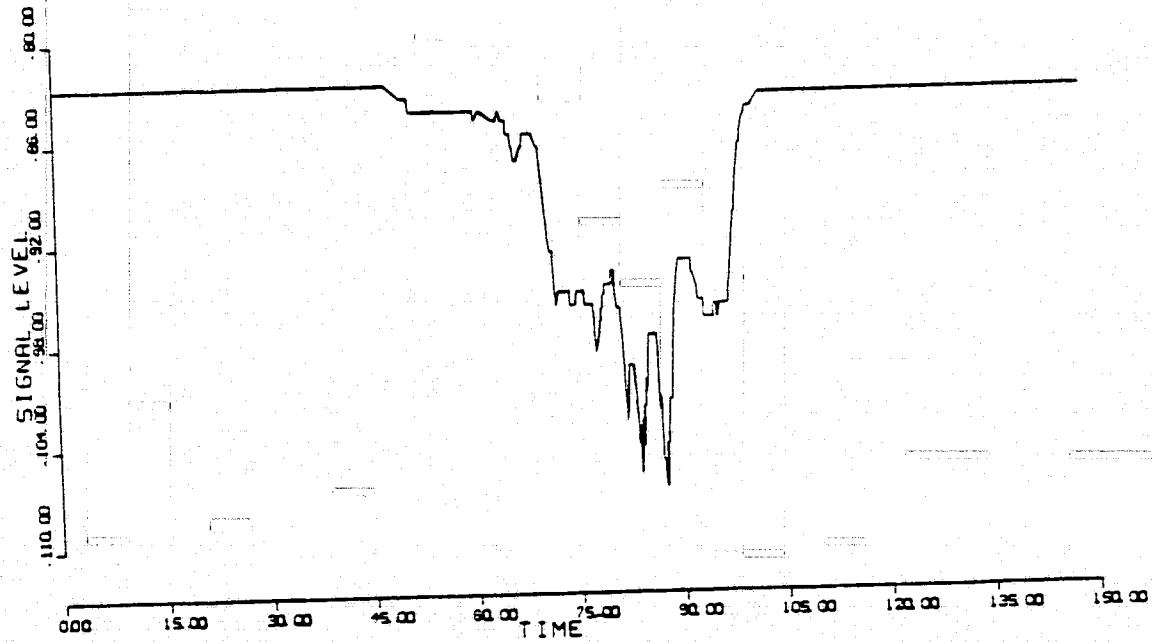
Figure 4-16. Copolarized signal level for storm presented in Figure 4-15.

the same region.

Figure 4-17 shows data from a typical 28 GHz depolarization event. The theoretical phase bounds are also included in the figure to show that in this case, as in most, the observed data falls within the prediction bounds.

Figure 4-18 illustrates another summer event associated with, in this case, a 12 dB fade. A considerable degradation in isolation and a larger than normal phase change are indicated in the figure.

Figures 4-19 through 4-21 show data from an early winter rain storm. The rain persisted for a three day period of almost continuous light rain intermittently increasing to higher rates for brief periods of time. During the first day (Figure 4-19) a maximum fade of 15 dB was experienced. The polar plot shows very typical behavior. During day two (Figure 4-20) a maximum fade of 20 dB occurred and the receiver lost lock briefly during some prolonged fades. The polar plot shows the bulk of data lying near the 160° value with some scattering of points probably caused by the receiver intermittently loosing lock. During the third day (Figure 4-21) a considerably higher average rain rate occurred with some periods of prolonged receiver loss of lock. The polar plot shows a wide scatter of points most likely due to receiver problems. Still the bulk of data is in the vacinity of 160°.

Figure 4-22 shows another early winter rain event where the data shows a larger than normal scatter. Again the bulk of points lie near the predicted values. An 18 dB fade was experienced during

ISOLATION VS PHASE
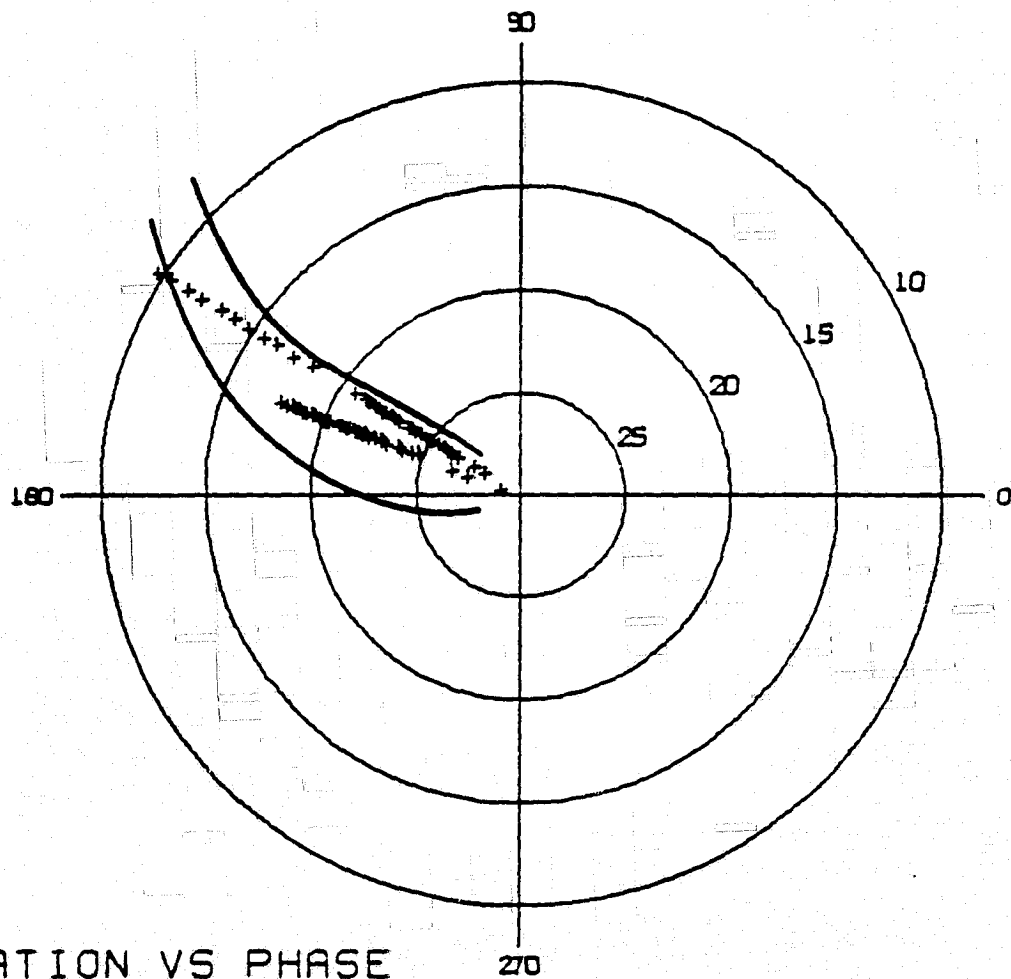
Figure 4-17. Typical 28.56 GHz phase data with maximum theoretical prediction bounds. The storm occurred at 1700 EST September 6, 1977.
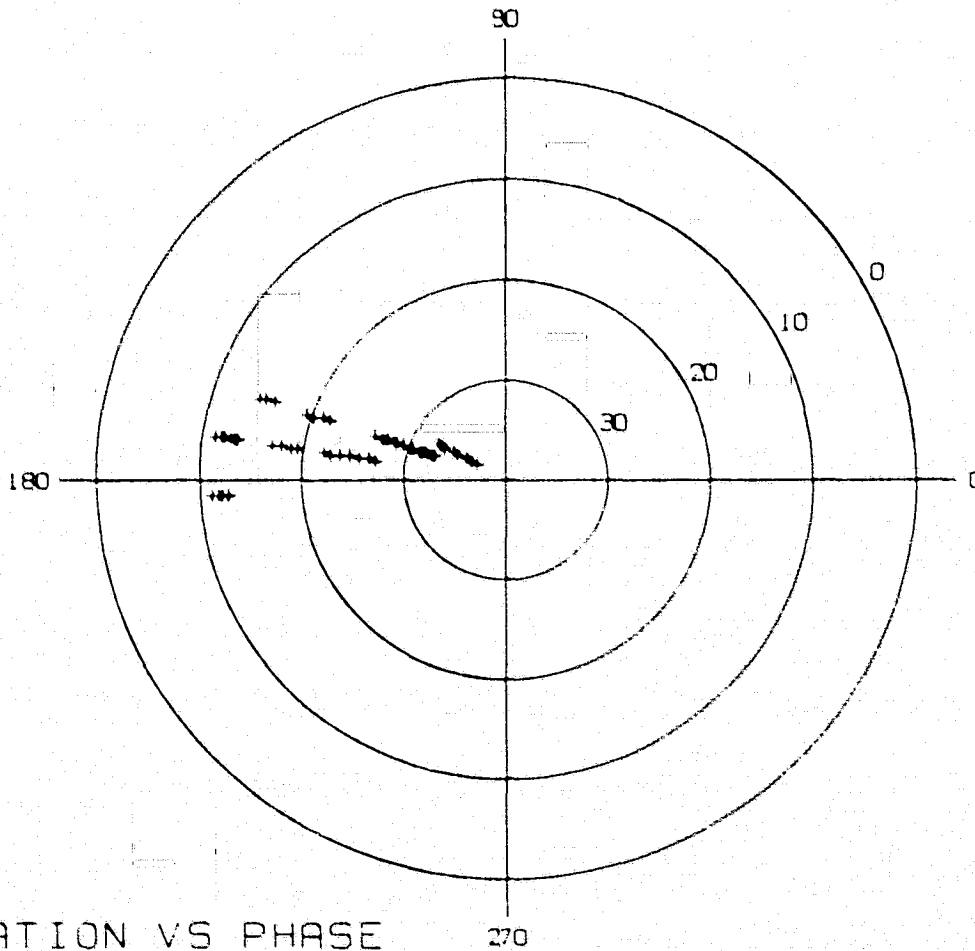
ISOLATION VS PHASE

Figure 4-18. 28.56 GHz phase data showing a larger
than normal phase change which was
associated with a severe depolari-
zation event. The storm occurred
at 1930 EST August 29, 1977.
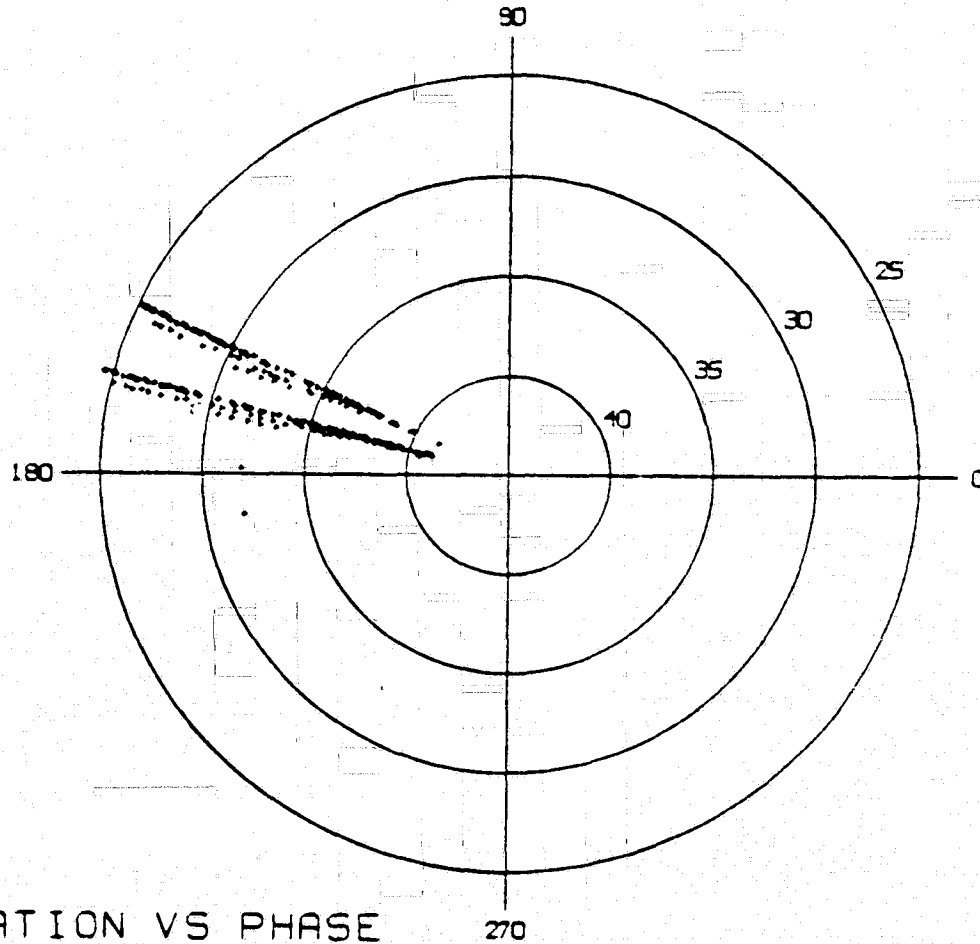
ISOLATION VS PHASE

Figure 4-19. 28.56 GHz phase data taken during a one
day period of continuous rain. The
typical behavior is illustrated here.
The storm occurred all day December
26, 1977.

ISOLATION VS PHASE
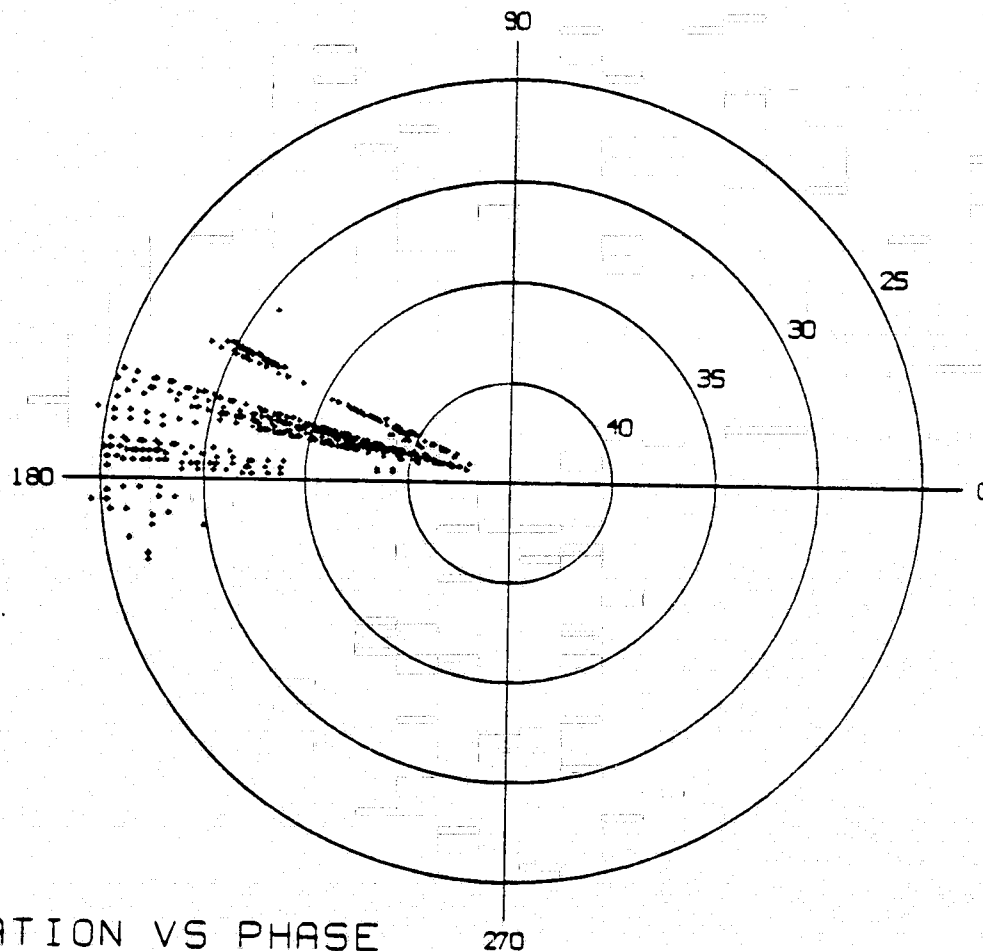
Figure 4-20. 28.56 GHz phase data covering a one day period.
Receiver intermittent loss of lock increased
the scatter. The storm occurred all day
December 27, 1977.
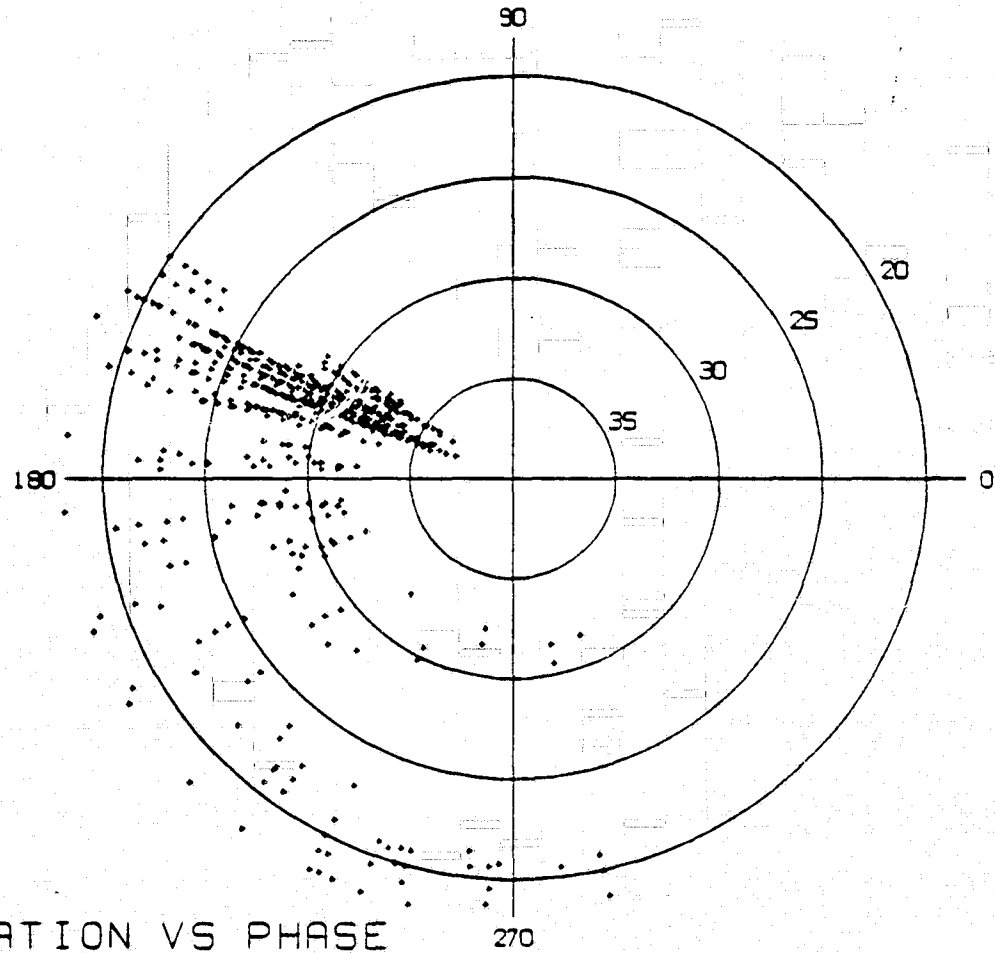
ISOLATION VS PHASE

Figure 4-21. 28.56 GHz data covering a one day period.
Periods of prolonged receiver unlock
contribute to severe scatter of data.
The storm occurred all day December 28,
1977.
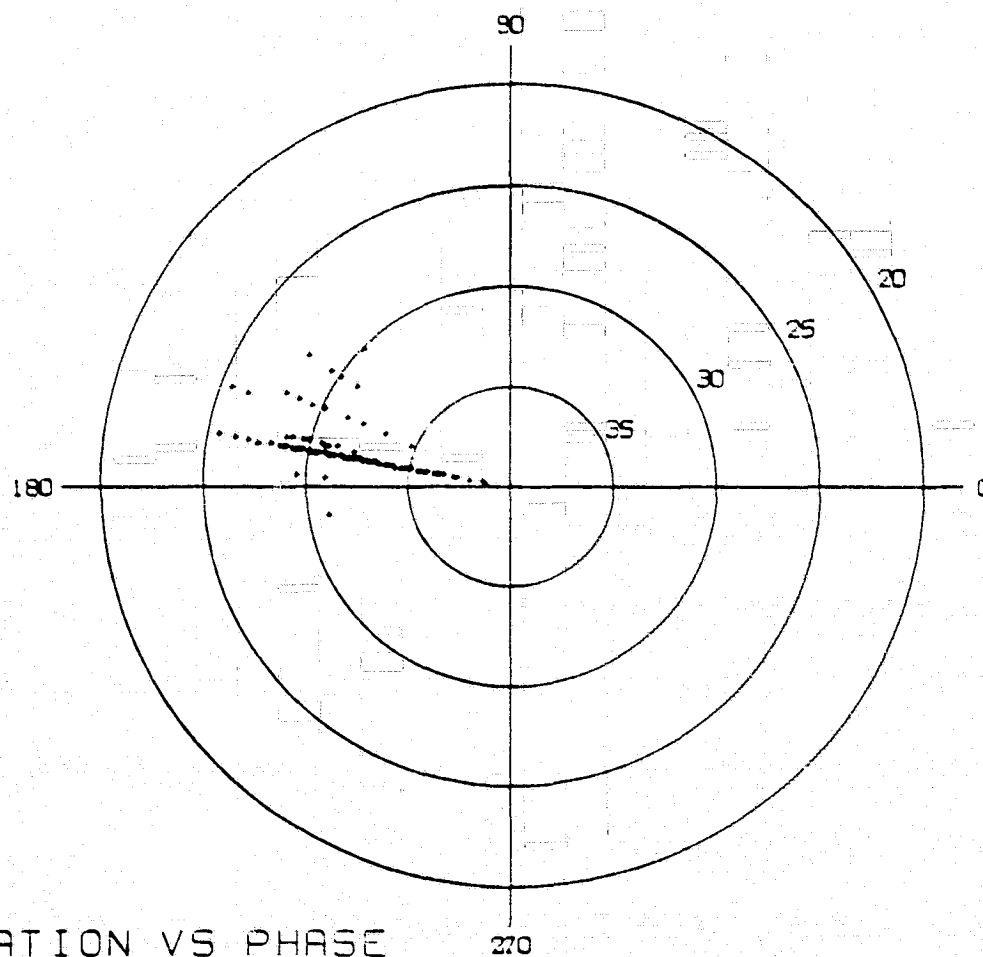
ISOLATION VS PHASE

Figure 4-22. 28.56 GHz phase data from early winter
rain storm. The storm occurred at
2330 EST December 7, 1977.

this event.

Many more events could be shown where the crosspolarized phase remained within 10° of its average value. The most dominant behavior exhibited with 28 GHz linear polarization is the small phase variation. This is attributable to the slight canting angle dependence of phase with linear polarization. Such stability is a positive aspect if a cancellation system is being considered.

CHAPTER 5

ELIMINATION OF CROSSTALK CAUSED BY DEPOLARIZATION

5.1 Discussion

It has been stated that precipitation degrades the performance of microwave communications links operating above 10 GHz. Precipitation effects include depolarization and attenuation of which only the problem of attenuation has a relatively straightforward solution. Large antennas and sensitive receivers provide system margin to allow for rain attenuation but depolarization is not affected by system margin and none of the classical methods of increasing the margin are of help. Several methods are available to decrease the effects of depolarization, though, and they will be discussed in this chapter. In the design of such depolarization compensation systems attenuation must be considered for it is of no use to maintain high channel isolation beyond the point in which a fade has disabled the communications link.

5.2 Systems

A number of methods have been proposed for increasing the channel isolation on a dual-polarized communications link during a rain event [18,19,20]. These methods fall within two basic categories, (1) the use of polarization matching antennas, and (2) the use of cancellation systems. The polarization matching antenna generally has devices in the circular waveguide ahead of the

orthomode transducer (OMT) that provide a differential phase and a differential attenuation exactly opposite to that of the rain propagation medium. The magnitude of these variables and the physical angle at which they are applied are adjusted so that the waves entering the OMT are orthogonal. Although not a requirement of this technique, all proposed systems of this type use a real-time computer to search for and maintain the correct feed network adjustment. This results in a fully adaptive system. The advantages of this system include (1) some of the waveguide components needed already exist in most feed networks, and (2) the system performance is good. Some disadvantages are (1) the possible increase in system noise temperature due to the increased feed complexity and (2) the large expense involved.

An alternative crosspolarization compensation scheme is the cancellation network shown in Figure 5-1. This network is inserted at some point after the OMT. The principle of cancellation has been known for years; the sum of two equal amplitude sinusoids which are 180° out of phase is zero. This cancellation system may be inserted before the low noise amplifier (LNA) but the couplers and attenuators will increase the system noise temperature. If the receiver components are of high phase stability and if care is taken in the design of the system, the cancellation network may be placed after the LNA or in the receiver IF section. This system can be made fully adaptive by providing variable attenuators and phase shifters controlled by a real-time computer. If implementation at
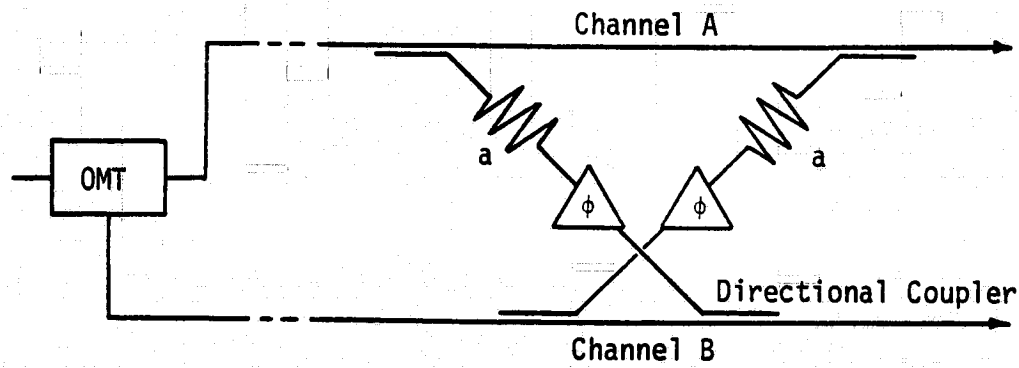
Figure 5-1. A general cancellation network which can be
inserted before or after the LNA.

RF is desired various ferromagnetic and PIN-diode attenuators and phase shifters are available [21]. Many of these are well suited to computer control. Advantages of this system include its simplicity.

Both techniques are applicable to an uplink as well as a down-link by applying, in effect, a predistortion to the wave which will be cancelled by the rain propagation medium. Both systems require a criterion for adjustment on both the downlink and uplink; i.e. the system controller should known on what basis to judge if an adjustment is necessary.

5.3 A Simple but Effective Cancellation System

Work has been done on the fully adaptive systems discussed previously and practical systems have been developed [22]. These systems are somewhat complex and expensive and are therefore suited to the large high volume earth station.

The purpose here is to propose a simple, inexpensive system that will be useful on the small domestic or private earth terminal. The fully adaptive systems can maintain isolation above an acceptable level for a large percent of the rain events that occur. No such claim will be made about this simple system but this system will provide improved performance during a significant amount of time that would otherwise be down-time.

The system consists of a cross-coupled cancellation network of the type previously discussed. One arm of this network is reproduced in Figure 5-2. The operation of a single arm is sufficient to
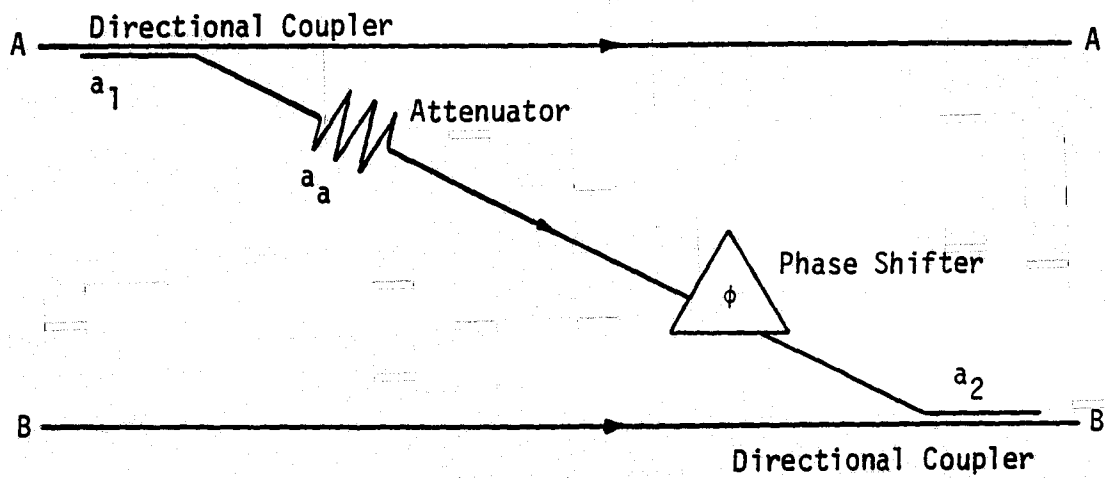
Figure 5-2. One cross-coupling arm of
a cancellation network.

describe the operation of the total system. Neglect the signal in channel B for the moment and consider that channel B contains only the crosspolarized component of channel A. The crosspolarized component is undesired.

Total cancellation of the undesired component requires that the total attenuation $a_a + a_1 + a_2$ and the phase shift ϕ be continuously changed in order to follow the changes in rain propagation conditions. The circuitry required for this can become exceedingly complex.

Several simplifications can be made to reduce the system complexity considerably. If enough is known about the characteristics of the crosspolarized signal level and phase, the attenuation $a_a + a_1 + a_2$ and the phase ϕ can be preset accordingly. Also if total cancellation is not required (say the acceptable minimum isolation is X dB) the values of a and ϕ can be fixed at an optimum point and isolation can be maintained higher than X dB over a large range of inputs.

With linear polarization it has been shown by theory and experiment that the crosspolarized signal phase will change very little during the progress of a rain event. This is illustrated in Figure 5-3 for 11.7 GHz and $\theta = 45°$. It has also been shown that the crosspolarized phase and signal level are very closely correlated during a majority of propagation events. Therefore in a simple cancellation system such as the one being proposed the attenuator and phase shifter are set to a value based on theory or previous measurement but remain disconnected from the system until the isolation falls below

ISOLATION VS PHASE
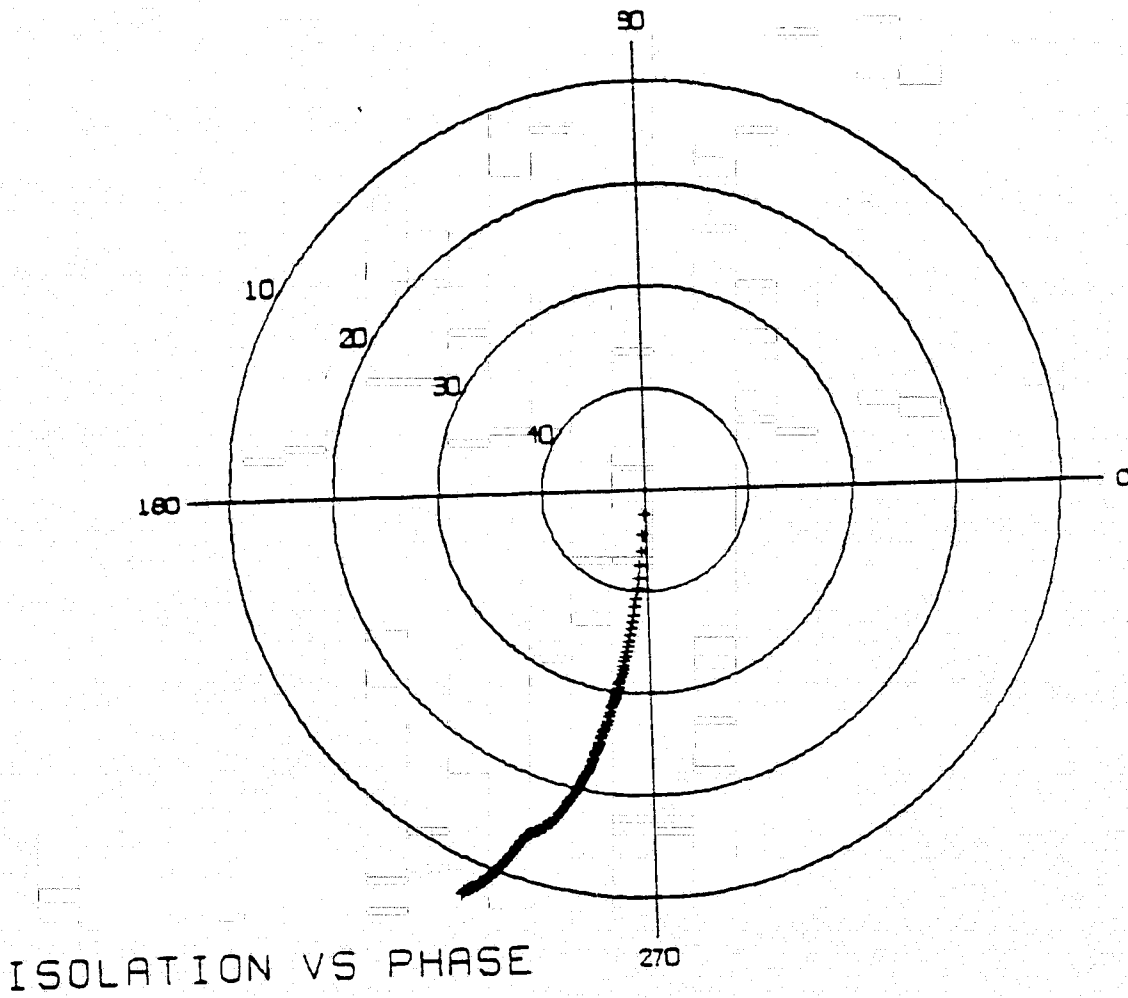
Figure 5-3. Predicted phase for 11 GHz linear
polarization indicates a maximum
of 25° phase change.

a threshold value. This provides a two state cancellation system, the two states being on and off.

Instead of an off state, certain advantages can be realized by cancelling the crosspolarization due to antennas along with any other incidental clear weather crosspolarization. The clear weather isolation can be increased to a very high level[1] by this method and the antenna phase errors can be eliminated thus enhancing the performance of the second cancellation state.

5.4 Analysis of the Two State System

In this analysis it is assumed that either perfect antennas are in use or that a clear weather cancellation state has already been applied. If this is not the case there will be errors in the cross-polarized phase and signal level that will degrade system performance but these errors will be small at low isolations where the performance of the system is most critical.

Figure 5-4 shows an approximation to isolation as a function of path rain rate for an 11 GHz linearly polarized wave, a canting angle $\theta = 45°$, and the Blacksburg 11.7 GHz effective path length. The relationship (82)

$$I = 20 \log_{10} \left\{ \frac{1 + d \tan^2 \theta}{(1 - d) \tan \theta} \right\} \tag{123}$$

----

[1] This clear weather enhancement has applications to propagation research systems [23]. With very high clear weather isolation very low levels of rain generated crosspolarization can be measured.
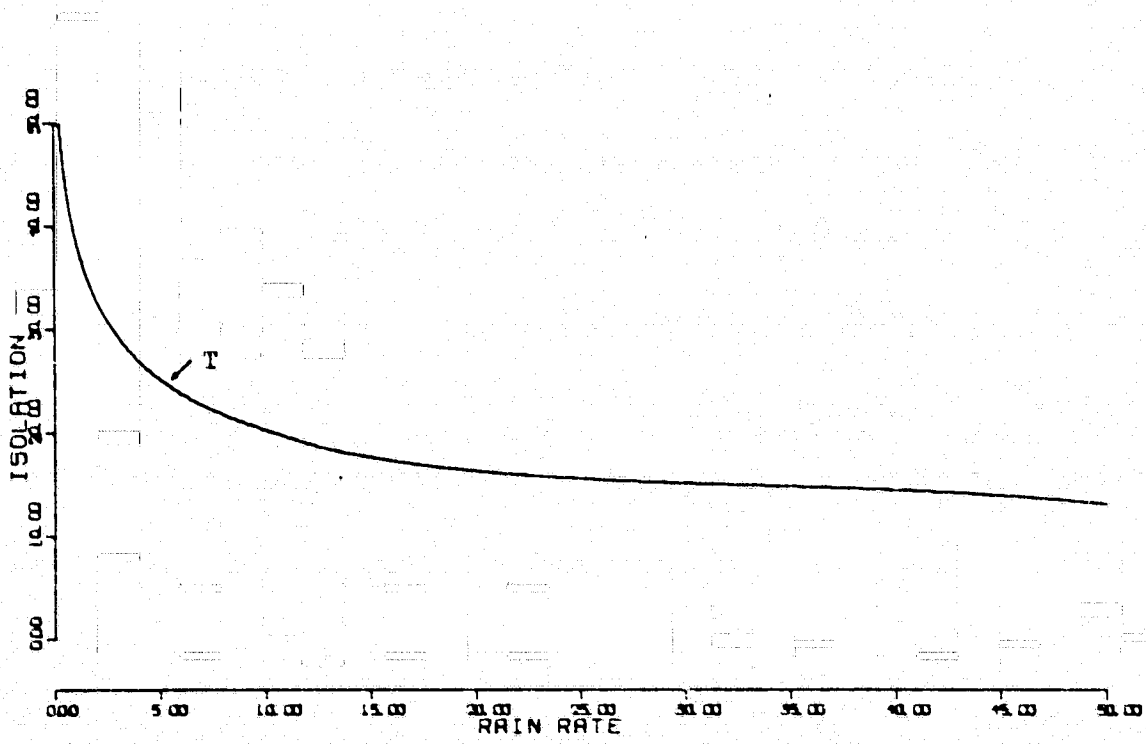
Figure 5-4.   Theoretical isolation versus rain rate.   The
point T indicates a possible threshold for a
cancellation system.

where

$$d = e^{-(\alpha + j\beta)L}$$

was used to generate the curve.

This curve also represents the crosspolarized signal level (in dB) normalized to a copolarized signal level of 1 (0 dB). Therefore this curve gives the amount of copolarized signal that must be fed through the cross-coupling arm in order to obtain full cancellation.

Assume that 25 dB is the threshold isolation below which the link will not operate. This is indicated by the point T in Figure 5-4. The crosspolarized signal level at this point is known and its phase is known by the equations developed in Chapter 2.

$$\Delta = \tan^{-1} \left\{ \frac{-e^{-\alpha L} \sin \beta L (1 + \cot^2 \theta)}{e^{-2\alpha L} \cot^2 \theta + e^{-\alpha L} \cos \beta L (1 - \cot^2 \theta) - 1} \right\} . \quad (124)$$

This phase is shown in the polar plot of Figure 5-3.

The cancellation network with 25 dB total attenuation and $\Delta + 180°$ phase shift is switched in at this point. Near perfect cancellation occurs, but as rain rate increases the level of cancellation becomes less sufficient and perfect cancellation no longer occurs. A substantial improvement over a large range of rain rates has been achieved, though, and it will be at a much higher rian rate that the isolation will again fall below 25 dB.

An improvement to this system can be made by injecting a cancellation signal which is twice the magnitude of the interfering signal

and 180° out of phase (at the threshold point). The isolation will not be improved at this point, but it will improve as the cross-polarized signal magnitude increases with increasing rain rate. The isolation will increase through a maximum then begin to decrease again. The point where isolation falls below the threshold of 25 dB will be moved to a singificantly higher rain rate.

Figure 5-5 is an illustration of the expected performance of this system with a 25 dB threshold. Also shown in this figure are the isolation without cancellation and the isolation with a cancellation network having a 20° phase error. As can be seen, the errors are small at high rain rates where performance is most critical.

An average improvement in isolation of 5 to 10 dB has been accomplished, but more improtant is that the system threshold (25 dB) has been moved from a rain rate of 5 mm/hr to 25 mm/hr ($\approx$ 18 mm/hr with a 20° phase error). If this system could stand a 22 dB isolation, the threshold point has been moved from 8 mm/hr to 35 mm/hr.

Figure 5-6 illustrates the performance of a system which was designed for a 22 dB isolation threshold. By switching in the cancellation network later during the progress of a storm much can be gained at the higher rain rates. In this case isolation has been maintained above 22 dB for rain rates in excess of 50 mm/hr.

Of course a system with a margin of 6 to 10 dB would probably be disabled due to the fade caused by a 50 mm/hr rain. Therefore the higher thresholds are advantageous. An optimum exists for each
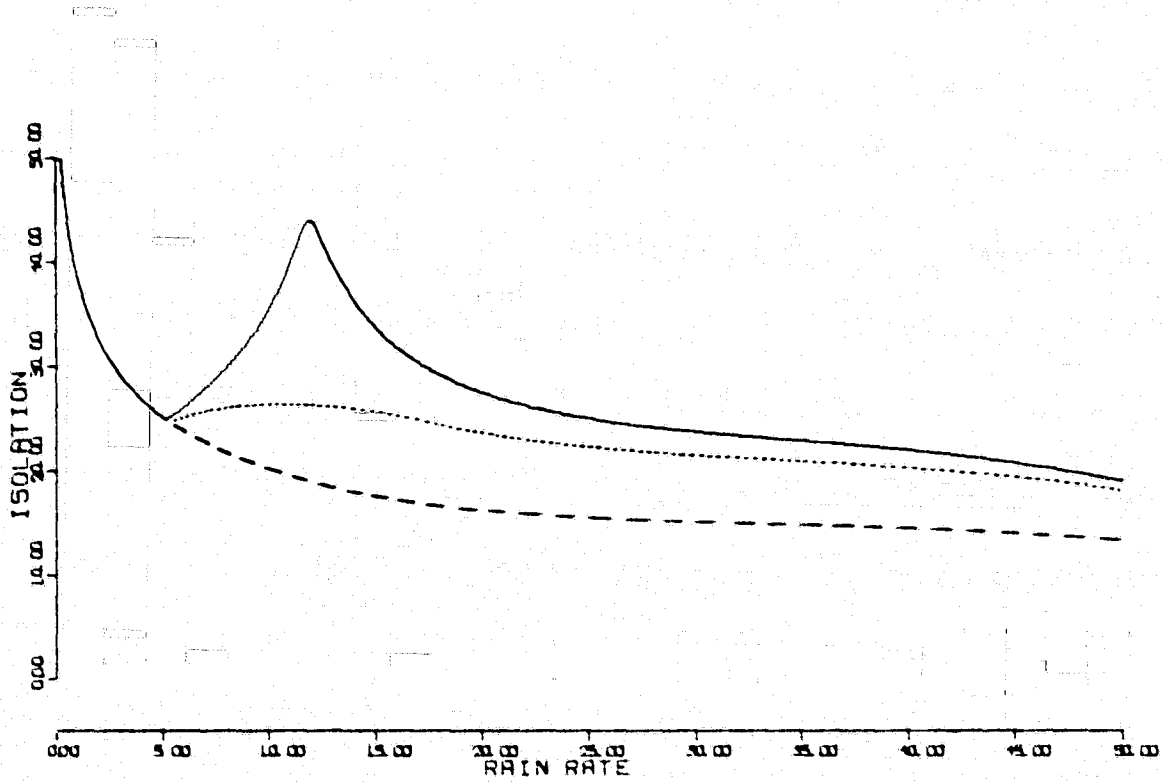
Figure 5-5. Isolation with a two state cancellation
network switched at 25 dB.
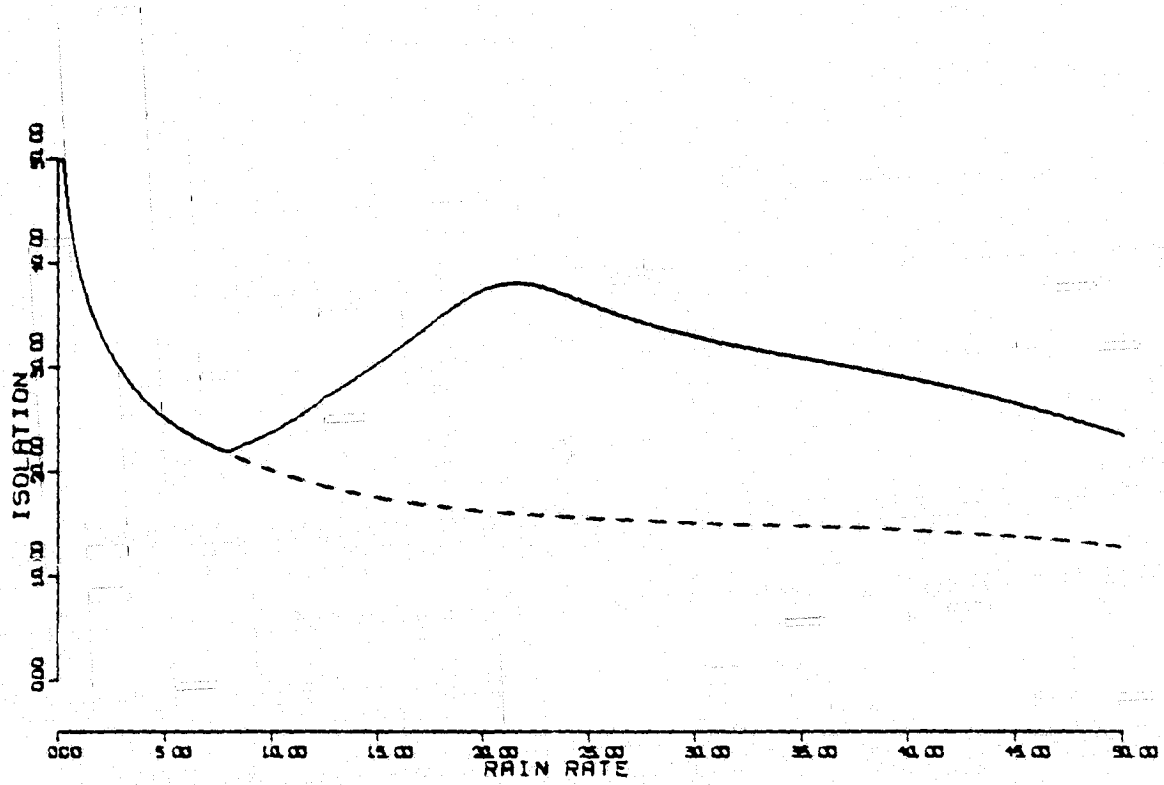
Figure 5-6. Isolation with a 22 dB threshold two state cancellation system.

particular system with its given fade margin.

The weather characteristics at the location are also important. If the location rarely experiences high rain rates and if the margin is designed accordingly, then depolarization is the dominant factor in limiting performance. Figure 5-7 illustrates the isolation of a system with a 30 dB threshold. The cancellation system moves the 30 dB isolation point from 2.5 mm/hr to 10 mm/hr. This example again emphasizes that the optimum design is determined by several factors particular to a given earth station.

The concept of the two state cancellation system may be extended to three or more states. For example, a third state is switched in when the isolation with state two in effect again reaches the threshold. Figures 5-8 through 5-10 illustrate the performance of such a system with 28, 31, and 34 dB thresholds respectively. Also included in these figures is the isolation without cancellation. The optimum threshold for switching is again relative to the situation at the particular earth station.

5.5 Criterion for Switching

It has been assumed that the cancellation network would be switched in when the isolation reaches a threshold value. This is easy to measure and implement if a beacon signal is available, but this requires a dedicated channel in the receiver and an extra carrier on the satellite transponder. Other possibilities exist for control. It has been shown that by minimizing the total power in a
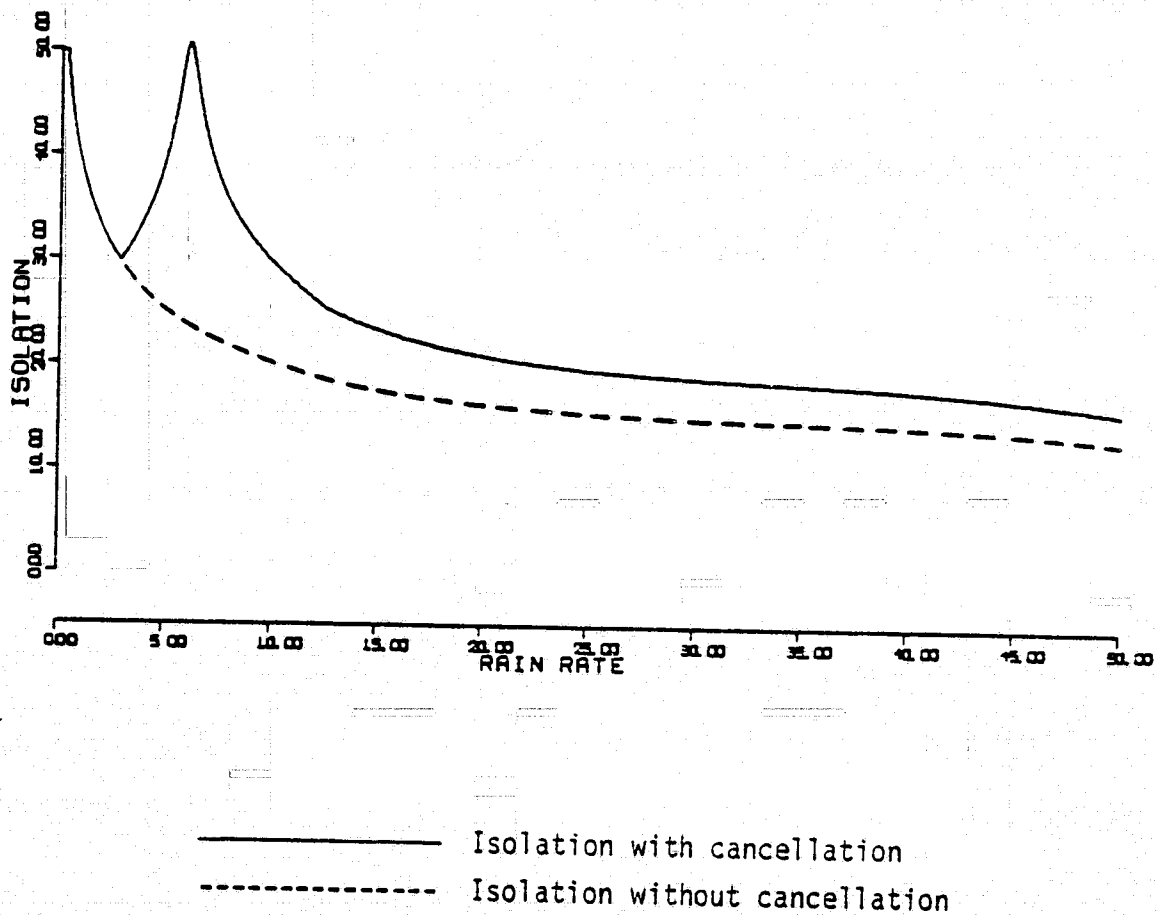
Figure 5-7. Isolation with a 30 dB threshold
two state cancellation system.

Figure 5-8. Isolation with a 28 dB threshold three state cancellation system showing improved performance.
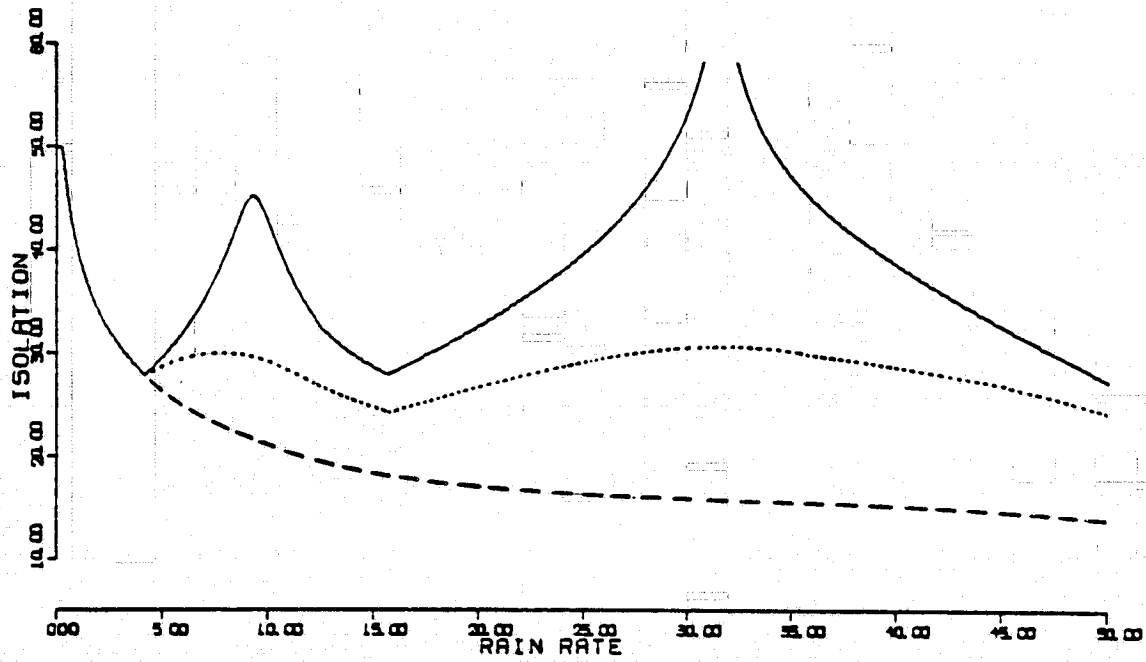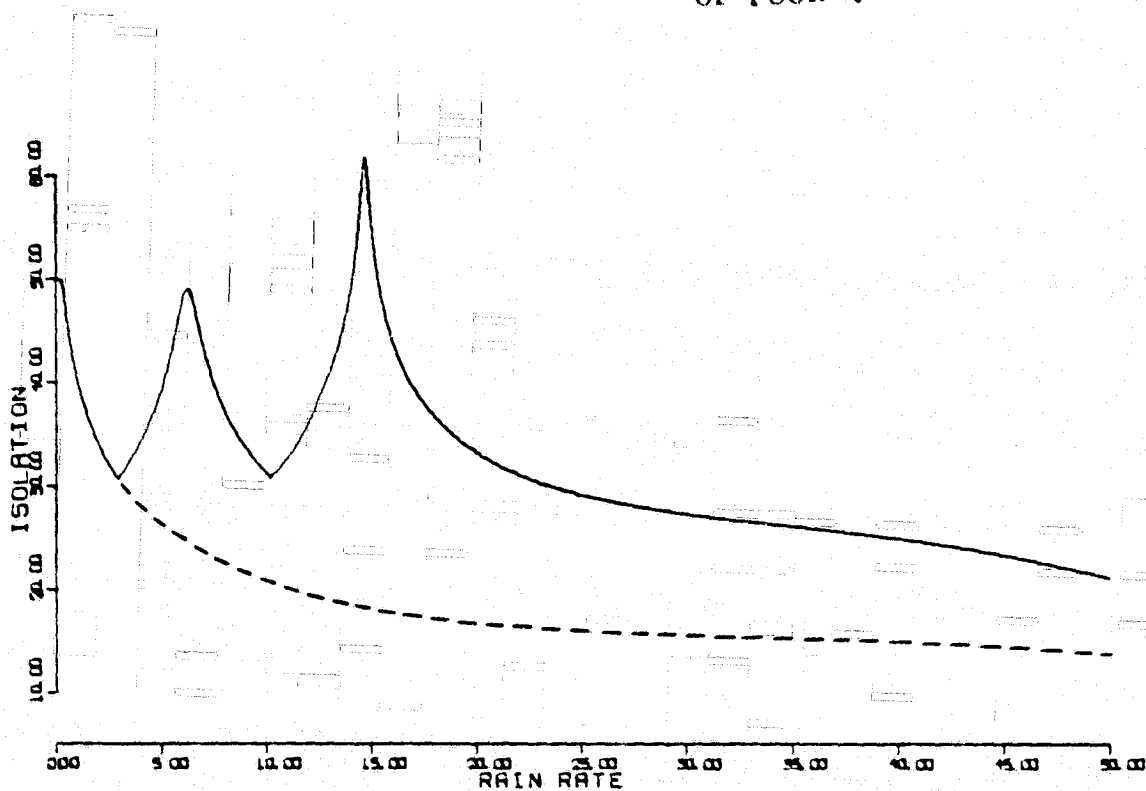
——————— Isolation with cancellation

- - - - - - - - - - Isolation without cancellation

Figure 5-9.   Isolation with a 31 dB threshold
three state cancellation system.

Figure 5-10. Isolation with a 34 dB threshold three state cancellation system.

channel that the interference is also minimized [24]. Therefore the total power in a communications channel could in some way be used as a criterion. Another approach is to place one or more raingauges under the path within several kilometers of the earth station and to switch the system at given rain rate thresholds [25]. A problem with this scheme is that a time delay between ground rainfall and rain in the path often exists. The fade measured with an AGC voltage is another possible criterion for switching [26]. Other possibilities of this type exist and many could be implemented with small expenditures.

5.6 Polarization Angle

The polarization angle of the incoming wave relative to the raindrop canting angle has an effect upon the isolation and cross-polarized phase. Depolarization is reduced when the angle θ is near $0°$ or $90°$ but the variable nature of the canting angle eliminates using this fact to improve system performance. Also a linearly polarized wave transmitted by a satellite arrives at different angles relative to the local horizon at different locations on the earth's surface. This further eliminates transmitting with an optimum polarization angle.

The possibility exists that for many polarization angles the crosspolarized signal in channel B will be different in amplitude and phase than that in channel A since differently polarized waves propagate through the rain differently. If the polarization angles

are known the difference in propagation can be included in the design of cancellation hardware.

5.7 Implementation

The multi-state cancellation system need not be implemented by separate cascaded networks, although this technique will work. A single cross-coupling network with switchable elements is the simpler method to construct such a system. Elements can be switched in parallel or series such that their phasor sum yields the desired result.

This system can be installed in the RF section of a system by using waveguide components or it may be installed in the receiver IF section. If cancellation is applied at IF it must be assured that both receiver channels preceeding the cancellation network exhibit nearly identical phase characteristics.

5.8 Performance Expectations

Perfect isolation cannot be maintained with this simple system but as the figures have indicated a substantial improvement can be realized. Several hundred dollars for this system can buy between 5 and 10 dB improvement in isolation over a reasonable range of rain rates. This several dB may mean that a system is down during only a fraction of the time that it would otherwise be disabled.

As seen in the linear polarization data in Chapter 4 some propagation events do not conform to the large bulk of data or to

the predictions. A cancellation system could likely be defeated in these cases. It is unlikely that any condition could arise in which the isolation with cancellation is worse than that without. A much larger phase change than that seen in the data must occur.

CHAPTER 6

CONCLUSION

The questions stated in Chapter 1 of this thesis were, (1) what can the phase indicate about the propagation medium, (2) is there a desired set of conditions to enhance the use of cancellation, and (3) how will phase variations affect cancellation? All of these questions have been answered; let us consider them separately.

First, the phase of a circularly polarized wave is directly dependent upon the canting angle of the raindrops in the medium. Circularly polarized radars use this fact to study a rain medium and circularly polarized satellite beacons can use this to provide additional information about the medium. It is imperative that antenna errors be eliminated if research of this type is to proceed. The static (clear weather) cancellation system can reduce antenna errors to near zero and additionally provide improved isolation measurement capability [23].

Second, linear polarization is an obvious answer to the question of what type of polarization to use. Research has shown that linear polarization has superior depolarization properties [27] and it has been shown in this thesis that linear polarization is well suited for use with cancellation systems. Furthermore polarization angles near 0° or 90° (relative to the local horizon) show decreased depolarization.

Third, phase variations in the crosspolarized wave will not

affect a fully adaptive cancellation system because the system will compensate for the changes. The system must be designed such that it can track fast phase changes that might occur [28]. A two or three state simple cancellation system will be degraded by phase errors but an allowed error of 30° to 45° will still provide some improvement. Larger variations will probably disable a simple system.

The phase has been a subject treated very briefly in the literature. It is hoped that this work will add some new insight into the problem and possibly encourage more needed work on the subject of phase and cancellation techniques.

LITERATURE CITED

1. D. C. Hogg and T. S. Chu, "The Role of Rain in Satellite Communications", _Proceedings of the IEEE_, Vol. 63, pp. 1308-1331, Sept. 1975.

2. American Heritage Dictionary of the English Language, American Heritage Publishing Co., Inc., Boston, 1973.

3. M. L. Kales, "Elliptically Polarized Waves and Antennas," _Proceedings of the IRE_, pp. 544-549, May 1951.

4. H. C. van de Hulst, _Light Scattering by Small Particles_, New York: John Wiley & Sons, Inc., 1957.

5. T. S. Chu, "Rain Induced Crosspolarization of Centimetre and Millimetre Wavelengths, _Bell Syst. Tech. J._, 1974, 53. pp. 1557-1579.

6. N. K. Uzunoglu, B. G. Evans, A. R. Holt, "Scattering of Electromagnetic Radiation by Precipitation Particles and Propagation Characteristics of Terrestrial and Space Communication Systems," _Proc. IEE_, Vol. 124, No. 5., May, 1977, pp. 417-424.

7. N. J. McEwan, "Phase of Crosspolarized Signals on Microwave Satellite Links," _Electronics Letters_, Vol. 13, No. 16, pp. 489-491.

8. J. A. Morrison and M. J. Cross, "Scattering of a Plane Electromagnetic Wave by Axisymmetric Raindrops," _Bell Syst. Tech. J._, 1974, 53 pp., 955-1019.

9. J. O. Laws and D. A. Parsons, "The Relation of Raindrop-size to Intensity," _Trans. Am. Geophysical Union_, Vol. 24, 1943, pp. 432-460.

10. W. L. Stutzman, "Theoretical Modelling of Millimeter Wave Propagation through Precipitation Media", to be published.

11. R. R. Persinger, "Millimeter Wave Propagation Modeling of Inhomogeneous Rain Media for Satellite Communications Systems", M. S. Thesis, VPI&SU, Blacksburg, Virginia, June, 1978.

12. B. O. Maher and P. J. Murphy, "Variation of Canting-Angle Distribution as a Function of Wind Velocity --- Rain-Induced Cross Polarization Prediction Models," _Electronics Letters_, Vol. 13, September 15, 1977, pp 567-668.

13. G. Brussaard, "Rain-induced Crosspolarization and Raindrop Canting", <u>Electronics Letters</u>, Vol. 10, No. 20, pp. 411-412.

14. W. L. Stutzman, <u>Mathematical Formulations and Definitions for Dual Polarized Reception of a Wave Passing Through a Depolarizing Medium (A Polarization Primer)</u>, VPI&SU, Blacksburg, Virginia, June 1977.

15. R. Rotollo, LNR Communications, Inc., Hauppage, N.Y., 1978, private correspondence.

16. C. W. Bostian, S. B. Holt, S. R. Kauffman, E. A. Manus, R. E. Marshall, W. L. Stutzman, and P. H. Wiley, "Final Report: A Depolarization and Attenuation Experiment Using the CTS Satellite", NASA Contract NAS5-22577, VPI&SU, Blacksburg, Virginia, November 18, 1976.

17. P. H. Wiley and E. A. Manus, "A Four-Quadrant Phase Indicator", Patent Disclosure, VPI&SU, Blacksburg, Virginia, May 1976.

18. T. S. Chu, "Restoring the orthogonality of two polarizations in radio communications systems - Part I", <u>Bell System Technical Journal</u>, 1971, Vol. 50, pp. 3063-3069.

19. T. S. Chu, "Restoring the orthogonality of two polarizations in radio communications systems - Part II", <u>Bell System Technical Journal</u>, 1973, Vol. 52, pp. 319-27.

20. R. W. Kreutel, D. F. DiFonzo, W. J. English, and R. W. Gruner", Antenna Technology for Frequency Reuse Satellite Communications", <u>Proceedings of the IEEE</u>, Vol. 65, pp. 370-378, March, 1977.

21. L. Stark, "Microwave Theory of Phased-Array Antennas, A Review", <u>Proceedings of the IEEE</u>, Vol. 62, pp. 1661-1701, Dec. 1974.

22. A. E. Williams, "A Dual-Polarized 4/6 GHz Adaptive Polarization Control Network", <u>Comsat Technical Review</u>, Vol. 7, pp. 247-262, Spring 1977.

23. B. G. Evans and P. T. Thompson, "Use of cancellation techniques in the measurement of atmospheric cross-polarization", <u>Electronics Letters</u>, 1973, Vol. 9, No. 19, pp. 447-448.

24. B. Widrow et. al., "Adaptive Noise Cancelling: Principles and Applications," <u>Proceedings of the IEEE</u>, Vol. 63, pp. 1692-1716, Dec., 1975.

25. W. L. Stutzman, VPI&SU, Blacksburg, Virginia, 1978, private correspondence.

26. R. E. Castle, VPI&SU, Blacksburg, Virginia, 1978, private correspondence.

27. R. A. Semplak, "Simultaneous Measurements of Depolarization by Rain Using Linear and Circular Polarizations at 18 GHz," Bell System Technical Journal, pp. 400-404, Feb., 1974.

28. N. J. McEwan and P. A. Watson, "Raindrop vibration spectra on a microwave link", IUCRM Colloquium preprints "on the fine scale structure of precipitation and EM propagation," Nice, 23-31, Oct. 1973, pp. I6-1 to I6-6.

29. M. L. Kales and J. I. Bohnert, "Elliptically Polarized Waves and Antennas," NRL Report 3686, Naval Research Laboratory, Washington, D.C., June 22, 1950.

30. J. S. Hollis, T. J. Lyon, and L. Clayton, Jr., Microwave Antenna Measurements, Scientific-Atlanta, Atlanta, Georgia, 1971; Chapter 3.

31. P. Beckman, The Depolarization of Electromagnetic Waves, Golem Press, Boulder, Colorado, 1968; Chapter 7.

APPENDIX 1A

PROOF THAT $\vec{V} \propto \vec{E} \cdot \vec{e}_{a_r}^*$ FOR CIRCULARLY POLARIZED WAVES

Given a RHCP wave

$$(R + jS) \begin{bmatrix} 1 \\ -j \end{bmatrix} \qquad \text{(A-1)}$$

and a LHCP wave

$$(L + jM) \begin{bmatrix} 1 \\ j \end{bmatrix} \qquad \text{(A-2)}$$

the sum of these waves is

$$\begin{bmatrix} R + jS + L + jM \\ -jR + S + jL - M \end{bmatrix}$$

$$= \begin{bmatrix} (R + L) + j(S + M) \\ (S - M) - j(R - L) \end{bmatrix} . \qquad \text{(A-3)}$$

This vector represents an arbitrary elliptically polarized wave. In order to extract the RHCP and LHCP components the complex vector formulation is used,

$$\vec{V} = C\vec{E} \cdot \vec{e}_{a_r}^* . \qquad \text{(A-4)}$$

The RHCP component is proportional to the phasor voltage at the terminals of a RHCP antenna. The normalized antenna vector is

$$\vec{e}_a = \frac{1}{\sqrt{2}} (\hat{x} - j\hat{y}) \quad . \tag{A-5}$$

Performing the coordinate transformation

$$\delta_r = 180° - \delta \tag{A-6}$$

yields

$$\vec{e}_{a_r} = \frac{1}{\sqrt{2}} (\hat{x} - j\hat{y}) \quad . \tag{A-7}$$

Therefore

$$\overline{V}_{RHCP} = C \vec{E} \cdot \vec{e}_{a_r}^{\star}$$

$$= \frac{C}{\sqrt{2}} ([(R + L) + j(S + M)]\hat{x} + [(S - M) - j(R - L)]\hat{y}) \cdot (1\hat{x} - j\hat{y})^{\star}$$

$$= \frac{C}{\sqrt{2}} ([(R + L) + j(S + M)]\hat{x} + [(S - M) - j(R - L)]\hat{y}) \cdot (\hat{x} + j\hat{y})$$

$$= \frac{C}{\sqrt{2}} [(R + L) + j(S + M)] + j[(S - M) - j(R - L)]$$

$$= \frac{C}{\sqrt{2}} [(R + L) + (R - L)] + j[(S + M) + (S - M)]$$

$$= C \sqrt{2} (R + jS) \quad . \tag{A-8}$$

A similar procedure yields

$$\overline{V}_{LHCP} = C \sqrt{2} (L + jM) \quad . \tag{A-9}$$

Q.E.D.

APPENDIX 1B

DISCUSSION OF THE $\overline{V} = \vec{E} \cdot \vec{e}_{a_r}^{\,*}$ FORMULATION

1B.1 Introduction

Several mathematical formulations exist for wave-antenna inter-action which may be used to calculate the magnitude of an antenna terminal voltage or the received power [14,29]. When both magnitude and phase of the terminal voltage are required the complex vector formulation must be used [30]. In this formulation the incoming wave and the antenna polarization state are represented by complex vectors. The antenna phasor voltage is given by

$$\overline{V} = C\vec{E} \cdot \vec{e}_{a_r}^{\,*} \tag{A-10}$$

where

$\overline{V} =$ the phasor voltage at the antenna terminals

$\vec{E} = \overline{E}_x \, \hat{x} + \overline{E}_y \, \hat{y} =$ a complex vector representing the
incoming wave in its own coordinate
system

$\vec{e}_{a_r} = e_x \, \hat{x} + e_y \, e^{j\delta} \, \hat{y} =$ a complex vector representing the
antenna polarization state in the
coordinate system of the incoming
wave

e_x, e_y are real numbers such that $e_x{}^2 + e_y{}^2 = 1$

C = a constant representing the antenna effective height

the "$\cdot$" indicates the vector dot product

the "$*$" indicates the complex conjugate .

Sometimes an equivalent form of the complex vector formulation is seen in which the wave and antenna states are represented as one-dimensional matrices.

$$\overline{V} = C[E]^t [e_{a_r}]^* \tag{A-11}$$

where

$$[E] = \begin{bmatrix} \overline{E}_x \\ \\ \overline{E}_y \end{bmatrix} \qquad [e_{a_r}] = \begin{bmatrix} e_x \\ \\ e_y\, e^{j\delta} \end{bmatrix} .$$

The "t" indicates the matrix transpose and the "$*$" indicates the complex conjugate of the matrix. It is immediately apparent that the complex vector representation and the matrix representation are identical. Henceforth the complex vector form will be used.

When used properly these equations yield correct results, but this involves several constraints that are not initially obvious. The antenna polarization state, $\vec{e}_a$, is usually defined by the wave that the antenna transmits, while the above relations require that the receiving state, $\vec{e}_{a_r}$, be used. An antenna is a reciprocal device

meaning that if it transmits a wave with a given axial ratio and tilt angle it will respond optimally to a wave with the same orientation in space. This wave to which the antenna responds optimally is <u>not</u> necessarily of the same polarization as the one that it transmits. This is because the waves are travelling in opposite directions and different coordinate systems are employed in defining their polarization state. Therefore a coordinate transformation must be performed before the complex vector formulation may be used. The complex conjugate appearing in the equations <u>does</u> <u>not</u> accomplish the transformation.

The placement of the complex conjugate is a point worth consideration. If the conjugate is placed on the wave state rather than the antenna state the resulting voltage is of equal magnitude but opposite phase. There is no immediately obvious reason for placing the conjugate on one member or the other. This point is not directly addressed in the literature, and this coupled with the fact that the absolute phase of a voltage is usually of little importance raises some suspicion about the validity of phase calculations. As it turns out, the placement of the conjugate is correct. This and the question of the coordinate transformation will be discussed in detail below.

It is necessary to establish and adhere to coordinate systems and conventions in calculations involving wave-antenna interaction. The standard convention used here consists of an xyz right-handed system with the positive z-axis in the direction of propagation.

This is illustrated for a general wave, a wave leaving a transmitting antenna, and a wave incident upon a receiving antenna in Figures A-1a, 1b, 1c. Figure A-1b also represents the transmitting antenna coordinate system and Figure A-1c represents the receiving antenna coordinate system.

1B.2 The Conjugate

Consider an antenna which can be represented by two elemental antennas A and B which are individually matched to orthogonally polarized waves, and some kind of a feed network that combines the outputs of the elements. This antenna is illustrated in Figure A-2. The antenna state is defined by the type of wave that it radiates. Establish a unit vector $\hat{a}$ which represents the polarization state of antenna element A and a vector $\hat{b}$ which represents the state of antenna element B. The unit vectors are orthogonal and fixed in their spatial orientation. The radiated field at plane M in the far field is then

$$\vec{E}_a = \overline{A}\,\hat{a} + \overline{B}\,\hat{b} \quad . \tag{A-12}$$

Consider the phase of $\overline{A}$ and the phase of $\overline{B}$, α and β respectively. Say α is greater than β. Upon receiving this antenna is matched to a wave which has an α less than β by the same amount [31]. This is essentially a statement of the fact that an advance for a wave travelling in one direction is a delay for a wave travelling in the opposite direction.
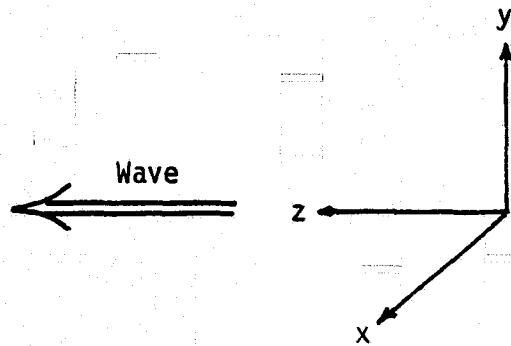
Figure A-1a. Wave coordinate system.

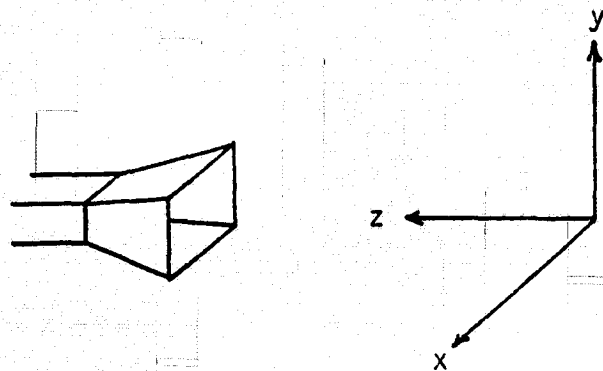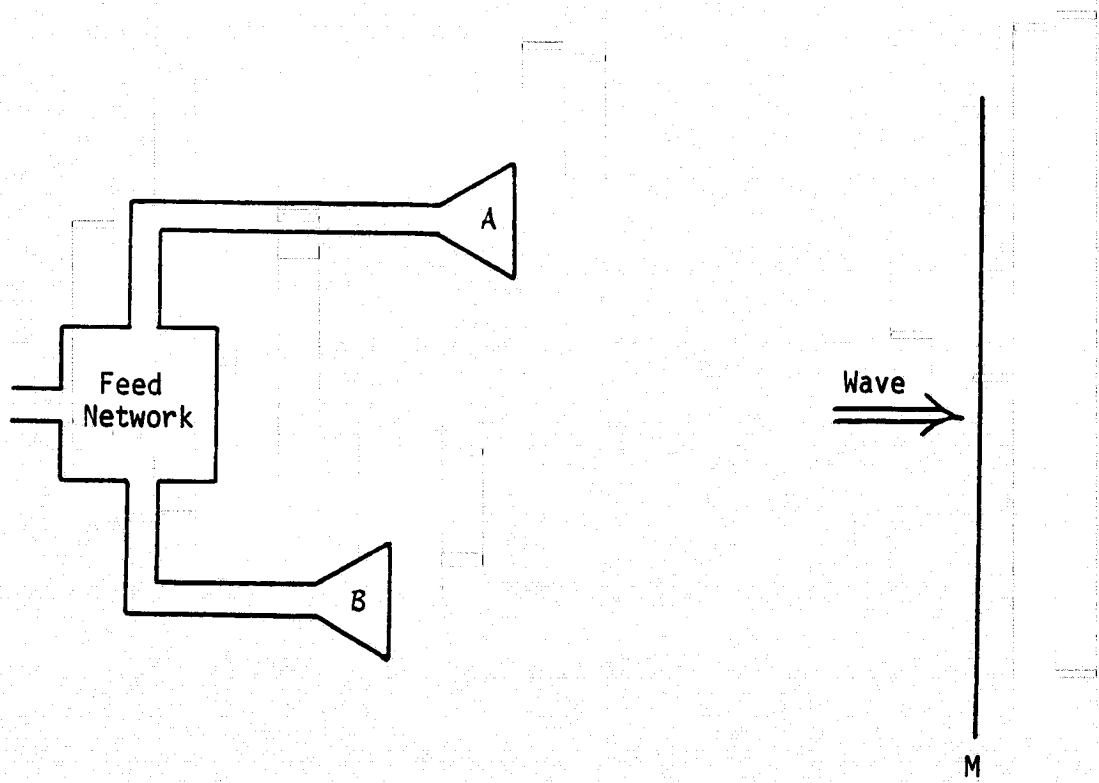Figure A-1b. Transmitting antenna coordinate system.

Figure A-1c. Receiving antenna coordinate system.

Figure A-1. The definition of coordinate systems
for waves and antennas.

Figure A-2. An arbitrarily polarized antenna
represented by two orthogonally
polarized elements.

This property is illustrated by examining two dipoles, one vertical and one horizontal spatially separated by $\lambda/4$ and fed with in-phase voltages as shown in Figure A-3. The transmitted wave has a vertical component which lags the horizontal component by 90°. Upon receiving the incident wave must have a vertical component which leads the horizontal component by 90° in order to have constructive addition of the voltages at the feed point.

The case shown in Figure A-2 is completely general. The orthogonal horizontal and vertical polarizations in the example of Figure A-3 are special cases of $\hat{a}$ and $\hat{b}$ orthogonal polarizations in the general case.

Considering now the general case of Figure A-2, the transmit wave of the antenna

$$\vec{e}_a = \overline{A}\,\hat{a} + \overline{B}\,\hat{b}$$

$$= |\overline{A}|\ e^{j\ \text{Phase}\{\overline{A}\}}\ \hat{a} + |\overline{B}|\ e^{j\ \text{Phase}\{\overline{B}\}}\ \hat{b} \qquad (A-13)$$
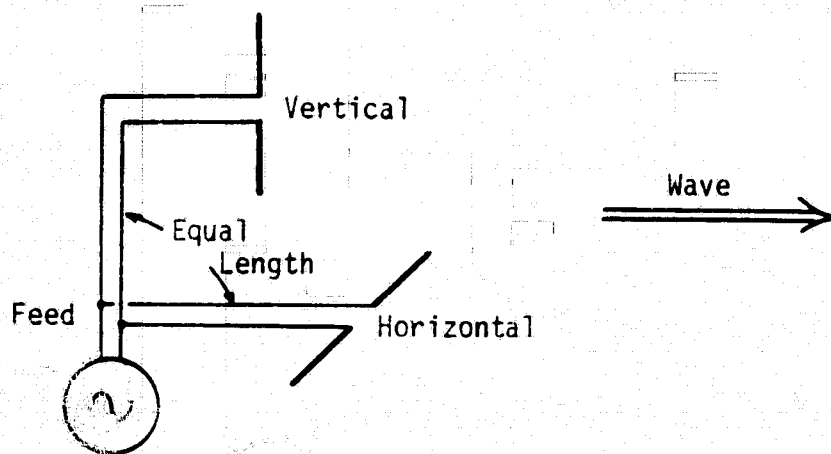
defines the polarization state of the antenna according to convention.

The phases of the components are

$$\text{Phase}\{\overline{A}\} = \alpha$$
$$\text{Phase}\{\overline{B}\} = \beta \qquad (A-14)$$

and the relative phase is

$$\phi = (\alpha) - (\beta) \ . \qquad (A-15)$$
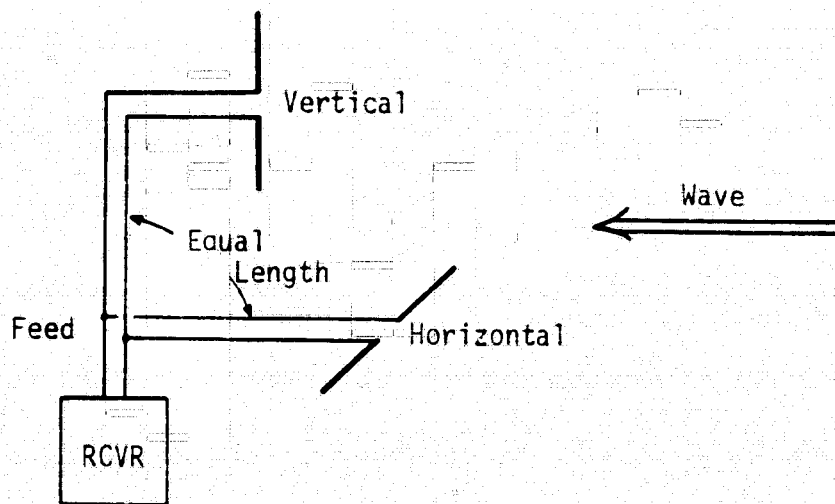
ORIGINAL PAGE IS
OF POOR QUALITY

Figure A-3. The properties of an antenna upon
transmitting and receiving.

In the receiving case the required condition for the antenna to be polarization matched to the wave is that the relative phase must equal $-\phi$. This is satisfied by

$$-\phi = (-\alpha) - (-\beta)$$
$$= (-\text{Phase}\{\overline{A}\}) - (-\text{Phase}\{\overline{B}\}) \quad . \tag{A-16}$$

Therefore the wave to which the antenna is polarization matched on receiving is

$$\vec{e}_a' = |\overline{A}| \, e^{-j \, \text{Phase}\{\overline{A}\}} \, \hat{a} + |\overline{B}| \, e^{-j \, \text{Phase}\{\overline{B}\}} \, \hat{b}$$
$$= \overline{A}^\star \, \hat{a} + \overline{B}^\star \, \hat{b}$$
$$= \vec{e}_a^\star \quad . \tag{A-17}$$

This vector represents the antenna state upon receiving. The antenna state upon receiving is defined as the wave state to which the antenna is optimally responsive and is the conjugate of the transmit antenna state.

The dot product of the incoming wave vector and the receive antenna vector is proportional to the terminal voltage.

$$\overline{V} = C\vec{E} \cdot \vec{e}_a^\star \quad . \tag{A-18}$$

This is the complex vector representation.

It is essential to remember that the $\hat{a}$ and $\hat{b}$ vectors form a coordinate system to which all waves have been referenced. However, the normal circumstance is that the same coordinate system is not used to define the incoming wave and the antenna state. This is

especially important to realize when the conventional polarization
state parameters ε, τ, γ, and δ are defined for a wave in its own
coordinate system and the coordinate system is then suppressed.

1B.3 The Coordinate System

The wave state and the antenna state must be represented in the
same coordinate system in order to use the complex vector formula-
tion [30]. Any arbitrary system may be used but since coordinates
have already been defined for the incoming wave and for the antenna
transmitted wave it is logical to use one of these. The coordinate
system of the incoming wave will be used, thus the antenna coordinate
system must be transformed.

In all of the discussions to follow in this section a reference
point at the antenna feed is used for all abso e phase values.

The wave will be decomposed into two orthc nal polarizations.
The most general case is two orthogonal elliptical polarizations, but
in this discussion the wave is to be decomposed into orthogonal
linearly polarized waves. These two polarizations are used to
establish an x-axis and y-axis respectively. These x and y axes
must form a right hand coordinate system with z in the direction of
propagation.

The incoming wave coordinate system is established first; then
the antenna coordinate system is defined with the y-axis in the same

direction as the y-axis of the incoming wave coordinate system[1] as illustrated in Figure A-4.

Transformation of the antenna coordinate system requires a reversal of the positive x-axis and reversal of the direction of propagation. The x and y axes of the antenna coordinate system and the transformed coordinate system are also shown in Figure A-4 where the transformed coordinate system is also the coordinate system of the incoming wave.

Phasor fields from the antenna (while transmitting) as they appear in a reference plane in the far field are shown in Figure A-5a where the absolute phase of the fields is referenced back to the feed terminals of the antenna. The relative phase of the two component fields (which are along the positive axes in the antenna coordinate system) is δ.

In the coordinate system of the receiving antenna a sign change is necessary on the x-axis which translates to a 180° phase change in the x-component of the wave. This is illustrated in Figure A-5b where the angle δ' is the relative phase of the orthogonal components (still from the antenna while transmitting) along the positive axes of the transformed coordinate system.

Now referencing absolute phase back to the common phase reference point of the antenna feed recall that the antenna upon receiving

---

[1] The antenna coordinate system could be defined with the x-axis in the same direction as the x-axis of the wave coordinate system with equivalent results.
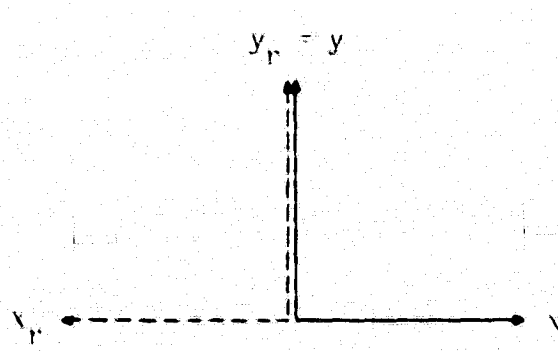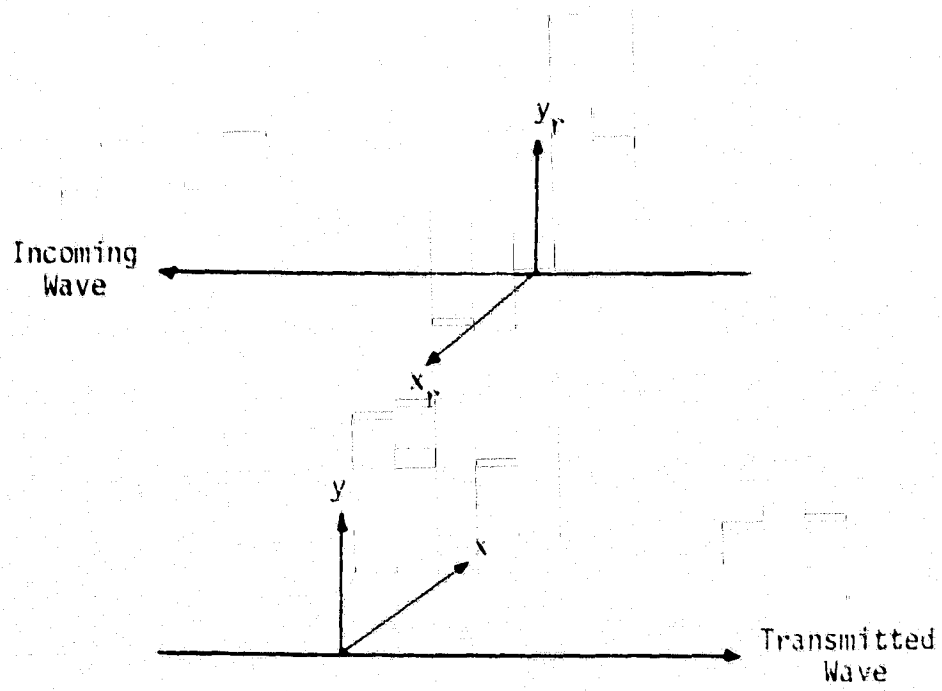
Figure A-4. The change in coordinate system between transmitting and receiving.
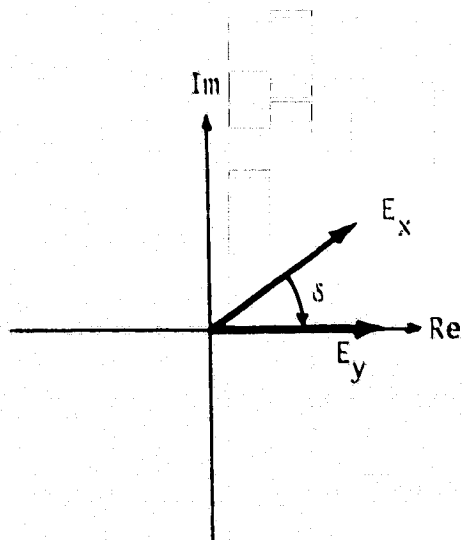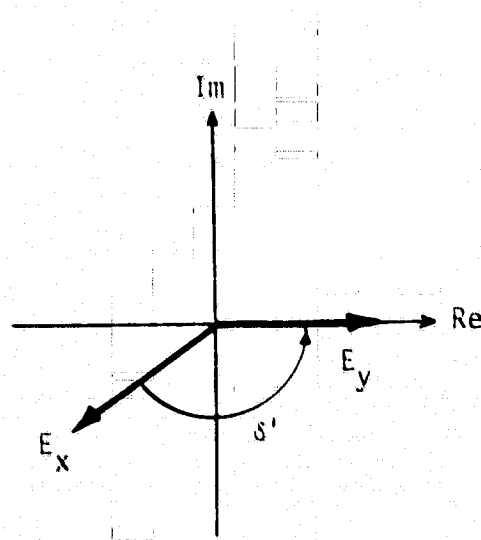
Figure A-5a. Transmitting.
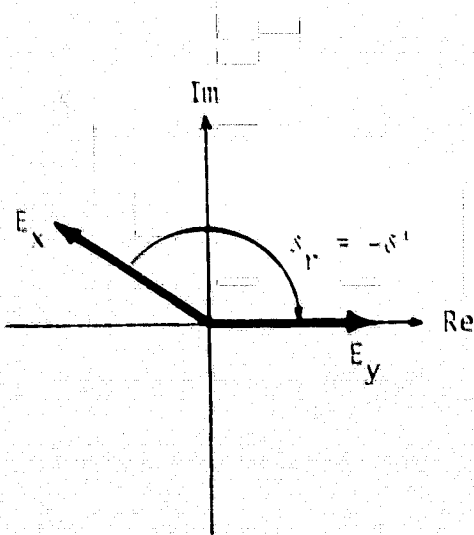

Figure A-5b. Receiving.

Figure A-5c. Receiving antenna with
proper phase reference.

Figure A-5. Phasor fields related to transmitting
and receiving.

will be optimally responsive to a wave with phase of $-\delta'$. This is illustrated in Figure A-5c where $-\delta'$ is called δ_r. From the figures it is apparent that the coordinate transformation has resulted in

$$\delta_r = -\delta' = 180° - \delta \quad . \tag{A-19}$$

Using the definition

$$\gamma = \tan^{-1} \frac{|E_y|}{|E_x|} \tag{A-20}$$

it is noted that the x-axis sign reversal in the coordinate transformation has no effect on γ. Therefore

$$\gamma_r = \gamma \tag{A-21}$$

Using equations relating δ, γ, ε (the inverse cotangent of the axial ratio) and τ (the tilt angle of the polarization ellipse) it is found that

$$\varepsilon_r = \frac{1}{2} \sin^{-1}(\sin 2\gamma_r \sin \delta_r)$$

$$= \frac{1}{2} \sin^{-1}(\sin 2\gamma \sin(180° - \delta))$$

$$= \frac{1}{2} \sin^{-1}(\sin 2\gamma \sin \delta)$$

$$= \varepsilon \quad , \tag{A-22}$$

and

$$\tau_r = \frac{1}{2} \tan^{-1}(\tan 2\gamma_r \cos \delta_r)$$

$$= \frac{1}{2} \tan^{-1}(\tan 2\gamma \cos(180° - \delta))$$

$$= \frac{1}{2} \tan^{-1}(\tan 2\gamma(-\cos \delta))$$

$$= -\frac{1}{2} \tan^{-1}(\tan 2\gamma \cos \delta)$$

$$= 180° - \tau \quad . \tag{A-23}$$

Therefore the coordinate transformation that must be performed in order to use the formulation

$$\overline{V} = C\vec{E} \cdot \vec{e}_{a_r}^{\,*} \tag{A-24}$$

is

$$\tau_r = 180° - \tau$$
$$\varepsilon_r = \varepsilon \tag{A-25}$$

or

$$\delta_r = 180° - \delta$$
$$\gamma_r = \gamma \tag{A-26}$$

where the r subscript indicates the antenna parameter transformed to the new coordinate system.

It might seem as though referencing phase back to the feed termi-nals has duplicated the process of conjugation in the complex vector formulation. This is not the case! The use of the feed reference is

necessary because of the conjugate appearing in the formulation. In
a later section a method will be presented which eliminates the
conjugate and the feed reference point.

An example will now be presented to illustrate the use of the
complex vector formulation. This example is presented as a verifica-
tion of the formulation, not a proof. Since the intention is to
verify the correctness of the voltage phase angle magnitudes will be
suppressed.

1B.4 Example: A Linearly Polarized Wave and Circularly Polarized Antennas

Shown in Figure A-6 are a RHCP antenna, a LHCP antenna, and an
incident linearly polarized wave. The antennas are crossed dipoles
fed 90° out of phase. The incident wave is at an angle of 45° in
its coordinate system (see inset) but it appears to be at 135° as
viewed receding.

Also shown are the induced voltages in each dipole at the feed
points and the sum voltage at the feed points. This indicates that
$\overline{V}_{RHCP}$ leads $\overline{V}_{LHCP}$ by 90°.

The complex vector representation of the wave is

$$\vec{E} = (\vec{x} + \vec{y})$$

and that of the RHCP antenna is

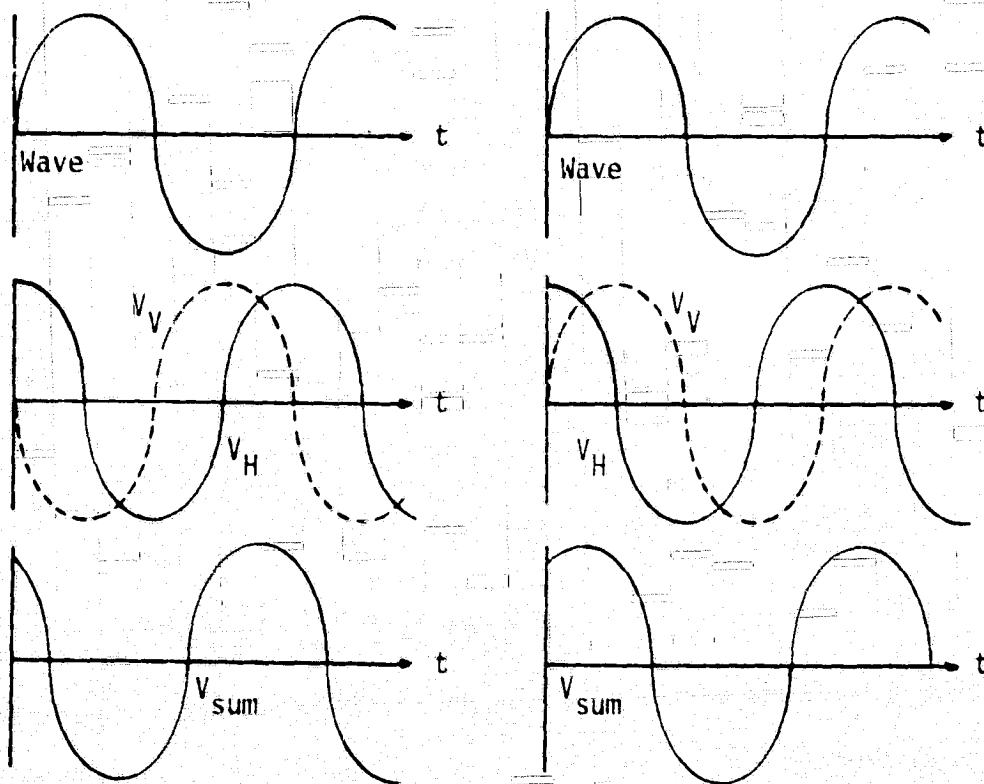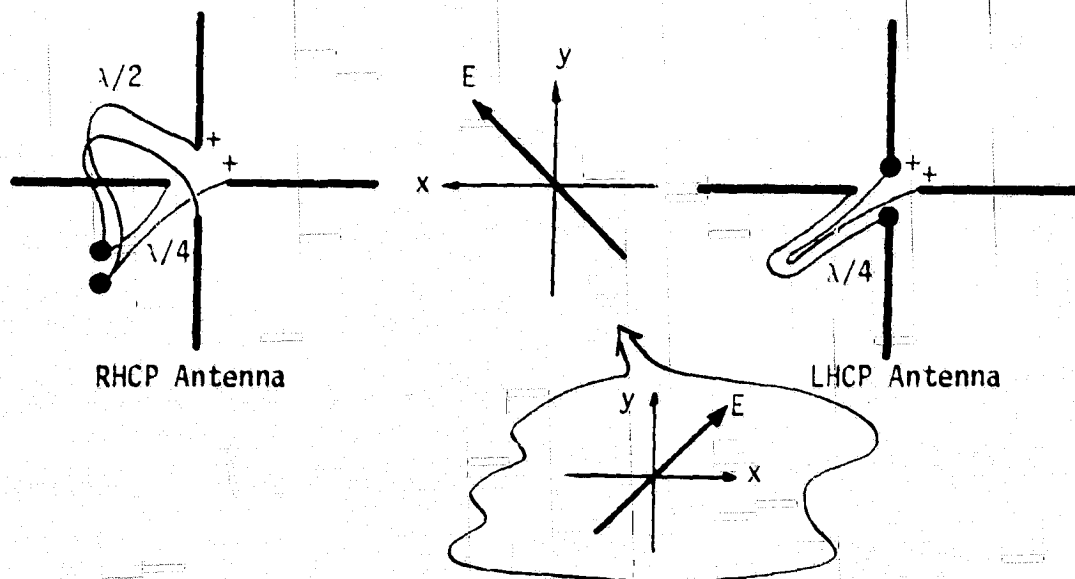$$\vec{e}_{RHCP} = (\vec{x} - j\vec{y}) \qquad (s = -90°)$$

Figure A-6. A linearly polarized wave at 45° incident
upon circularly polarized antennas.
$\overline{V}_{RHCP}$ leads $\overline{V}_{LHCP}$ by 90°.

and that of the LHCP antenna is

$$\vec{e}_{LHCP} = (\hat{x} + j\hat{y}) \ . \qquad (\delta = +90°)$$

Performing coordinate transformations on the antenna states yields

$$\vec{e}_{RHCP_r} = (\hat{x} - j\hat{y}) \qquad (\delta_r = 180° - \delta = 180° - (-90°)$$
$$= 270° \leftrightarrow -90°)$$

and

$$\vec{e}_{LHCP_r} = (\hat{x} + j\hat{y}) \ . \qquad (\delta_r = 180° - \delta = 90°)$$

Thus

$$\overline{V}_{RHCP} = \vec{E} \cdot \vec{e}^{\ *}_{RHCP_r} = (\hat{x} + \hat{y}) \cdot (\hat{x} - j\hat{y})*$$
$$= (\hat{x} + \hat{y}) \cdot (\hat{x} + j\hat{y})$$
$$= 1 + j$$

and

$$\overline{V}_{LHCP} = \vec{E} \cdot \vec{e}^{\ *}_{LHCP_r} = (\hat{x} + \hat{y}) \cdot (\hat{x} + j\hat{y})*$$
$$= (\hat{x} + \hat{y}) \cdot (\hat{x} - j\hat{y})$$
$$= 1 - j \ .$$

Therefore $\overline{V}_{RHCP}$ leads $\overline{V}_{LHCP}$ by 90° which agrees with the previous analysis.

1B.5 Another Method

Define a new complex vector formulation

$$\overline{V} = C\vec{E} \cdot \vec{e}_{a_r} \qquad\qquad (A-27)$$

with no complex conjugate. This formulation still requires the coordinate transformation but it eliminates the need to reference all phase values to a point at the antenna feed.

Consider the coordinate system of the incoming wave and the antenna as shown in Figure A-7. The coordinate transformation in the xy plane of the field components is as before

$$x_r = -x$$
$$y_r = y \qquad\qquad (A-28)$$

where unsubscripted variables represent the antennna state on transmitting and the subscript r represents the antenna state on receiving.

The phasor fields in the transmitting antenna coordinate system are shown in Figure A-8a. The relative phase between the two components is δ. The phasor fields in the transformed coordinate system are shown in Figure A-8b where the minus sign on the x-component has resulted in a 180° phase reversal on the x-directed field. The relative phase between the two components is δ_r. It is seen from this that the coordinate transformation has resulted in

$$\delta_r = \delta \pm 180° \quad . \qquad\qquad (A-29)$$

As before $\gamma_r = \gamma$. Substituting these values for δ_r and γ_r into the relations for ε and τ results in:
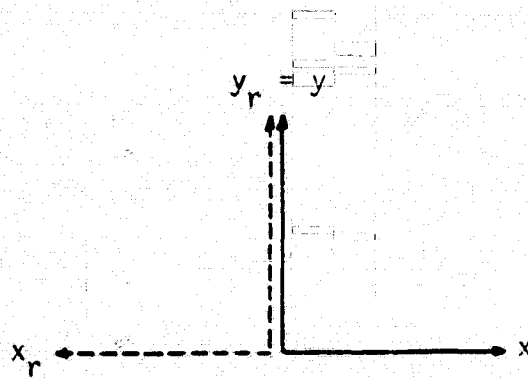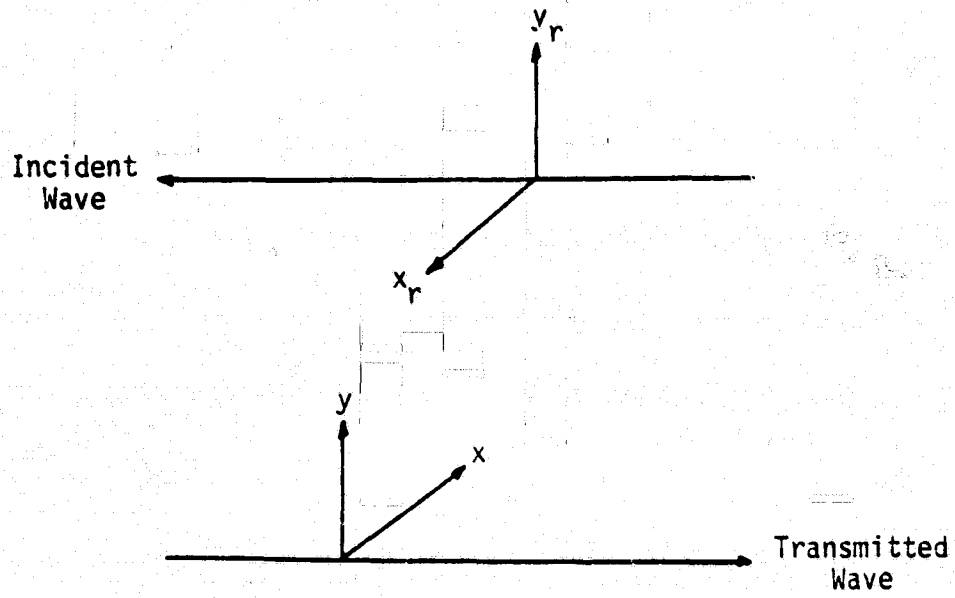
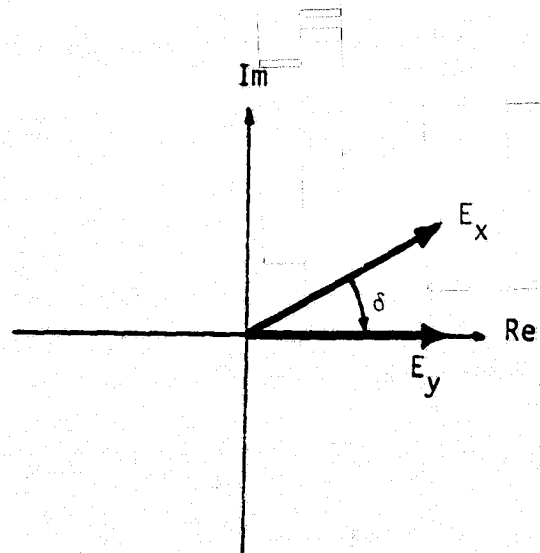Figure A-7. The change in coordinate system between transmitting and receiving.
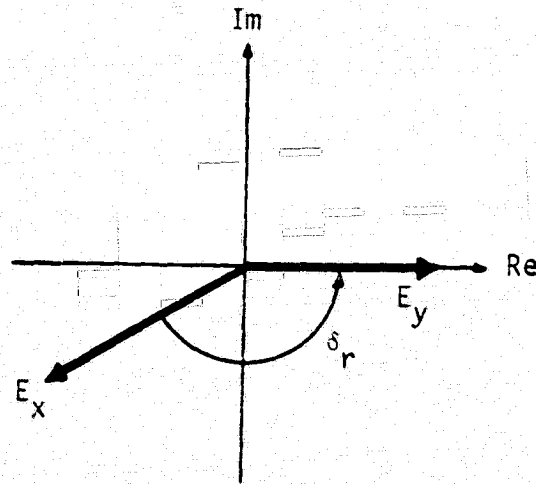
- 182 -

Figure A-8a. Transmitting.

Figure A-8b. Receiving.

Figure A-8. Phasor fields related to
transmitting and receiving.

$$\varepsilon_r = \frac{1}{2} \sin^{-1}(\sin 2\gamma_r \sin \delta_r)$$

$$= \frac{1}{2} \sin^{-1}(\sin 2\gamma \sin(\delta \pm 180°))$$

$$= \frac{1}{2} \sin^{-1}(\sin 2\gamma (-\sin \delta))$$

$$= -\frac{1}{2} \sin^{-1}(\sin 2\gamma \sin \delta)$$

$$= -\varepsilon \quad . \tag{A-30}$$

And,

$$\tau_r = \frac{1}{2} \tan^{-1}(\tan 2\gamma_r \cos \delta_r)$$

$$= \frac{1}{2} \tan^{-1}(\tan 2\gamma \cos(\delta \pm 180°))$$

$$= \frac{1}{2} \tan^{-1}(\tan 2\gamma (-\cos \delta))$$

$$= -\frac{1}{2} \tan^{-1}(\tan 2\gamma \cos \delta)$$

$$= 180° - \tau \quad . \tag{A-31}$$

Therefore, to use the formulation proposed here the following coordinate transformation is required.

$$x_r = -x$$
$$y_r = y \tag{A-32}$$

or

$$\tau_r = 180° - \tau$$
$$\varepsilon_r = -\varepsilon \tag{A-33}$$

or

$$\delta_r = \delta \pm 180°$$
$$\gamma_r = \gamma \quad . \tag{A-34}$$

Apparently Kales [3,29] originated the complex vector formulation for use with elliptically polarized waves and upon close inspection of his work it appears that he proposed the formulation without the conjugate. Kales gives

$$\overline{V} = k \ \vec{E} \cdot \vec{\rho}* \tag{A-35}$$

where

$\vec{E}$ is the complex vector representation of the incoming wave

and

$\vec{\rho}$ is the complex vector representation of the "antenna state" .

As it turns out, $\vec{\rho}$ is defined to be proportional to $\vec{g}*$ where $\vec{g}$ is the polarization vector of the transmitting antenna state. A double conjugation is "hidden" in the definitions he proposes. Kales makes no direct mention of coordinate transformations.

1B.6 Summary

The following forms are valid with their corresponding coordinate transformations:

$$\vec{V} = \vec{CE} \cdot \vec{e}_{a_r}^{*} \quad , \tag{A-36}$$

coordinate transformation:

$$\delta_r = 180° - \delta$$
$$\gamma_r = \gamma \tag{A-37}$$

or

$$\varepsilon_r = \varepsilon$$
$$\tau_r = 180° - \tau \tag{A-38}$$

and

$$\vec{V} = \vec{CE} \cdot \vec{e}_{a_r} \quad , \tag{A-39}$$

coordinate transformation:

$$x_r = -x$$
$$y_r = y \tag{A-40}$$

or

$$\delta_r = \delta \pm 180°$$
$$\gamma_r = \gamma \tag{A-41}$$

or

$$\varepsilon_r = -\varepsilon$$
$$\tau_r = 180° - \tau \quad . \tag{A-42}$$

APPENDIX 2

MATHEMATICAL ANALYSIS OF LIMIT OF

CROSSPOLARIZED PHASE AT ZERO RAIN RATE

Consider the phasors d_1 and d_2 which represent the propagation properties of a rain-filled medium.

$$d_1 = e^{-(\alpha_1 + j\beta_1)L}$$

$$d_2 = e^{-(\alpha_2 + j\beta_2)L} \qquad . \qquad (A\text{-}43)$$

Expanding the complex exponentials

$$d_1 = e^{-\alpha_1 L}(\cos \beta_1 L - j \sin \beta_1 L)$$

$$d_2 = e^{-\alpha_2 L}(\cos \beta_2 L - j \sin \beta_2 L) \qquad . \qquad (A\text{-}44)$$

As an aid to visualization consider now the equivalent vectors $\vec{d_1}$ and $\vec{d_2}$

$$\vec{d_1} = e^{-\alpha_1 L}(\cos \beta_1 L \; \hat{x} - \sin \beta_1 L \; \hat{y})$$

$$\vec{d_2} = e^{-\alpha_2 L}(\cos \beta_2 L \; \hat{x} - \sin \beta_2 L \; \hat{y}) \qquad . \qquad (A\text{-}45)$$

The vector $\vec{d_1}$ and the path it follows with varying rain rate are shown in Figure A-9. This path may be determined by calculating the unit tangent vector at all points along the path

$$T_1 = \frac{d}{ds} \vec{d_1} = (\frac{d}{dRR} \vec{d_1}) (\frac{d}{ds} RR) \qquad (A\text{-}46)$$

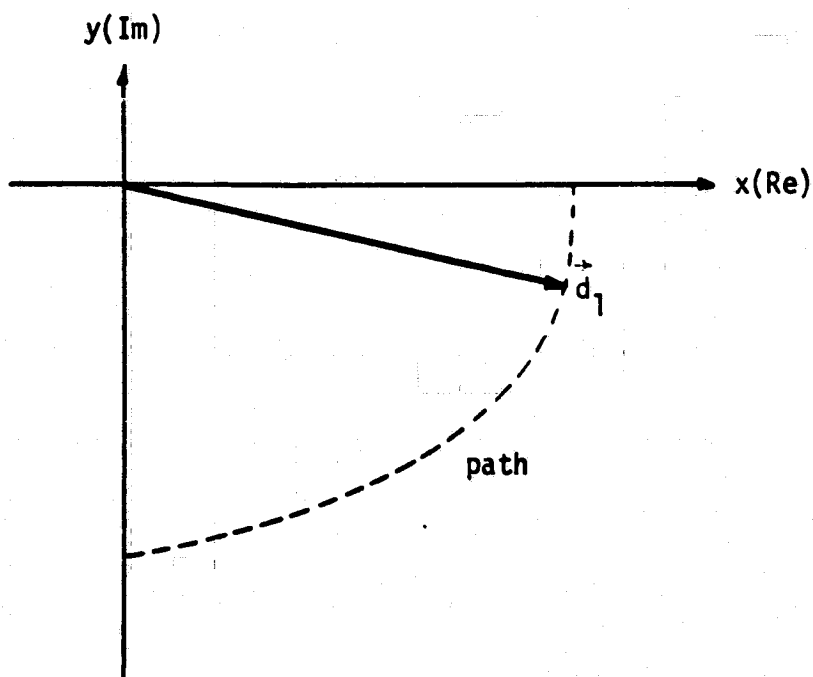where the variable RR represents rain rate. In this analysis only

Figure A-9. The vector $\vec{d_1}$ and the path it follows with changing rain rate.

the direction of the tangent is of concern.   Therefore

$$T_1 \propto \frac{d}{dRR} \vec{d}_1 \quad .$$
(A-47)

Recalling that both α_1 and β_1 are functions of rain rate

$$
\begin{aligned}
\frac{d}{dRR} \vec{d}_1 &= \frac{d}{dRR} \{ e^{-\alpha_1 L} (\cos \beta_1 L \, \hat{x} - \sin \beta_1 L \, \hat{y}) \} \\
&= -L \, e^{-\alpha_1 L} \frac{d}{dRR} \{\alpha_1\} \, (\cos \beta_1 L \, \hat{x} - \sin \beta_1 L \, \hat{y}) \\
&\quad - e^{-\alpha_1 L} (\sin \beta_1 L \, \hat{x} + \cos \beta_1 L \, \hat{y}) \, L \frac{d}{dRR} \{\beta_1\} \quad .
\end{aligned}
$$
(A-48)

Now, since $\alpha(0) = 0$ and $\beta(0) = 0$

$$\lim_{RR \to 0} T_1 \propto \frac{d}{dRR} \{\alpha_1\} \, \hat{x} + \frac{d}{dRR} \{\beta_1\} \, \hat{y} \quad .$$
(A-49)

Similarly

$$\lim_{RR \to 0} T_2 \propto \frac{d}{dRR} \{\alpha_2\} \, \hat{x} + \frac{d}{dRR} \{\beta_2\} \, \hat{y} \quad .$$
(A-50)

The angle at which the vectors approach the x-axis depends on the ratios

$$\frac{d\beta_1/dRR}{d\alpha_1/dRR} \quad \text{and} \quad \frac{d\beta_2/dRR}{d\alpha_2/dRR} \quad .$$

For very low rain rates these ratios are nearly equal and it can be assumed that $\vec{d}_1$ and $\vec{d}_2$ approach the x-axis along the same path. Therefore the angle of the difference vector $\vec{d}_1 - \vec{d}_2$ must be equal to the path angle as illustrated in Figure A-10.   Therefore
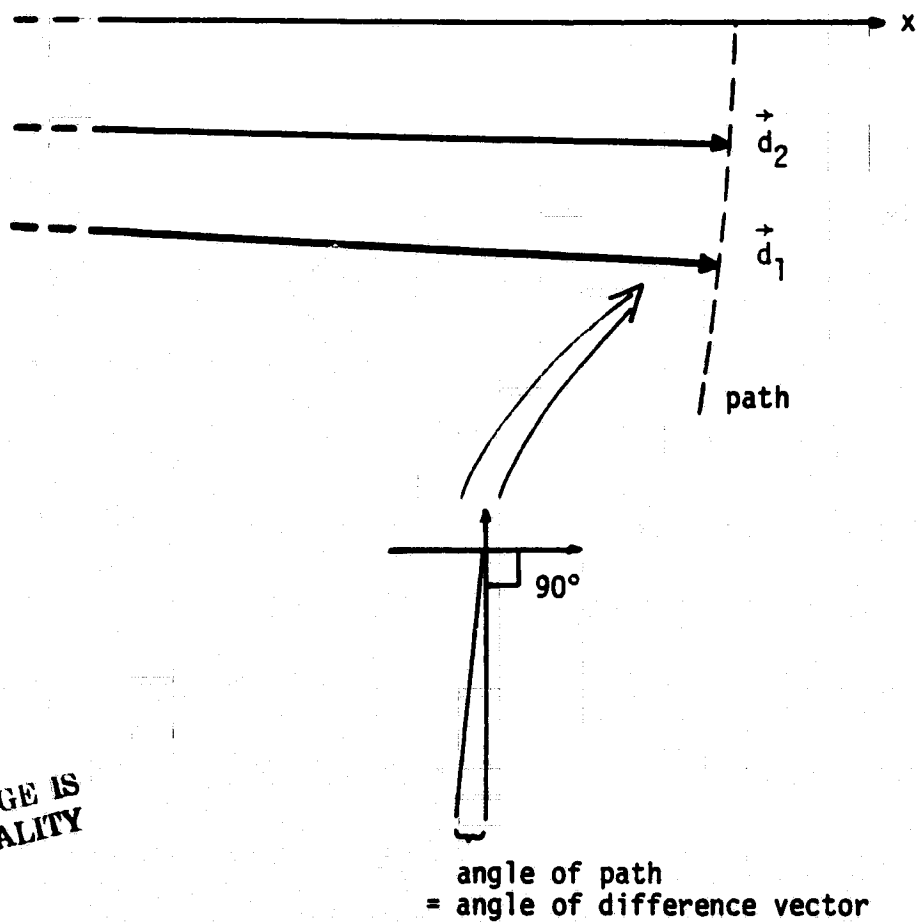
Figure A-10. The angle of $\vec{d}_1 - \vec{d}_2$ at very low rain rates is nearly -90°.

$$\lim_{RR \to 0} \text{Phase}\{d_1 - d_2\} \approx -90° - \tan^{-1} \left\{ \frac{d\beta_1/dRR}{d\alpha_1/dRR} \right\}$$

$$\approx -90° - \tan^{-1} \left\{ \frac{d\beta_2/dRR}{d\alpha_2/dRR} \right\} . \qquad (A-51)$$

Published [5] attenuation and phase data indicates that the inverse tangent term is small. Therefore

$$\lim_{RR \to 0} \text{Phase}\{d_1 - d_2\} \approx -90° . \qquad (A-52)$$